

**THESIS**

**FEED ZONE MICROMIXING AND ITS EFFECT  
ON CONTINUOUS CULTURES OF *SACCHAROMYCES*  
*CEREVISIAE***

**Submitted by**

**Paul Mondani**

**Department of Chemical and Bioresource Engineering**

**In partial fulfillment of the requirements**

**for the Degree of Master of Science**

**Colorado State University**

**Fort Collins, Colorado**

**Spring, 1995**

TP  
248.25  
.B55  
M65  
1995

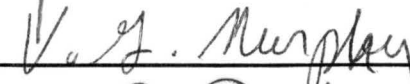
COLORADO STATE UNIVERSITY

March 27, 1995

WE HEREBY RECOMMEND THAT THE THESIS PREPARED UNDER OUR SUPERVISION BY PAUL RICO MONDANI ENTITLED THE EFFECT OF FEED ZONE MICROMIXING ON THE METABOLISM OF SACCHAROMYCES CEREVISIAE GROWN IN CONTINUOUS CULTURES BE ACCEPTED AS FULFILLING IN PART THE REQUIREMENTS FOR THE DEGREE OF MASTER OF SCIENCE.

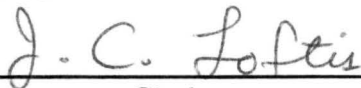
Committee on Graduate Work







Adviser



Department Chair

COLORADO STATE UNIVERSITY LIBRARIES

## **ABSTRACT OF THESIS**

### **FEED ZONE MICROMIXING AND ITS EFFECT ON CONTINUOUS CULTURES OF *S. CEREVISIAE***

**Inadequate mixing is known to be a common problem in the scale-up of bioprocesses, often leading to decreases in yield and productivity. To investigate the role of nutrient dispersion in continuous cultures, growth medium was fed into a laminar flow section of a loop that recirculates broth from a laboratory scale bioreactor. The intensity of micromixing at the feed site could be controlled by varying the axial distance a static mixer was placed upstream of the site. The intensity of the turbulent wake shed by the mixer was quantified by laser Doppler velocimetry and the Bourne dye reaction. By decreasing the size of the smallest turbulent eddy in the feed zone, less of the population is exposed to regions of either inadequate or excessive substrate concentrations. Yield vs. dilution rate curves were obtained through various mixing and feeding strategies. Reduced mixing was shown to delay the onset of the Crabtree effect and therefore improve the bioreactor's productivity.**

**Paul Rico Mondani  
Department of Chemical and  
Bioresource Engineering  
Colorado State University  
Fort Collins, CO 80523  
Spring, 1995**

## TABLE OF CONTENTS

<b>1. Introduction</b>	<b>1</b>
<b>1.1 Scope and Significance</b>	<b>1</b>
<b>1.2 Background</b>	<b>2</b>
<b>1.2.1 Mixing Effects in Biological Systems</b>	<b>2</b>
<b>1.2.2 Turbulence Quantification</b>	<b>12</b>
<b>1.3 The Crabtree Effect in <i>Saccharomyces cerevisiae</i></b>	<b>19</b>
<b>1.4 Objectives</b>	<b>25</b>
<b>2. Experimental</b>	<b>27</b>
<b>2.1 Fermentation Experiments</b>	<b>27</b>
<b>2.1.1 General Description</b>	<b>27</b>
<b>2.1.2 System Characteristics</b>	<b>33</b>
<b>2.1.3 Mixing and Feeding Strategies</b>	<b>37</b>
<b>2.2 Turbulence Quantification at the Feed Site</b>	<b>38</b>
<b>2.2.1 Laser Doppler Velocimetry</b>	<b>38</b>
<b>2.2.1.a General Description</b>	<b>38</b>
<b>2.2.1.b Specifications of Setup for Microscale                     Quantification Behind the Static Mixer</b>	<b>40</b>
<b>2.2.2 Bourne Dye Reaction</b>	<b>42</b>
<b>2.2.3 Photography of Dye Dispersion in the Feed Zone</b>	<b>45</b>
<b>3. Preliminary Fermentation Experiments</b>	<b>46</b>
<b>3.1 Flip-Flop Experiment #1 (FF1)</b>	<b>47</b>
<b>3.2 Flip-Flop Experiment #2 (FF2)</b>	<b>52</b>
<b>3.3 Culture History Effect Experiment #1 (CHE1)</b>	<b>60</b>
<b>3.4 Culture History Effect Experiment #2 (CHE2)</b>	<b>69</b>

<b>4.</b>	<b>Results and Discussion</b>	<b>77</b>
<b>4.1</b>	<b>Fermentation Results</b>	<b>77</b>
<b>4.1.1</b>	<b>Culture History Effect Experiment #3 (CHE3)</b>	<b>77</b>
<b>4.1.2</b>	<b>Culture History Effect Experiment #4 (CHE4)</b>	<b>85</b>
<b>4.2</b>	<b>Turbulence Quantification</b>	<b>92</b>
<b>4.2.1</b>	<b>Scale Determination from LDV Time Series</b>	<b>92</b>
<b>4.2.2</b>	<b>Scale Determination from Bourne Dye Reaction</b>	<b>98</b>
<b>4.2.3</b>	<b>Comparison of Different Mixing Results</b>	<b>103</b>
<b>4.3</b>	<b>Photographs of Dye Dispersion at Different Mixing Conditions</b>	<b>104</b>
<b>5.</b>	<b>Conclusions and Recommendations</b>	<b>107</b>
<b>6.</b>	<b>Notation</b>	<b>111</b>
<b>7.</b>	<b>Acknowledgments</b>	<b>112</b>
<b>8.</b>	<b>Literature Cited</b>	<b>113</b>
<b>9.</b>	<b>Appendix A</b>	<b>118</b>

## LIST OF FIGURES

No.		Page
1.1	Yield vs Dilution rate results of Fowler (1985)	9
1.2	Ye "Flip-Flop" Data (1990)	10
1.3	Summary of Ye Experiments (1990)	11
1.4	Schematic of the two major metabolic routes of <i>S. cerevisiae</i>	21
1.5	Cytochrome spectra for <i>S. cerevisiae</i> cultures using different metabolisms	24
2.1	The fermentation system with feed zone isolated in recirculating loop	28
2.2	The cyclone gas/liquid separator	30
2.3	The feed bulb used to dampen flow pulses and prevent backgrowth	31
2.4	The autoclavable dissolved oxygen flowcell	32
2.5	The two dimensional Laser Doppler Velocimetry system	39
3.1	Yield vs Dilution rate -- FF1	49
3.2	Ethanol vs Dilution rate -- FF1	50
3.3	Carbon dioxide evolution rate vs Dilution rate -- FF1	51
3.4	Yield vs Dilution rate -- FF2	54
3.5	Ethanol vs Dilution rate -- FF2	55
3.6	Carbon dioxide evolution rate vs Dilution rate -- FF2	56
3.7	Dissolved oxygen concentration vs time	57
3.8	Yield vs Dilution rate -- CHE1	62

<b>3.9</b>	<b>Productivity vs Dilution rate -- CHE1</b>	<b>63</b>
<b>3.10</b>	<b>Ethanol vs Dilution rate -- CHE1</b>	<b>64</b>
<b>3.11</b>	<b>Dissolved oxygen levels vs Dilution rate -- CHE1</b>	<b>65</b>
<b>3.12</b>	<b>Cytochrome levels vs Dilution rate -- CHE1</b>	<b>66</b>
<b>3.13</b>	<b>Yield vs Dilution rate -- CHE2</b>	<b>70</b>
<b>3.14</b>	<b>Productivity vs Dilution rate -- CHE2</b>	<b>71</b>
<b>3.15</b>	<b>Ethanol vs Dilution rate -- CHE2</b>	<b>72</b>
<b>3.16</b>	<b>Cytochrome levels vs Dilution rate -- CHE2</b>	<b>73</b>
<b>3.17</b>	<b>Low mixing conditions: CHE1 vs CHE2</b>	<b>74</b>
<b>4.1</b>	<b>Yield vs Dilution rate -- CHE3</b>	<b>80</b>
<b>4.2</b>	<b>Productivity vs Dilution rate -- CHE3</b>	<b>81</b>
<b>4.3</b>	<b>Ethanol vs Dilution rate -- CHE3</b>	<b>82</b>
<b>4.4</b>	<b>Cytochrome levels vs Dilution rate -- CHE3</b>	<b>83</b>
<b>4.5</b>	<b>Yield vs Dilution rate -- CHE4</b>	<b>86</b>
<b>4.6</b>	<b>Productivity vs Dilution rate -- CHE4</b>	<b>89</b>
<b>4.7</b>	<b>Ethanol vs Dilution rate -- CHE4</b>	<b>90</b>
<b>4.8</b>	<b>Cytochrome levels vs Dilution rate -- CHE4</b>	<b>91</b>
<b>4.9</b>	<b>The autocorrelation function of a LDV time series collected at the well mixed condition</b>	<b>92</b>
<b>4.10</b>	<b>The power spectrum of a LDV time series collected at the well mixed condition</b>	<b>93</b>
<b>4.11</b>	<b>Radially averaged values of total turbulent energy at the well mixed condition</b>	<b>96</b>
<b>4.12</b>	<b>Radially averaged values of total turbulent energy at the poorly mixed condition</b>	<b>97</b>

<b>4.13</b>	<b>Dye reaction and E model predictions of microscales at the four mixing conditions</b>	<b>101</b>
<b>4.14</b>	<b>Color photos of dye dispersion at degassed mixing conditions</b>	<b>106</b>

## LIST OF TABLES

No.		Page
2.1	Feed medium composition	34
4.1	Extinction coefficients for dye products	99
4.2	Comparison of microscale estimates from different experimental methods	103
4.3	Comparison of feed zone mixing conditions in similar studies	104

## CHAPTER I: Introduction

### 1.1 Scope and Significance

This thesis is concerned with the system response of a continuously fed *Saccharomyces cerevisiae* bioreactor to changes in the intensity of micromixing at the feed site. Specifically, the yield of dry cell mass vs. substrate concentration and other metabolic indicators were measured at different mixing intensities over a range of dilution rates. The objective is to understand how the extent of nutrient dispersal can affect the productivity of the bioreactor.

This research in the area of biological responses to changes in the physical bioreactor environment is significant for several reasons. The degree of mixing attained between two reacting fluid streams in any chemical process is known to have an affect on the product distribution and the rate of product formation in the system (Oldshue, 1982). In a bioreactor environment, the extent of mixing affects the performance of the system in many ways. Sufficient agitation must be provided to: (1) transfer enough oxygen from the gaseous to the aqueous phase in order to insure that dissolved oxygen concentrations are kept above repressive levels and, (2) decrease substrate concentration gradients so that nutrient starvation and/or repressive levels are minimized. Any cell, when placed in a moving fluid with

velocity gradients, experiences a shear force, the magnitude of which depends on the dynamic viscosity of the fluid, the fluid velocity gradients, and the size and properties of the cell. High shear gradients created by excessive agitation are known to cause lytic and sub-lytic effects in cultures of cells from higher organisms (Namdev, 1994). In contrast to microbial cells, insect and mammalian cells are very sensitive to shear force due to their relatively large size (10-20 micron range) and lack of cell wall (Cherry, 1988).

All living cells respond to the concentration of nutrients and toxins in their environment in a manner which can be very sensitive to threshold limits. There seems to be no clear means of determining and describing local concentration variations, particularly in poorly agitated vessels. Even more difficult is to predict what effect these gradients may have. Traditional chemical engineering methods are therefore difficult to apply to biological processes because of the lack of design equations which can reliably and consistently predict the output of a bioreactor. The development of an optimum "process recipe" requires one or two years of on-line experimentation and analysis. The time spent on this research represents a small portion of continuing efforts by many researchers to evaluate similar situations in hopes of optimizing a bioprocess' variables.

## 1.2 Background

### 1.2.1 Mixing Effects and Biological Systems

In a review of micromixing studies, Bourne (1983) stated that micro-mixing studies in general represent a risk of solving a non-problem. In light of this, I will

first address the requirements of system must have in order to exhibit a sensitivity to micromixing. The first requirement is that the system must have variable intensity of segregation. Secondly, either the product distribution of the reaction must be sensitive to the concentration of reactants in the local environment, or the rate of reaction must be non-first order, so that the product yield is a function of the segregation existing within the system. If the response to different states of segregation is to be appreciable, there is a further requirement that the characteristic reaction time not be much longer than the time spent in the different segregated regions. This is also represented by stating the system must have a large Damkohler number.

With respect to a biological system, the overall growth process is quite slow. Eucaryotes replicate a DNA strand every 30 minutes to 2 hours, (Alberts *et al.*, 1983), and this is only one segment of the growth cycle. However, the uptake of substrate and its subsequent reaction can be quite fast. This fact has been confirmed in a number experiments by Humphrey and co-workers (1966). When attempting to develop fluorometry methods as an on-line measurement of cell density, they showed spatial variations in the intracellular NADH pool concentrations were detected. Subsequent studies found that the NADH pool, interacting principally with the oxidative- phosphorylation steps of metabolism, reached a new steady state level in the 4.3 to 4.4 seconds after a step change in glucose supplied (Fiechter *et al.*, 1978). This fact is significant when considering that NAD<sup>+</sup> does not accept a proton until the sixth step of glucose metabolism. The

next reduction of NAD<sup>+</sup> does not occur until the fourteenth reaction. These figures are reinforced by data collected by Brooks and Meers (1983), who found that intermittent and periodic addition of medium on a 20 second cycle caused a reduction of biomass yield in their culture of *Pseudomonas methylotrpha*. This indicates periods of alternating bursts of growth with periods of starvation.

The effects of complete segregation vs. maximum mixedness were simulated on a growth model using Michaelis-Menten kinetics by Tsai *et al*, (1969). Ideal micromixing (maximum mixedness) produced greater degrees of conversion than complete segregation. It is implied that when the difference in concentration between the feed and the bulk is great and when the dilution rate is low, a chemostat may experience segregation.

In studying the mass transfer to particles similar in size to microbes, Armenante and Kirwan (1989) determined that the diffusional lower limit of Sherwood number equals 2 applies. Also noted is that as the diameter of the particle decreases, diffusion plays a more significant role in mass transfer than does fluid turbulence. Therefore, greater energy dissipation and smaller eddy sizes creating a smaller diffusion path can be a factor in determining the availability of substrate and the rate of its uptake. The mass transfer coefficient was not related to agitation intensity for the smallest particles.

Sweere *et al.* (1988) studied the effect of dissolved oxygen fluctuations using *S. cerevisiae* as a model system. In a fermenter in which oxygen and nitrogen were alternately sparged, the dissolved oxygen level was cycled between repressive and non-repressive levels. The actual dissolved oxygen concentrations were difficult to

measure due to a slow response time of the probe relative to the speed of the fluctuations. When air and nitrogen were sparged for equal times, substantial effects on biomass and metabolite production rates were observed at frequencies between one and two minutes. Higher frequencies approached values for zero dissolved oxygen fluctuations, while lower frequencies resulted in decreased biomass and increased ethanol, glycerol and acetate levels.

Continuous cultures of *S. cerevisiae* grown by Humphrey et al. (1966) at low dilution rates achieved improved yields when the feed was injected into well mixed regions of the tank. The proposed reason for this was that when feed was poorly dispersed, a greater portion of the culture population was ineffectively fed and suffered a reduced capacity to grow because of the lack of substrate availability. Mixing times in this system varied between two and three seconds with a stirrer speed of 500 rpm. The greatest effect was seen at a dilution rate of  $0.03 \text{ hr}^{-1}$ , but the yield of biomass from substrate was significantly lower at all dilution rates below  $0.10 \text{ hr}^{-1}$  when the feed was injected at the poorly mixed feed site.

Toma et al (1991) studied the effect of turbulence on microorganisms. They found that the limiting substrate concentrations for microbial growth depended on the intensity of agitation. By measuring the turbulence intensity with a piezoelectric crystal, the velocity fluctuations in the medium are transduced. They found that in vessels of different geometries, agitators with similar power input per unit volumes had vastly different distributions of the energy within the vessel. Dissolved oxygen concentrations in these experiments were kept constant by altering the percentage of

pure oxygen vs. air in the total gas flowrate. Their data suggests that an optimum agitation rate of 900 rpm exists for batch fermentations of *Brevibacterium flavum*. Here is an example where excessive agitation has an adverse effect on productivity of a microbial culture, as ATP levels began to drop significantly along with specific lysine production at stirrer speeds greater than 900 revolutions per minute.

*Trichoderma reesei*, a filamentous fungi grown on wheat straw, was found to have an optimum agitation rate of 150 rpm in a batch culture. *S. cerevisiae*, grown on molasses showed optimum viability at a 800 rpm stirrer speed.

Multiple methanol feed sites improved the yield compared to a single site in a 1500 m<sup>3</sup> continuous single cell protein fermenter at ICI's facility in England (Senior and Windass, 1980). Excessive methanol concentrations are known to be inhibitory in this process. Fields and Slater (1984) found the respiratory quotients depended on the location of the feed site in an airlift fermenter where *Methylophilus methylotrophus* was grown to in a fed batch culture.

Funahashi (1977) studied the effects of agitation by a flat bladed turbine Rushton style impeller on the microbial production of xanthan gum. An increase of stirrer speed increased the specific production rate of xanthan gum by *Xanthomonas campestris*. The effect was isolated from the dissolved oxygen concentration which also led to an increased specific production rate. Experiments in a rotating drum reactor, an apparatus with a similar defined shear field as in a Couette viscometer, showed the optimal xanthan gum production occurred at shear stresses up to a value of 40 Pascals. Production was found to be independent of shear rate.

Moes *et al.* (1985) investigated the scale-up of a culture of *Bacillus subtilis* using geometrically similar 0.045, 0.45, and 4.5 m<sup>3</sup> bioreactors. This organism was chosen because of its known sensitivity to dissolved oxygen levels represented by the metabolic production of different ratios of butanol to acetoin. Gassed power values for the three fermentors ranged from 0.16-3.6 kW/m<sup>3</sup>. By maintaining a constant superficial velocity and varying stirrer speeds, scale up experiments were run as a function of  $k_L a$ . Contrary to expectations, the fermentors did not show scale up dependence to this parameter. Product ratios in the smallest reactor were three to four times as sensitive to power input as were the large vessels. The authors determined the product distribution was therefore a function of both power input per unit volume (turbulence intensity) as well as the ratio of circulation time to reaction time.

Models of feed zone effect on *S. cerevisiae* include one by Bajpai and Reuss (1982). This model has the feed start in a small perfectly mixed region at the impeller's tip and then flow around the tank in a segregated manner analogously to circulation times measured in stirred tanks. Lower circulation times result in higher yields according to this model. This model also accurately predicts the results shown by Humphrey *et al.* (1966) where at low dilution rates (<0.10 hr<sup>-1</sup>) biomass yield suffered when fresh medium was poorly dispersed when fed to the system. The data of von Meyenberg (1969) is often used as a reference in baker's yeast experiments because of its thoroughness and because there appears to be a high degree of feed zone mixing in the system. The results are explained by stating

better mixing transports glucose to the cell surface more effectively, therefore stimulating growth at low dilution rates and causing cell surface glucose concentrations to rise above a repressive level at higher dilution rates.

Fowler and Dunlop (1989) developed a model system attempting to find these boundaries at higher dilution rates. In this system, nutrient broth was fed into a recirculation stream from a stirred bioreactor. Poor dispersal in this system resulted in reduced yields, as locally high glucose concentrations caused the onset of the Crabtree effect (Crabtree, 1929) and fermentative growth (see Figure 1.1).

A similar experiment was carried out by Ye and Dunlop (1990), where the effect of injection point location in a 3-liter stirred tank bioreactor was studied in a continuous culture of *S. cerevisiae*. Two types of experiments were conducted: in the first, the dilution rate was held constant at  $0.16 \text{ hr}^{-1}$ , and feed was injected through either of two different ports within the fermenter, one directly adjacent to the impeller tip's region and the other behind a baffle near the vessel wall. When the injection point location was changed at a supposed constant flowrate, significant changes in steady state biomass yields were reported (Figure 1.2). This type of experiment where injection point location is changed while dilution rate is held constant will from here on after be referred to as a "flip-flop" type experiment.

In another experiment, a yield versus dilution rate curve is constructed for various microscale levels at the different port locations (Figure 1.3). This data indicates a decrease in biomass yield with an increase in smallest turbulent eddy diameters at the injection point. The data differs most significantly from the

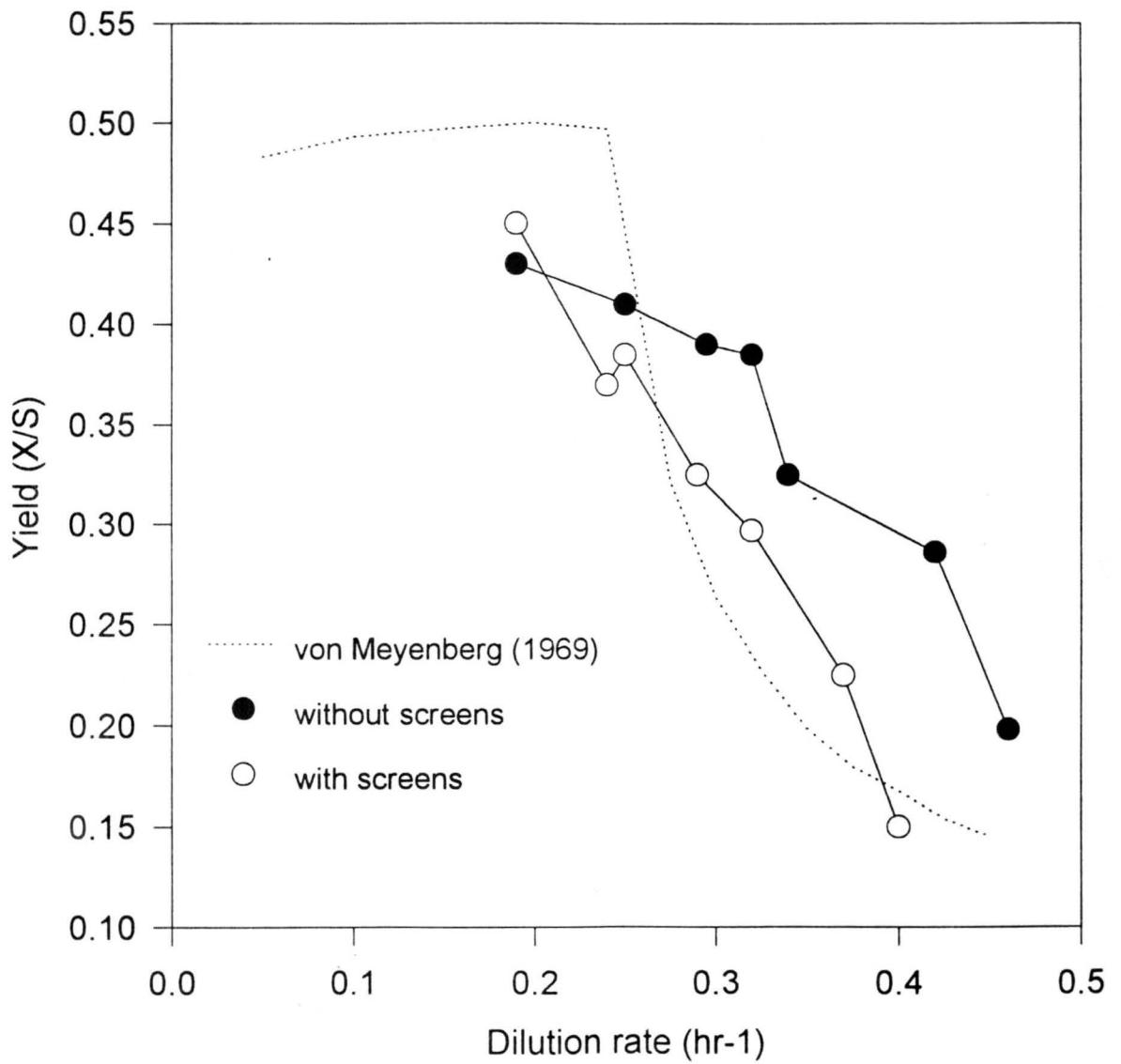


**Figure 1.1**

Yield vs Dilution rate as reported by Fowler (1985)

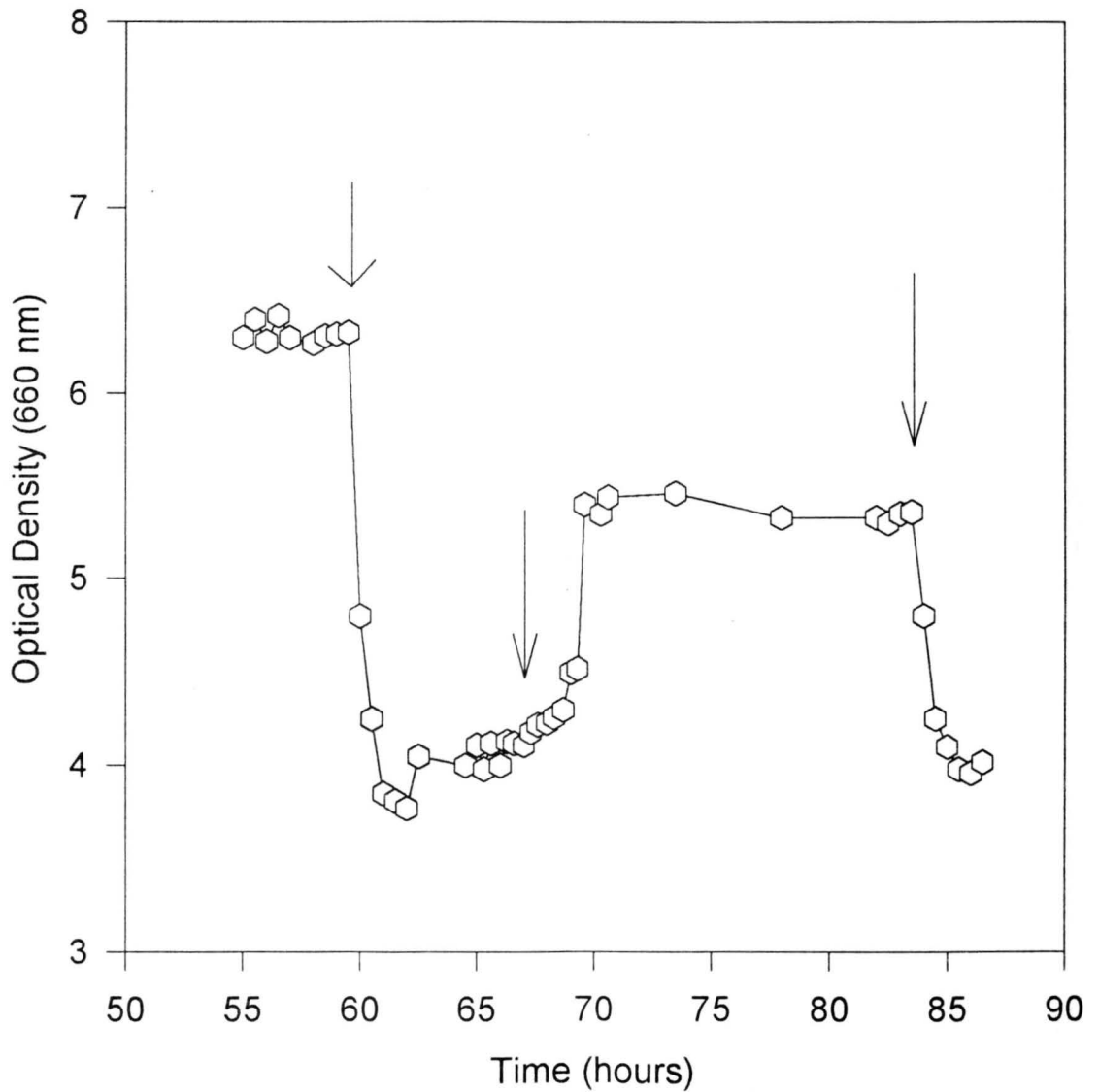


**Fig 1.2** Ye Flip-Flop Data (1990) -- Arrows indicate switch of injection point location.

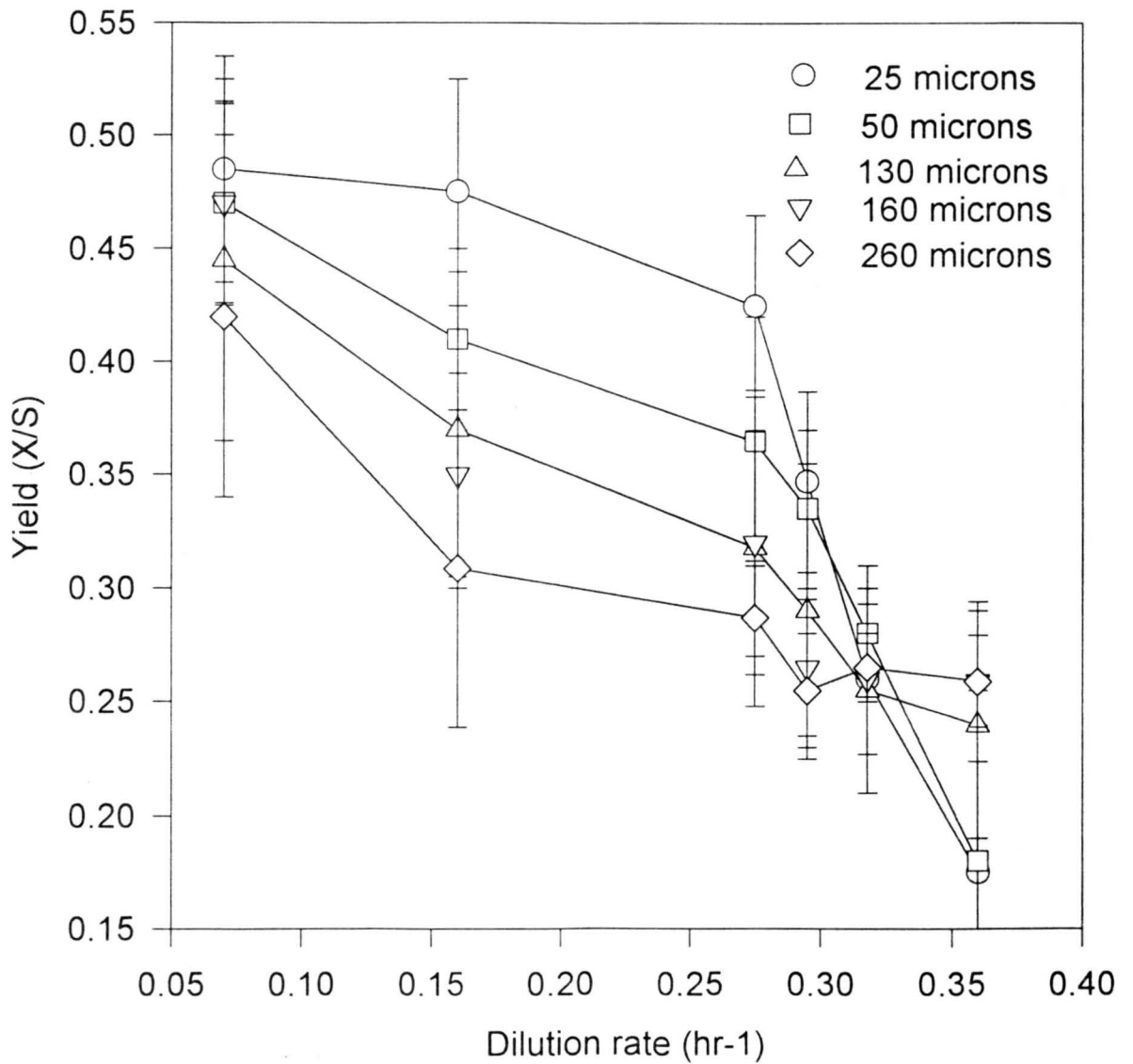


**Figure 1.3**

Summary of all experiments from Dunlop and Ye (1990)

classical von Meyenberg reference data in the middle dilution rates just prior to the critical dilution rate. It should be noted that these experiments differ greatly from those of Humphrey and co-workers in that they are carried out at a higher range of dilution rates where the cultures are no longer synchronous in nature and the organism will eventually switch to fermentative metabolism.

Wenger (1994) pointed out several limitations of all of these previous experiments. They include: (1) Lack of quantification of micromixing levels. The most common means of quantifying micromixing levels is by determination of the Kolmogorov or microscales of turbulence. These scales represent the size and turnover rate of the smallest turbulent eddies within the flow field. It is expected that different reactor geometries will have vastly different spatial distribution of microscale levels. (2) Failure to isolate micromixing from macromixing. Gross mixing parameters like stirrer speed have an effect on both macro- and micromixing properties. Since these properties scale-up and scale-down with distinct differences, the importance of this factor should not be overlooked. (3) Because the critical dilution rate is effected by low dissolved oxygen concentrations (Furakawa *et al.* 1983), the failure of some of these studies to isolate the mixing parameter in question from this and other similarly important factors has led to gross errors in conclusions made from the data acquired.

### 1.2.2 Turbulence Quantification

By mapping the turbulence levels simply in a feeding zone as opposed to throughout an entire fermentor, one could simplify the task of developing a suitable

model for scaling up bioreactors. In order to accurately predict reactor performance, a physical understanding of the reactors fluid environment is essential and quantification of turbulence levels is therefore imperative.

Three of the most common methods are quantifying degrees of turbulence will be discussed here. They are: 1) laser Doppler velocimetry, 2) the Bourne dye reaction, and 3) piezoelectric transduction of velocity gradients. Laser Doppler velocimetry (LDV) provides a means of measuring particle velocities in a non-intrusive manner. Intersecting beams of light create a "measuring volume" where particles scatter a Doppler shift created by a change in the periodicity of one laser beam. An estimate of the particle's component velocity is required to estimate the period shift necessary for the scattering to be detectable. The output of the LDV is a randomly sampled time series of velocity measurements as the particles in the fluid arrive in the measuring volume at random times and velocities. If a single particle's instantaneous velocity,  $U$ , is measured, then this time series consists of an average of the series,  $\bar{U}$ , plus or minus a fluctuating component,  $u$ . The mean square velocity,  $u^2$ , equals the variance of the time series' velocities.

The LDV has the potential to measure momentum transfer and, as stated by Hinze (1975), the similarity hypothesis may be used to relate this to the transport of a scalar property, like concentration. The similarity hypothesis has not held up well in practice with several authors such as Kindler *et al.* (1991) and Helgesen *et al.* (1991) have noticed greater transport of mass than of momentum. Townsend (1949) has shown that these two processes are independent of one another.

Hinze (1975) also states the mean axial momentum is distributed by a gradient type diffusion, while turbulent energy is similar to convective transport and scalar properties are distributed by gradient type diffusion as well as convective type transport. Townsend also notes that bulk jet movement carries out the turbulent transfer of energy and heat while the turbulent motion within the jet is responsible for the momentum transfer.

While the LDV is a very powerful tool, it does have the limitation of not being able to directly measure microscale levels because they are often smaller than dimensions of the measuring volume. An indirect method for determining the Kolmogorov microscales with laser Doppler velocimetry was developed by Beyerinck (1992). By measuring the decay of total turbulent energy behind a grid, a value for the turbulent energy dissipation rate,  $\varepsilon$ , was estimated and used in the equations for smallest turbulent eddy diameter,  $\eta$ , and turnover rate,  $\tau$ , developed by Kolmogorov.  $\nu$ , in these equations, is kinematic viscosity. Corrsin (1957) showed that turbulence is generally isotropic at these levels. The condition of local isotropy, which is met at Reynolds numbers greater than 100, is important because it allows simpler descriptions of the turbulent state.

The Schmidt number,  $Sc$ , defined as the relative rate of energy dissipation by viscosity divided by the concentration dissipation by diffusion plays an important role in fluids where concentration gradients exist. In fluids of high Schmidt number, substantial concentration gradients may still exist at the Kolmogorov scales. The Batchelor microscale defines the range where molecular diffusion play a

more significant role. This occurs in the viscous-subrange of the energy spectrum according to Tennekes and Lumley (1972).

The Bourne (1977) dye reaction is one of the most notable methods for determining microscales via fast consecutive chemical reactions whose product distributions are dependent on the degree of agitation at the feed port. The azo coupling of reactants 1-naphthol (A) and diazotized sulfanilic acid (B) form two dye products R and S, which resemble red and deep purple solutions, respectively. The reaction scheme for this test is as follows:  $A + B \rightarrow R$ ;  $R + B \rightarrow S$ . Samples of product are analyzed using the Lambert-Beer law and product concentrations are entered into a model developed by Baldyga and Bourne (1985) which predicts the Kolmogorov length scale.

Test reactions with similar strategies have been used by others including Paul and Treybal (1971). Iodination of acetone by Plasari et al. (1978), bromination of resorcin by Bourne (1977), imidization by Frey et al. (1988), and an acid into an alkaline solution of Barium-EDTA complex and sulfate ions by Barthole *et al.* (1982) all are fast consecutive reactions which have been used in micromixing studies. Bourne's dye reaction remains the most accurate and popular of these test reactions, however.

A third method for determining turbulence intensity within vessels, the piezoelectric transducer, was developed by Toma et al. (1991) and Ruklisha et al. (1989). Medium flow interactions are transformed into an electrical signal which is proportional to the momentum gradients. They have successfully used this probe to

map turbulence levels within a reactor by placing it at various points within the apparatus.

### *Models of Mixing Processes*

The first type of model to be reviewed is phenomenological. Within this type of model a distinction can be made between those in an Eulerian frame of reference and those in a Lagrangian frame of reference.

Models in the Eulerian frame of reference include two of the most popular in chemical engineering literature. The first, a coalescence-dispersion model (C-D), is from the work of Curl (1963). The basic principle is that the fluid consists of perfectly-mixed "packets" in which reaction proceeds by classical kinetics during the intervals between periodic coalescence of pairs of packets. After homogenization of the two packets, they divide and separate. Behavior of the system is thus governed by two parameters; the frequency of coalescence and the maximum distance of separation of interacting packets. Both of these parameters can be interpreted in the light of turbulence theory, where coalescence frequency is a function of energy dissipation rate and the integral length scale. The maximum separation is normally also related to the integral length scale. Unfortunately, *a priori* predictions of these parameters has met with little success and awaits the development and application of more detailed experimental data on the nature of turbulent energy spectra in real systems, according to Villermaux (1983). Computation of C-D simulations proceeds by Monte Carlo simulations or

probability density functions. Life expectancy of the packets is fixed by RTD considerations.

The second model of this type was developed by Villermaux (1983) and is referred to as the Interaction by Exchange with the bulk Model (IEM), in which fluid elements undergo continuous mass transfer with a hypothetical body of fluid at the mean exit concentration. Life expectancy of any particular packet is once again fixed by RTD considerations of the system. The single parameter in this model may be interpreted either as a mass transfer coefficient or as a micromixing time scale. This can also be equated with one of the time scales of turbulence theory, but parameter prediction as opposed to parameter fitting has proved difficult. Simulations of this scheme are iterative, as the exit concentration must be known to calculate the system conditions; convergence is usually rapid.

A major problem with these phenomenological model is there inability to represent spatial variations in segregation, and also their failure in certain cases where reaction schemes are complex. To overcome this it is necessary to turn to distributed models.

Models in a Lagrangian frame can adopt a more physically reasonable interpretation of the mixing process, in which three operation are distinguished: (1) Distribution of fluid elements to homogenize the mean concentration gradient, but without reduction of local concentration gradients, (2) Reduction of the size of fluid elements, either by laminar shear or by turbulent erosion, and (3) Intimate mixing of the fluid elements by molecular diffusion.

**Bourne (1983) noted that these processes do not necessarily occur consecutively. This formalism has been used extensively by Bourne and his co-workers to analyze results from his dye experiments. Ottino *et al.* (1979, 1980) have developed a more rigorous formalism for laminar shear and the convolution of fluid elements, defining a warped time scale which allows an analytical solution to the diffusion and reaction (mass balance) equation for first order kinetics.**

**It is important to recognize that in these models the interfacial area between elements, or more generally, the surface area to volume ratio, is the key parameter is determining the model's performance. In fact, Ottino describes the mixing process (the diffusion process as he refers to it) solely by the rate of generation of intermaterial area. Thus, the initial shape assigned to the element will strongly affect results of his model.**

**Another revolutionary approach to this problem was presented by Danckwerts (1953), in which he formally defines segregation (a measure of unmixedness), and introduces some of the concepts of residence time distributions. While the intensity of segregation is a difficult characteristic to determine experimentally, RTD's have been extensively developed and applied. Following this, the notions of regions of maximum mixedness and complete segregation have, together with interaction between such regions, formed the physical basis and interpretation of numerous other model. An excellent discussion on the importance of Danckwerts work is presented by Nauman and Buffham (1983).**

### 1.3 The Crabtree Effect in *Saccharomyces cerevisiae*

*Saccharomyces cerevisiae* possesses a metabolic feature known as the Crabtree effect, as discovered by Crabtree (1929), who originally noticed this phenomenon in resting tumor cells. This feature is alternatively known by the glucose effect, glucose repression, catabolite repression, or aerobic fermentation, and may be referred to as any of these terms in other references.

This phenomenon occurs in *S. cerevisiae*, as well as other yeasts which are grown on glucose. When an excess of glucose is present within a system, many glycolytic and Krebs cycle enzymes become saturated with substrate and therefore become repressed. Lim *et al.* (1982) provide an excellent review of the enzymes which are affected. When these pathways are no longer in use, the amount of ATP produced per mole of substrate is reduced along with the culture's oxidative capacity and therefore overall biomass yield.

In batch culture, growth proceeds under Crabtree effect conditions until all of the glucose is consumed. In a continuous culture, repressed growth does not occur until higher dilution rates (those approaching  $0.3 \text{ hr}^{-1}$ ). Researchers, including Fiechter (1978), have suggested that *S. cerevisiae* will grow at Crabtree effect conditions whenever the bulk glucose concentration exceeds 0.10 grams per liter.

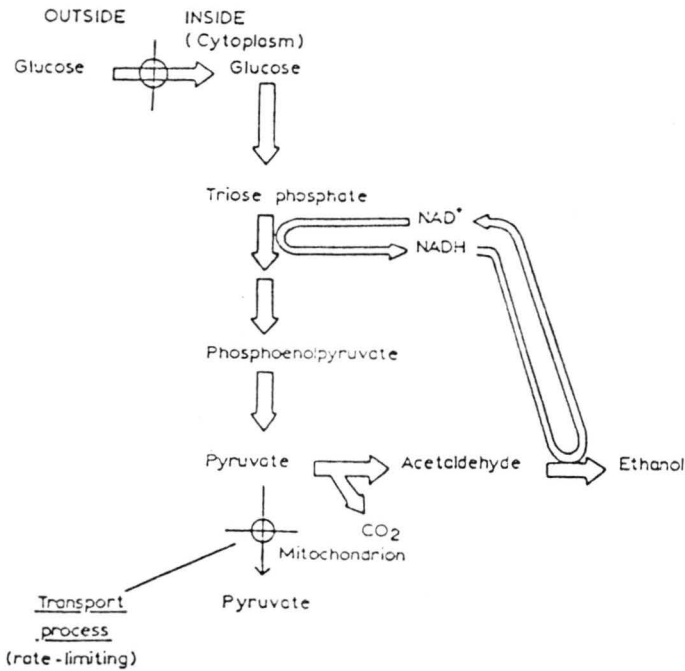
Growth under the Crabtree effect is evidenced by biomass yields of approx. 0.15 g biomass/g substrate, increased respiratory quotients (RQs), increased metabolite concentrations, and decreased cytochrome contents. Respiring continuous cultures of *S. cerevisiae* have biomass yield near 0.50 g biomass/g substrate. Fully respirative

(de-repressed) growth may only occur in fed-batch or continuous cultures where the feed rate is slow enough to keep the glucose concentration under the threshold limit. Figure 1.4 diagrams these two major catabolic routes of *S. cerevisiae*.

von Meyenberg (1969) observed intermediate values of biomass yield, indicative of a combination of catabolic routes being used. Others, such as Potsma et al. (1989), Sonnleitner (1991) and Wenger (1994) noticed much a sharper transition to and more distinct regions of repressed growth, with intermediate values being uncommon. Fiechter (1978) determined that this transition is dependent on the inlet glucose concentration as well as the dilution rate. The dilution rate where the organism starts to jump to its new metabolic route is referred to as the "critical" dilution rate or  $D_{crit}$ .

The existence of the glucose effect in this yeast makes it attractive for these type of experimental studies. Operation under conditions close to the critical dilution rate makes the system as a whole more sensitive to changes in glucose concentrations which will be near the threshold limit. This fact will be used later in selecting the operating conditions for these experiments.

Industrially, the glucose effect assumes a special significance. It is apparent that optimal processes will operate at conditions to maximize the productivity of the reactor, by insuring that the metabolic mode remains respirative and the biomass yield high.



**Metabolism of glucose under anaerobic conditions.**  
Respiration is now minimal and reducing equivalents (NADH) generated by glycolysis must now be re-cycled by being linked to the oxidation of some glycolytic intermediate, in this case, pyruvate to ethanol.

**Metabolism of glucose under aerobic conditions.**  
Glycolysis involves the oxidation to pyruvate; respiration involves the oxidation of pyruvate by the reactions in the Krebs cycle.

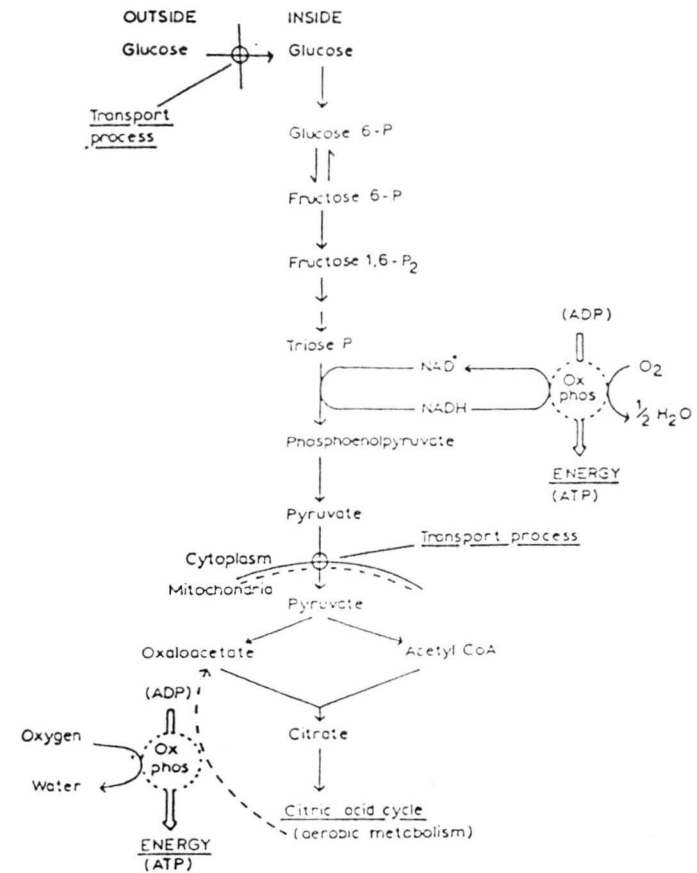


Figure 1.4 -- Schematic of the two major metabolic routes *S. cerevisiae* utilizes.

Several researchers have attempted to model the glucose effect for this reason. Sonnleitner and Kappeli (1986) proposed a model of this situation called a respiratory bottleneck. They hypothesize that during the Crabtree effect a saturation of the glycolysis pathway occurs and the overflow of glucose supply goes to the ethanol production pathway. This model shows long periods of adaptation necessary at super critical dilution rates where oxygen uptake remains constant, in contrast to von Meyenberg's linearly decreasing values for similar dilution rates. One possible reason for this discrepancy is that the two authors used different strains of *S. cerevisiae* species.

*S. cerevisiae* also has a metabolic characteristic known as the Pasteur effect (Pasteur, 1872). This effect simply states that the organism will switch to fermentative metabolism and produce ethanol when insufficient oxygen is present. Thus, it is similar to the Crabtree effect in the sense the metabolic pathway switches from respirative to fermentative, yet the stimulus for the change is different. It is therefore important to establish in any *S. cerevisiae* continuous culture what has caused the onset of fermentative metabolism and reduced biomass yield.

Jefferies *et al.* (1990) has suggested the reason for the conflict of saturated oxidative capacity versus repression of oxidative enzymes may be that an alternate form of respiration is necessary to compensate for the repressed respiration. Lievens *et al.* (1982) have noted that metabolic rates are more dominant in determining the pathway in use than the extracellular glucose concentration. They also noted that this phenomenon may occur with substrates other than glucose,

although not as dramatically. Levels of the mitochondrial cytochrome enzymes may help distinguish between low yields caused by glucose repression and those caused by oxygen limitation. Figure 1.5 gives cytochrome spectra for cultures in three different metabolic modes. The oxygen limited curve shows a culture whose biomass yield was low but still contained a measurable content of cytochrome oxidase.

The kinetics of glucose uptake for the fermentative and respirative pathways is clearly different. Fiechter *et al.* (1966) resolved all of their data into two distinct metabolic modes and found two distinctly different sets of constants when put to a Monod model. The reader should recognize the limitations of applying the Monod model to this situation. First, it is not applicable for short-term responses, by which is meant a response which occurs at time scales less than that of one cell division cycle. This error arises from the implicit assumption that a cell can instantaneously adjust its growth rate to its surrounding conditions. The second limitation of the Monod form concerns long-term responses. An organism will undergo adaptation to culture conditions over a long period of time, approximately 20 days for *S. cerevisiae* (Furukawa *et al.* 1983). Such adaptation may involve the loss of important organelles like mitochondria and therefore result in a completely different organism from the original one.

Wenger (1994) denotes three consequences of excessive glucose flux to such a system. In the short term, in response to sort of a glucose pulse, ethanol is produced without decrease of normal respirative capacity. Secondly, occurring over a longer

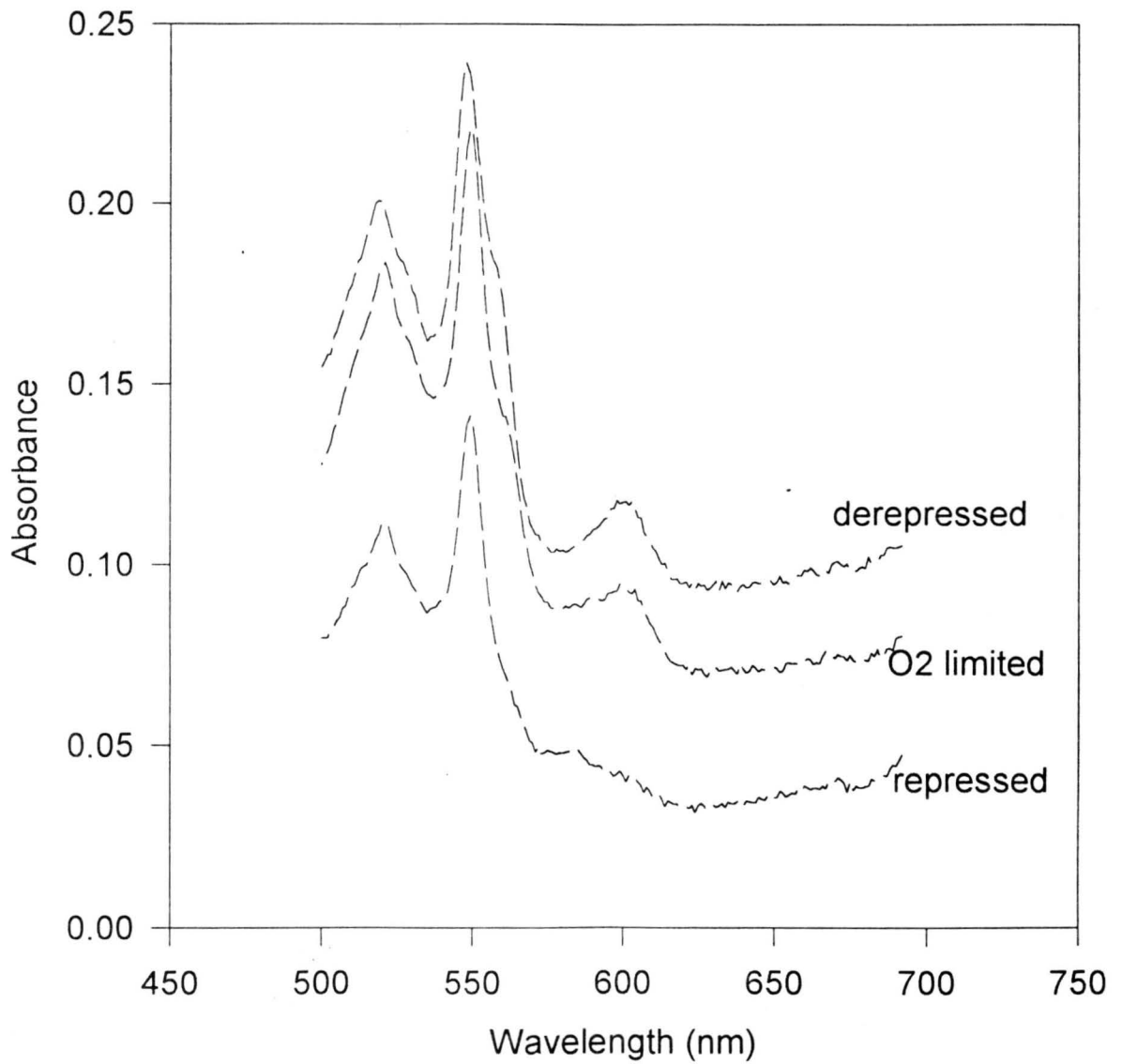


**Figure 1.5** Inverted Cytochrome Spectra for Cultures in Different Metabolic States

period of time, repression of Krebs cycle enzymes and mitochondrial cytochrome complexes begins to occur. Finally, after extended periods of adaptation, alternate pathways begin to develop as a result of the saturated oxidative capacity.

#### 1.4 Objectives

The research conducted sought to correlate the level of micromixing at the feed site, as quantified by laser Doppler velocimetry and the Bourne dye reaction, to the biomass yield of *S. cerevisiae* from glucose in continuous cultures at various mixing and feeding schemes. Of particular interest is the catabolic route the organism is utilizing (oxidative, fermentative, or a combination of the two), and other metabolic indicators such as ethanol production, cytochrome content, and off-gas analysis were measured. The role of dissolved oxygen levels on the output of the system will also be discussed.

The biological effect expected was that seen by Fowler and Dunlop (1989) when increased feed zone mixing caused a decrease in biomass yield and an increase in ethanol production. Their hypothesis was that increased nutrient dispersal caused an increase in the volume of the population where glucose levels exceeded the threshold for oxidative growth. The current fermentation system differs from theirs in that the mixing intensity in this system can be changed immediately by changing the axial distance upstream the static mixer is placed from the feed site; Fowler's system required disassembly of the recirculation loop, the insertion or removal of the mixing screens, and then re-autoclaving and re-installing to the stirred tank. Thus, a period of several hours passes before the mixing state is adjusted. This

study also has the advantage of monitoring dissolved oxygen at the end of the recirculating feed loop as well as in the stirred tank; this is significant because the previous results of Fowler and Dunlop (1989) and Dunlop and Ye (1990) overlook the role of dissolved oxygen in their results.

The smallest turbulent eddy in the feed zone will be quantified by laser Doppler velocimetry and Bourne dye reaction at the two different mixing extremes. A comparison of the results obtained by the two methods will be discussed with emphasis on repeatability and reliability. These various degrees of mixing were expected to cause different steady state biomass yields, with better nutrient dispersal leading to decreased yields.

## 2. EXPERIMENTAL

### 2.1 Fermentation Experiments

#### 2.1.1 General Description

The experimental system described here was developed with the intention of varying the energy dissipation rate, and thus the size of the smallest turbulent eddy, at the site where fresh sterile medium is fed into a continuous bioreactor. It is the aim of this thesis to investigate the role of *micromixing* of the feed stream, therefore care must be taken that the system's RTD not be affected coincidentally with the intensity of energy dissipation, to isolate the *micromixing* phenomena from the *macromixing* phenomena. The design must also allow for the level of turbulence to be quantified, as there is evidence that these mixing parameters are critical for the development of some scale ups.

To meet these criteria, the feed injection port was isolated in a recirculating loop from the chemostat (See Figure 2.1). Controllable energy dissipation rates were achieved with the use of a static mixer, which consisted of two 4 mm diameter steel cylinders, 11 mm in length, nestled perpendicularly halfway into each other so as to form the shape of a cross or a plus sign. Unlike the secondary mixing vessel used by Fowler and Dunlop (1989), where disassembly of the vessel, insertion of mixing screens, re-autoclaving, cooling, and re-assembly of the recirculation vessel is required to change the mixing intensity at the feed site, this system's mixing

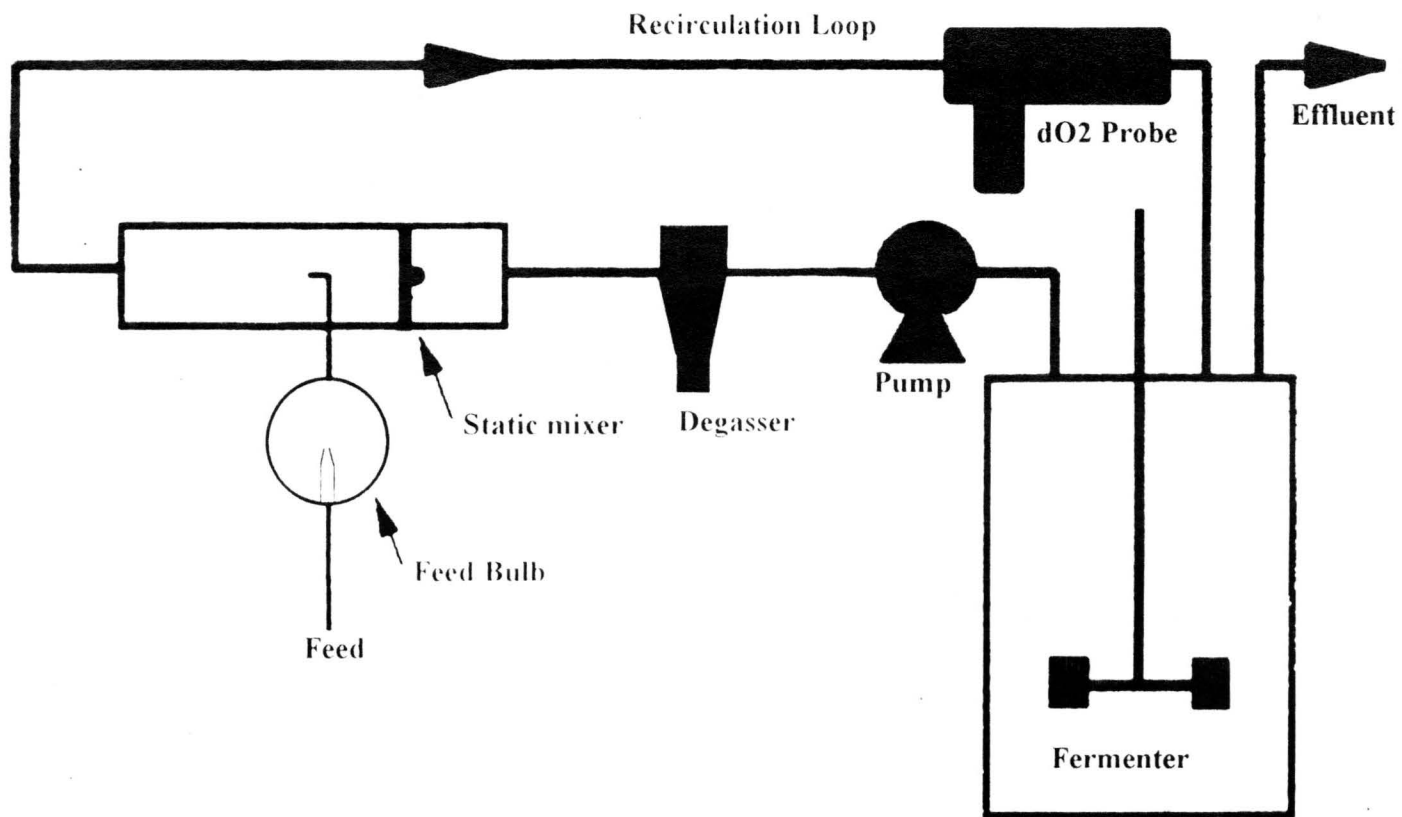


Figure 2.1 -- The entire fermentation system, the feed zone is isolated in the recirculation loop.

intensity may be changed instantly by varying the axial distance the static mixer is placed upstream of the feed site. A magnet external the glass loop held the mixer at its given location and allowed in axial position to be moved.

A cyclone shaped gas-liquid separator (figure 2.2) and a pulse dampener were placed upstream of the pipe's entrance to minimize the mixing effects of gas bubbles in the flow and pulses created by the peristaltic pump driving the flow, respectively. Figure 2.3 gives a schematic of the feed bulb placed above the 21 gauge hypodermic needle. This bulb created an air lock which prevented the yeast from growing up the feed line at contaminating the fresh sterile medium. Figure 2.4 shows a diagram of the autoclavable stainless steel flow cell for monitoring dissolved oxygen levels at the loop's end.

In an effort to maximize the difference in size of the Kolmogorov microscales at two different mixing intensities, the flowrate in the recirculation loop was chosen so that the Reynolds number was approximately 2000, just below the transitional range when turbulence begins to form. The idea here is that when the static mixer is pulled far upstream so that its wake has entirely decayed before it reaches the feed site, laminar conditions will prevail so that nutrient dispersion will be minimal. Conversely, when the static mixer is placed only 1 cm upstream of the feed site, this upper limit of laminar pipe flow ensures a high degree of variability in the fluctuating velocity component. The energy dissipation rate is nearly proportional to the square of this fluctuating component (to be discussed more thoroughly later), and therefore minimizing the size of the Kolmogorov eddy diameter.

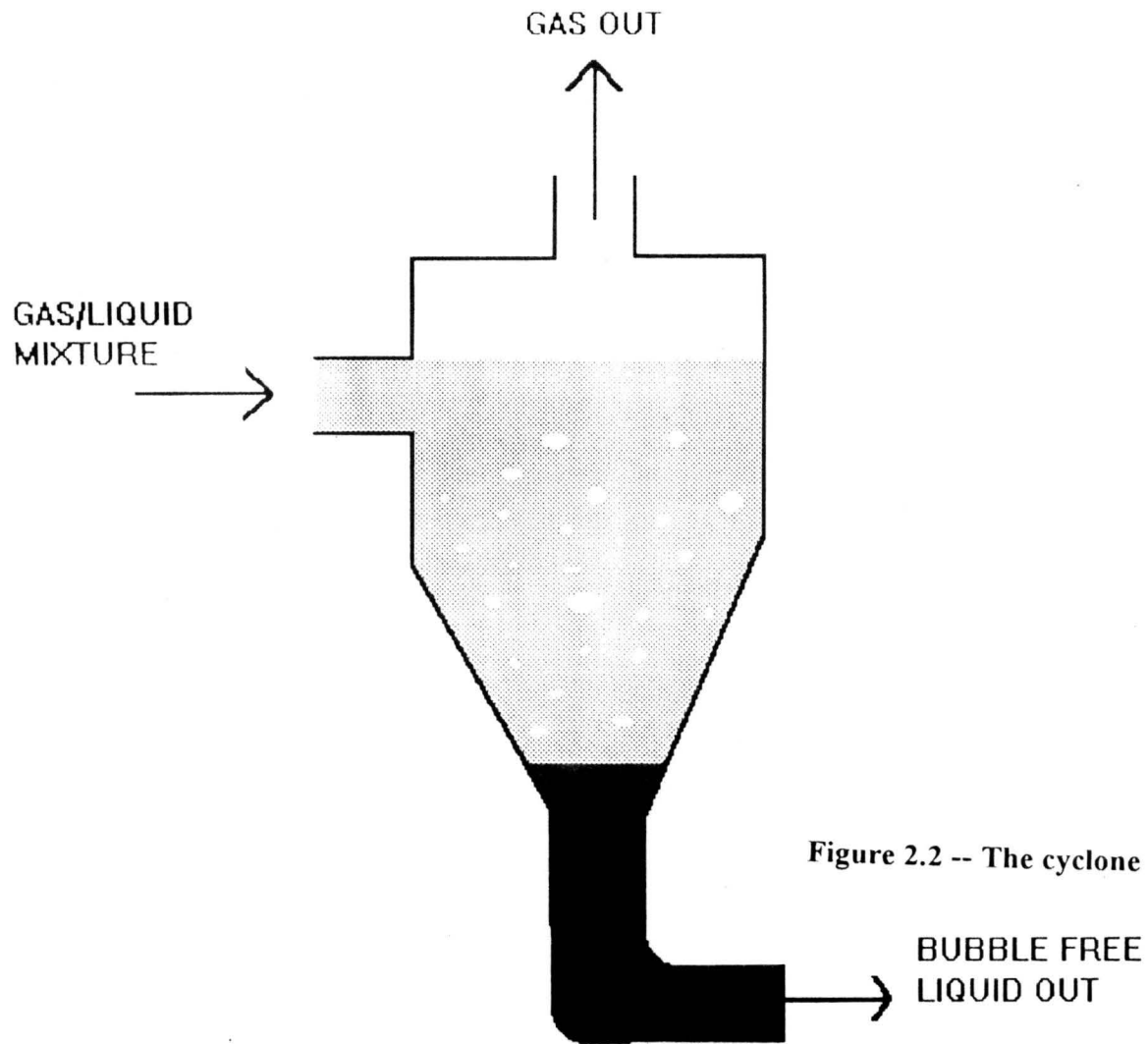


Figure 2.2 -- The cyclone gas/liquid separator

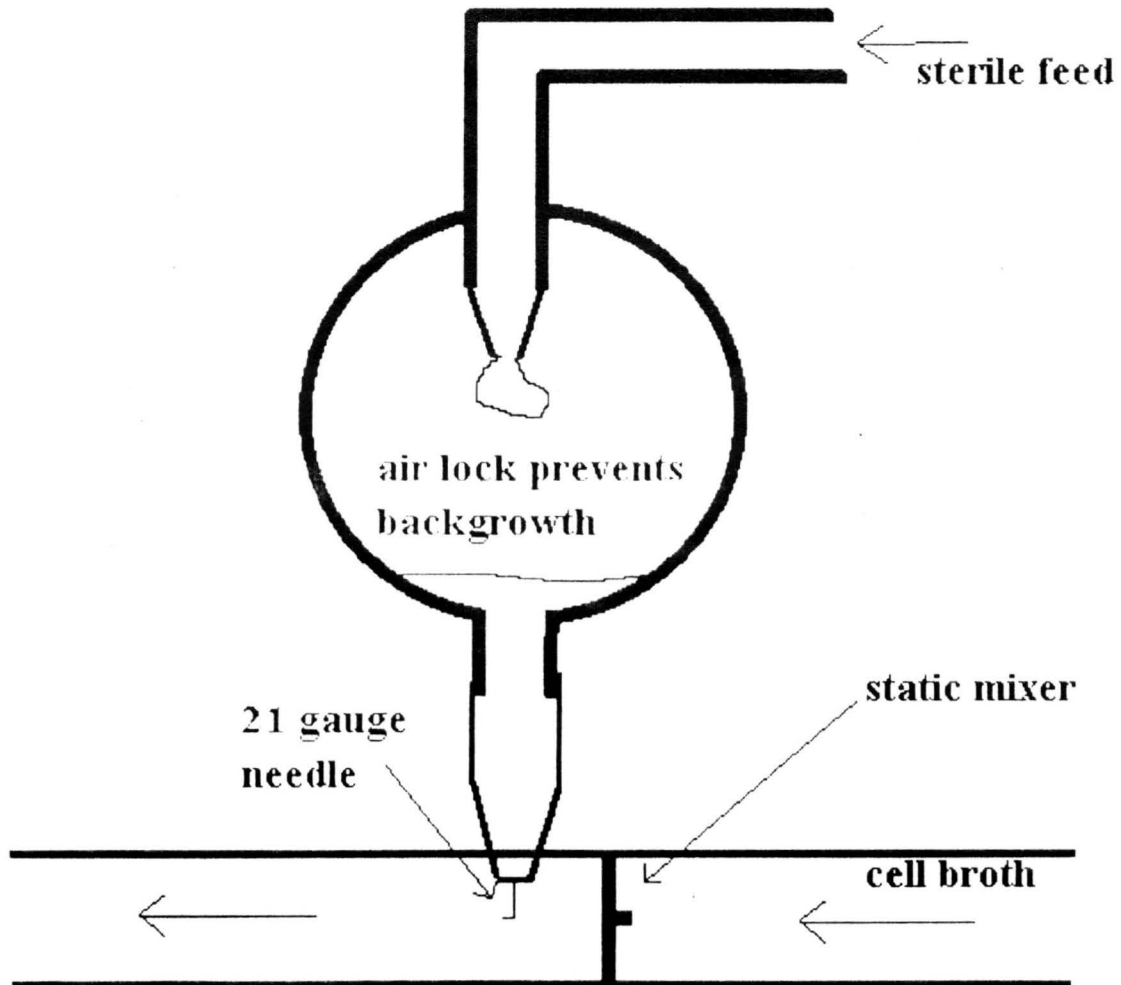


Figure 2.3 -- The feed bulb used to dampen pulses in the feed and prevent organisms growing back up the line to the feed tank.

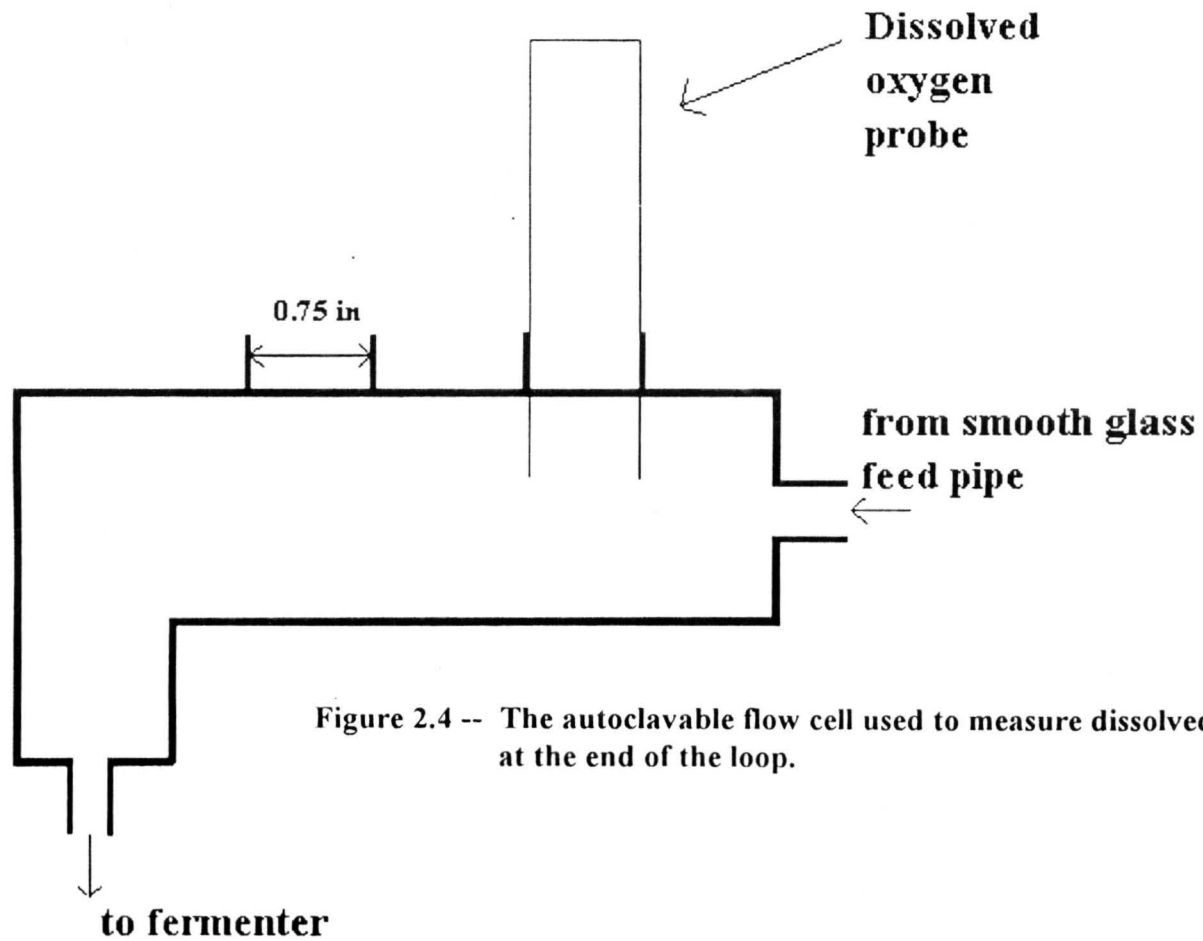


Figure 2.4 -- The autoclavable flow cell used to measure dissolved oxygen at the end of the loop.

### 2.1.2 System Characteristics

The primary vessel in this experiment was an Applikon 3 liter stirred tank bioreactor. The total culture volume was maintained at 1 liter by a constant effluent line. The volume of the entire loop was about 200 milliliters. The *S. cerevisiae* strain used in this experiment was ATCC 32167 and was grown on the medium given in Table 2.1.

An Applikon ADI 1030 Biocontroller was used to maintain system conditions of temperature = 30°C and pH = 3.10. Dissolved oxygen concentrations were also monitored by Ingold sterilizable dissolved oxygen electrodes at two locations in the system: 1) in the bulk of the stirred tank and, 2) at the end of the recirculation loop just before the culture broth returns to the stirred tank. Agitation was delivered by a 6-blade Rushton turbine at an RPM of 700. Total inlet gas flowrates were controlled with Cole-Parmer Co. rotameters (Serial # 046180) and held at a value of 2 vvm. Recirculation through the secondary vessel was held at a flowrate of 860 ml/min by a Masterflex peristaltic pump (Model No. 7523-00). Feed flow rates were controlled by a Watson-Marlow peristaltic pump (Model 101U/R).

The ATCC 32167 was maintained on slants and plates with a medium composing of 1% yeast extract, 2% peptone, 2% glucose, and 2% agar. Approximately 2 days of incubation at 30°C is required for colonies to form after which plates were stored under 4°C refrigeration. Multiple colonies are transferred to 250 ml baffled shake flasks containing 100 ml of the medium given in Table 2.1. Flasks are then incubated in a closed environment shaker where temperature is maintained at 30°C

**Table 2.1 -- Media composition**

<i>Component</i>	<i>Concentration (mg/l)</i>
CaCl <sub>2</sub>	755
CoCl <sub>2</sub> (6 H <sub>2</sub> O)	1.2
CuCl <sub>2</sub> (2 H <sub>2</sub> O)	41
FeCl <sub>3</sub> (6 H <sub>2</sub> O)	113
H <sub>3</sub> BO <sub>3</sub>	12
KH <sub>2</sub> PO <sub>4</sub>	6,530
KI	1.8
MgSO <sub>4</sub> (7 H <sub>2</sub> O)	1.5
MnSO <sub>4</sub> (H <sub>2</sub> O)	57
NaMoO <sub>4</sub> (2 H <sub>2</sub> O)	7.8
NH <sub>4</sub> Cl	10,700
ZnSO <sub>4</sub> (7 H <sub>2</sub> O)	66
citric acid (H <sub>2</sub> O)	115
EDTA	450
d-biotin	0.1
d-pantothenic acid (1/2 Ca)	100
i-inositol	200
thiamine (HCl)	20
pyridoxine (HCl)	27.6
nicotinic acid	20
Anitfoam 289 (Sigma)	0.05 ml/l
glucose	11.35 g/l

**YPD Agar:**

- 10 g/l yeast extract
- 20 g/l peptone
- 20 g/l glucose
- 20 g/l agar

and agitation at 250 RPM. Upon depletion of glucose, one of these flasks were used to inoculate the stirred tank/recirculation loop system. When the initial batch phase was complete, the system was operated at a fed-batch feed rate of 0.03 liters/hour for a few hours to achieve a high cell density. When cell density approached 5.00 grams/liter, the effluent pump was started to begin the continuous fermentation.

Samples of 10 ml were taken from the sample port and immediately placed in an ice bath to slow metabolic activity. Dry cell weights were determined by pipetting 5 ml of broth onto a pre-weighed 0.45 micron filter (Gelman Supor 450), rinsing with 10 ml distilled water, drying for 1 hour in a 65°C oven, and re-weighing. Part of the sample was also filtered and assayed for acetate, glycerol, glucose and ethanol concentrations on a BioRad Aminex-based HPLC column HPX-87C.

Steady-state in continuous experiments was assumed when biomass and ethanol (if present) concentrations were constant for at least 5 residence times since the last change in operating conditions. These steady states were maintained for periods of 3-8 residence times. Steady state values were determined from an average of the samples taken during this time.

#### *Cytochrome measurements*

Cytochrome measurements were made using the method of Borralho et al. (1989). Cell samples were collected from the effluent line, centrifuged and washed two times with distilled water, and concentrated to a cell density of 25 grams dry cell mass/ liter. An absorbance spectrum of the sample was taken on a Cary 3 double beam spectrophotometer (Varian Analytical Instruments, Sugar Land, TX) using

**2% lowfat milk diluted 1:5 with distilled water as a reference. About 5 milligrams of sodium hydrosulfite was added to the sample just before scanning in order to reduce the iron groups within the cytochromes.**

**The cytochrome spectra were quantitatively analyzed using Peakfit software (Jandel Scientific, San Rafael, CA). First the abscissa is inverted to give a spectrum of increasing wavenumbers. Two separate analyses are performed: one for the cytochrome reductase compound whose spectra's peaks lie at approximately 550 and 560 nm, and secondly on the cytochrome oxidase group whose absorbance maximum occurs at 600 nm. Peak areas were assumed proportional to the amount of each cytochrome present and served as an indicator of the metabolic pathways in use. Qualitative examination of the spectra shown in figure 1.5 gives insight to the metabolic pathway the organism is using. A derepressed culture whose major metabolic route is the oxidation of glucose will have significantly larger peaks than a repressed culture whose oxidative pathways enzymes have become saturated with substrate. The resulting fermentative metabolism does not require the use of the cytochromes in the electron transport chain and as the new steady state is reached, the diminishing of dull orange tint within concentrated cytochrome samples is visible to the naked eye. Interestingly, a third metabolic mode can be distinguished with the use of these cytochrome assays. A dissolved oxygen limited derepressed culture still contains a significant cytochrome oxidase peak, despite the reduction in biomass yield and the increase in ethanol yield. This suggests that cytochrome**

measurements can help distinguish between low yields caused by either low dissolved oxygen concentrations or glucose repression.

### 2.1.3 Mixing and Feeding Strategies

Two types of feeding and mixing strategies were used to distinguish between the short-term and long-term nutrient dispersal effects on the culture. The first strategy which focuses on the short-term effects is patterned after the flip-flop experiments of Dunlop and Ye (1990, see figure 1.2). The term flip-flop refers to the changing of the mixing conditions at a given dilution rate. The idea here is to elicit a biological response by merely altering the hydrodynamic environment at the feed site, thus changing the sizes of regions within the system which are substrate limited or repressed. The second feeding/mixing strategy focuses on the longer term effects, those which relate to culture history and adaptation. This design follows the one used by Fowler and Dunlop (1989, see figure 1.1), whereby the mixing intensity at the feed site is held constant while a set of points relating steady state biomass yield to dilution rate is collected. After the first curve is generated, the dilution rate is reduced to its original low value, the mixing intensity is instantly changed by the sliding of the static mixer, and the data for another yield versus dilution rate curve is collected. This type of feeding/mixing regimen will here on after be referred to as a CHE (Culture History Effect) type experiment.

## **2.2 Turbulence Quantification at the Feed Site**

### **2.2.1 Laser Doppler Velocimetry**

#### **2.2.1.a. General Description**

The TSI laser Doppler velocimeter generates a 750 milliwatt Ion Laser Technology argon ion laser beam. This beam is directed into TSI's model 9201 beam separator, where it is split into three different wavelengths of 465, 445, and 420 nanometers, corresponding to green, blue, and violet colors in the visible spectrum, respectively. Because this system is two dimensional, the pair of violet beams which gives the data in the third dimension is not used in any of these experiments. The intensity of each of these color beams is divided into two beams, one of which is passed through a Bragg cell and subsequently shifted 50 MHz. This phase shift is what generates the Doppler shift and fringe pattern which gets scattered. These divided beams are passed through individual fiber optic cables to a probe which directs the beams to a single point about 12.5 centimeters in front of the probe. Figure 2.5 contains a schematic of the two dimensional TSI LDV system.

The point where the beams intersect is known as the 'measuring volume', and has an ellipsoid shape with a major axis measuring 1.56 millimeters in length and a minor axis or diameter of 120 microns. In the measuring volume, each beam pair creates an interference pattern or Doppler shift because they are out of phase. The resulting fringe pattern has spacing of 4.888 microns for the green beam pair and 4.644 microns for the blue beams. The scattered light, including the Doppler frequencies and background light noise are both reflected back by a retroreflector to

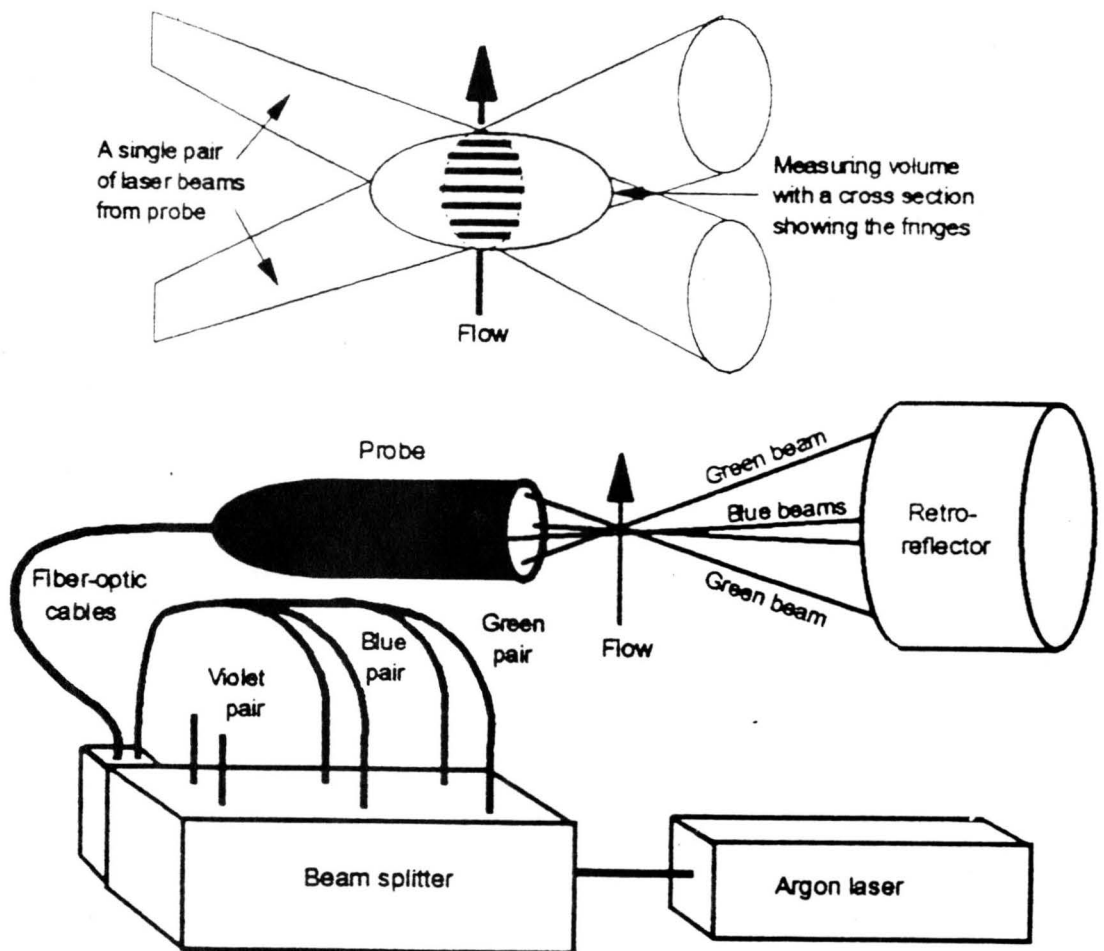


Figure 2.5 -- The two dimensional TSI LDV system.

the probe, through another fiber optic cable to a photomultiplier tube. The photomultiplier backshifts the electronic signals from the 50 MHz and fed into a TSI Intelligent Flow Analyzer (IFA) Model 550 signal analyzer where the Doppler signals are distinguished from the noise.

A valid velocity measurement occurred when ten consistent frequencies were detected in a periodic manner corresponding to a particle passing through the ten fringes with a consistent velocity. TSI's Flow INformation Display (FIND) software Version 2.1 was used to monitor the velocity measurements and time series of velocities were saved.

#### 2.2.1.b Specifications of Setup for Microscale Quantification of Static Mixer

A Plexiglas tube with diameter 1.07 cm and length 90 cm was used to house the static mixer. A 2 inch square Plexiglas window of length 50 cm was encased around the section of the tube to be measured. This window facilitates two purposes: first, the flat surface is necessary to prevent the beams from diffracting before they meet, thus never forming a measuring volume, and, secondly, the window holds a solution with a refractive index similar to the material the from which the vessel is made. Els, et al. (1985) and Yeh, et al. (1983) show how this solution also helps minimize the light refraction and ensures better data rates. Plexiglas or acrylic has a refractive index (RI) of 1.53 (CRC Handbook of Chemistry and Physics) and a solution of 80% sucrose was poured into the tube's window to match this RI. This differs from the glass tube (refractive index = 1.60) used by Beyerinck (1991) where the highly toxic methyl benzoate was needed to fill the window. Filtered double

distilled water seeded with 0.01% TSI metallic coated particles was used as the flow medium. These metallic coated particles have an average diameter of 2.6 microns and are responsible for the light scattering in the measuring volume which gives the Doppler signals and the individual velocity measurements. The seeded water was recirculated through the pipe from a 3 liter reservoir by a Masterflex pump (Model No. 7523-00) through size 18 tubing at a flowrate of 860 ml/min. The use of a peristaltic pump necessitates the presence of a 2 inch round bottomed pulse dampener upstream of the pipe entrance. When the pulse dampener is not present, the LDV is easily capable of detecting pulsation caused by this type of pump, which produces results which are not valuable for most practical calculations. The Reynolds number of the pipe flow was 2000; the Reynolds number based on the mixer's diameter was 750, which is high enough for the eddies shed in the wake to contain turbulent fluid, according to Roshko (1954). The same static mixer was used here as in the fermentation experiments described in Section 2.1.

The probe and the corner cube retroreflector were mounted in line with each other to allow axial movement of them together while ensuring proper reflection. Together, they were mounted on two dimensional platform whose position was quantifiable by micrometer spinners. This allowed the measurement of two orthogonal velocity components each at a 45 degree angle to the axis of the pipe and normal to its radius. The center of the pipe was located using the well known fact that, when pipe flow is laminar, the center of the pipe contains the maximum velocity in the pipe and is equal to exactly twice the average velocity over the pipe's

cross section. The average velocity was set at by adjusting the total flowrate to be 860 ml/min and dividing by the pipe's cross sectional area of 0.90 cm<sup>2</sup>. The position of the measuring volume was then adjusted until a velocity measurement as close to 32 cm/s was obtained; when an agreement of less than 1% between measured and calculated values, this position was assumed to be the pipe center.

The two extremes of mixing used in the fermentation experiments are ones of greatest concern here. Specifically, determination of turbulence intensity within the static mixer's wake at positions 1 cm and 20 cm downstream of it. The information calculated by the FIND software includes: the autocorrelation function, the turbulence power spectrum, instantaneous velocity histograms, the first four moments of turbulence, Reynolds' stresses, and intermittency factors.

#### 2.2.2. Bourne Dye Reaction

Fast, complex chemical reactions are another excellent means of quantifying micromixing at the feed site. Because they are fast, the reaction volume is actually confined to the region where the fluids are introduced to each other, therefore the bulk mixing characteristics of the system are not important. As the reaction products are distributed throughout the system by bulk circulation, the reaction zone is kept fresh with reactants; the complexity of these reactions makes them particularly sensitive to the mixing intensity, leading to different product distributions for different levels of mixing. Such a reaction was developed by Bourne and coworkers (1981) to study turbulence intensity within bioreactors.

The reaction consists of two competitive, consecutive chemical reactions:

$A + B \rightarrow R$  and  $R + B \rightarrow S$ , where the first order reaction constant of the first reaction is much greater than the second, ( $k_1 \gg k_2$ ). In these equations, species A is a 0.0055 millimolar solution of 1-naphthol dissolved in a carbonate solution buffered to pH = 10.1, species B represents a 0.0055 millimolar solution of diazotized sulfanilic acid (See Appendix A for recipes), and  $k_1/k_2 \sim 2500$ , which ensures the first reaction is diffusion controlled while the second is kinetically controlled. R and S are the monazo (ortho- or para- isomer) and diazo dye products, respectively. When equimolar quantities of solution B is added in semi-batch fashion to the vessel containing solution A, the relative amounts of R and S formed depend upon the energy dissipation rate at the injection port. As turbulence intensity is increased, the relative amount of S formed is decreased. After the entire solution of B is added to the reactor, a sample is spectrophotometrically analyzed using the Lambert-Beer law and extinction coefficients for the dye products. Concentrations were determined by doing a third order multiple linear regression on Lotus 1-2-3 spreadsheet (Lotus Development Corporation, 1993).

A product yield is defined as  $X_i = 2C_S / 2C_S + C_R$ , and this value is plugged into a model developed by Baldyga and Bourne (1989), called the E model, abbreviating engulfment. This model is a simplification of a previous model published by Baldyga and Bourne (1984) known as the EDD model, abbreviating engulfment-distortion- and diffusion and relates the engulfment rate to the local rate of energy dissipation.

The simplified E model may be used in place of the EDD model when two conditions are met: first, the Schmidt number of the reacting solutions must be much less than 4000, and, secondly, the dimensionless ratio of reactant concentrations for species A to B must be much less than 1. In these experiments, the first condition is met with the Schmidt number for these reactants in aqueous solution is approximately 1000. The second condition is met by the semi-batch feed approach, where the concentration of B in the feed solution is 10 times greater than the bulk concentration of A within the bioreactor. The E model requires inputting a value for the Kolmogorov microscale and gives outputs for local power input,  $X_s$ ,  $Da$ ,  $Da_{bar}$ , and the Strouhal number, which is the reciprocal of vortex spacing expressed in the number of obstacle diameters.

Semi-batch operation was carried out as followed: the reactor was initially filled with  $5.78 \times 10^{-4}$  mol of 1-naphthol in 1 liter double distilled water. This solution is buffered with 0.11 mol each  $Na_2CO_3$  and  $NaHCO_3$ . This buffering holds the pH constant at 10.1 and the ionic strength constant at 0.440 mol/l throughout the experiment.  $5.50 \times 10^{-3}$  moles of diazotized sulfanilic acid was dissolved in 100 ml ddH<sub>2</sub>O. This solution was fed into the loop via the same feed pump/bulb/needle complex used in the fermentation experiments. The feeding took place over a  $24 \pm 1$  minute period. If dissolved oxygen is present in any concentration within the solutions, side products other than R or S are formed; therefore, both solutions were degassed with nitrogen for 30 minutes prior to and throughout the feeding; nitrogen

flowrate was held constant at 2 liters/min by the same Cole-Parmer rotameter.

Temperature was held constant at  $25 \pm 0.5$  °C by the Applikon Biocontroller.

After each injection, the product solution was diluted to standard conditions as defined by Wenger (1992) of ionic strength = 0.0400 mol/l. The absorbance of the diluted product mixture was then recorded as a function of wavelength from 700 nm to 400 nm by the Cary 3 spectrophotometer. Absorbencies were plugged into the Lambert-Beer equation and product concentrations regressed from this equation.

The analysis was checked by using a mass balance on B. The percent closure, M, is given by the equation:  $M = (2C_s + C_{o-R} + C_{p-R}) * 5 (10^5) * 100$ .

### 2.2.3 Photography of Dye Dispersion in the Feed Zone

The renowned mathematician and philosopher, Euclid, once stated that the two best methods for proving a hypothesis are: 1) the use of numbers and mathematics, and 2) the use of pictures. This idea was the motivation to have photographs taken which highlight the differences in the two mixing extremes used in these experiments. The recirculating loop with degasser and pulse dampener in-line was set up as usual and the same Masterflex pump was used to generate a flow of tap water at 860 ml/min. A  $5.0 * 10^{-3}$  molar solution of para-R was used as the dye tracer and fed at 300 ml/hr (equivalent to  $D = 0.30 \text{ hr}^{-1}$ ) through the mixing bulb and hypodermic needle. Observations were also made as to how the dye dispersed when the water was withdrawn from the bottom of an aerated stirred fermenter.

## CHAPTER III: Preliminary Fermentation Results

### *Introduction*

The results of this thesis will be divided into two chapters: the first will describe preliminary results and the second will contain more definitive results. The criteria for distinguishing between the results is whether or not gas bubbles were effectively separated before the feed zone. Microscale quantification with azo dyes (See Results in Section 4.3) shows that gas has to be completely and reliably separated before the feed zone to avoid disrupting the flow conditions. All results in Chapter 3 did not have the cyclone separator before the feed zone; smallest turbulent eddy diameters for this case are estimated at 65 and 127 microns for the well-mixed and poorly-mixed conditions, respectively.

All fermentation experiments were conducted with the common objective of attempting to produce a biological response (change in steady state biomass yield and other metabolic indicators) in a continuous culture by manipulating one specific physical parameter (the intensity of micromixing at the feed site). However, each of the separate experiments described here investigated a different set of given physical conditions in hopes of gaining some insight on what factors are crucial in anticipating the system's behavior. Therefore, the results and discussion of each experiment will be preceded by a short section explaining the feeding/mixing

strategy used, the gas mixture sparged into the system, the purpose of various pieces of hardware added as the system evolved, and the objective(s) of that particular experiment.

### 3.1 Flip-Flop Experiment #1 (FF1)

#### *Preamble*

This experiment was conducted with the intention of reproducing the flip-flop mixing results reported by Dunlop and Ye (1990). Specifically, using a strategy whereby an increase in steady state biomass yield is expected when the feed site's mixing intensity is increased at a constant dilution rate. They report this effect due to smaller and fewer regions within the reactor where cells are carbon limited and therefore not using their full oxidative capacity. This system was aerated with 2 vvm of air and the dissolved oxygen level was monitored in the stirred tank only. Cell broth was recirculated to and from the stirred tank by a peristaltic pump with only a pulse dampener in-line to reduce the pressure fluctuations created by the pump.

Flip-flop experiments were conducted by establishing a steady state condition at a given dilution rate and mixing intensity. This steady state was maintained for at least 2-3 residence times, at which point the static mixer was slid to its opposite position. Culture parameters, dry cell weight, effluent glucose and ethanol concentrations, and off-gas composition were observed for another 2-3 residence times after the change.

## ***Results***

Figures 3.1 through 3.3 show the results of experiment FF1. As the figures indicate, the steady state outputs did not significantly vary with the feed site mixing intensity. Oxidative growth behavior was displayed at both mixing extremes up to a dilution rate of  $0.28 \text{ hr}^{-1}$ . Upon increasing the dilution rate to  $0.32 \text{ hr}^{-1}$ , the culture switched to a fermentative metabolism and both mixing intensities produced similar biomass and ethanol yields expected for that range.

## ***Discussion***

The results from this experiment were discouraging. We did not see similar effects as those published by Dunlop and Ye (1990), namely, short term changes in biomass yield associated with varying mixing intensities at the feed site.

Among the possible reasons brainstormed for the lack of a response in this experimental design was the difference in dissolved oxygen levels which arise from the disparate geometries of the reactor used here and the one used in Dunlop and Ye's system. Configuration of the sparging and stirring elements within a reactor as well as vessel dimensions are significant factors in determining the system's mass transfer capabilities. Because dissolved oxygen levels are known to play a critical role in deciding the metabolism in a *S. cerevisiae* continuous culture (Furakawa, 1983), and because Dunlop and Ye failed to isolate their mixing effects from this important factor, it was reasoned that the lack of a response in FF1 may have been due to a disparity in dissolved oxygen levels. It was decided a better effort should be made to keep dissolved oxygen at non-limiting levels for the next experiment.

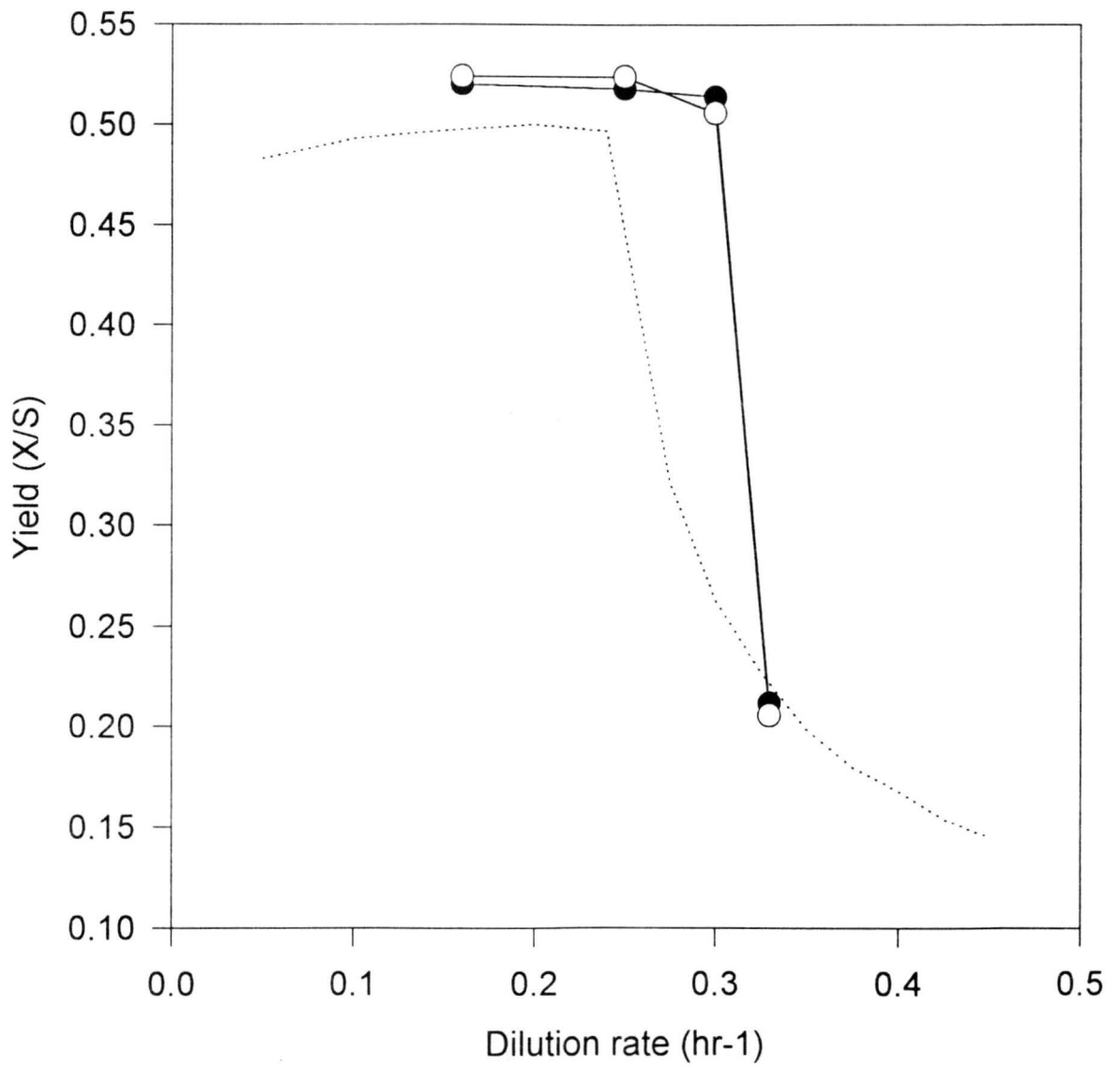


**Figure 3.1** Yield vs Dilution rate -- FF1

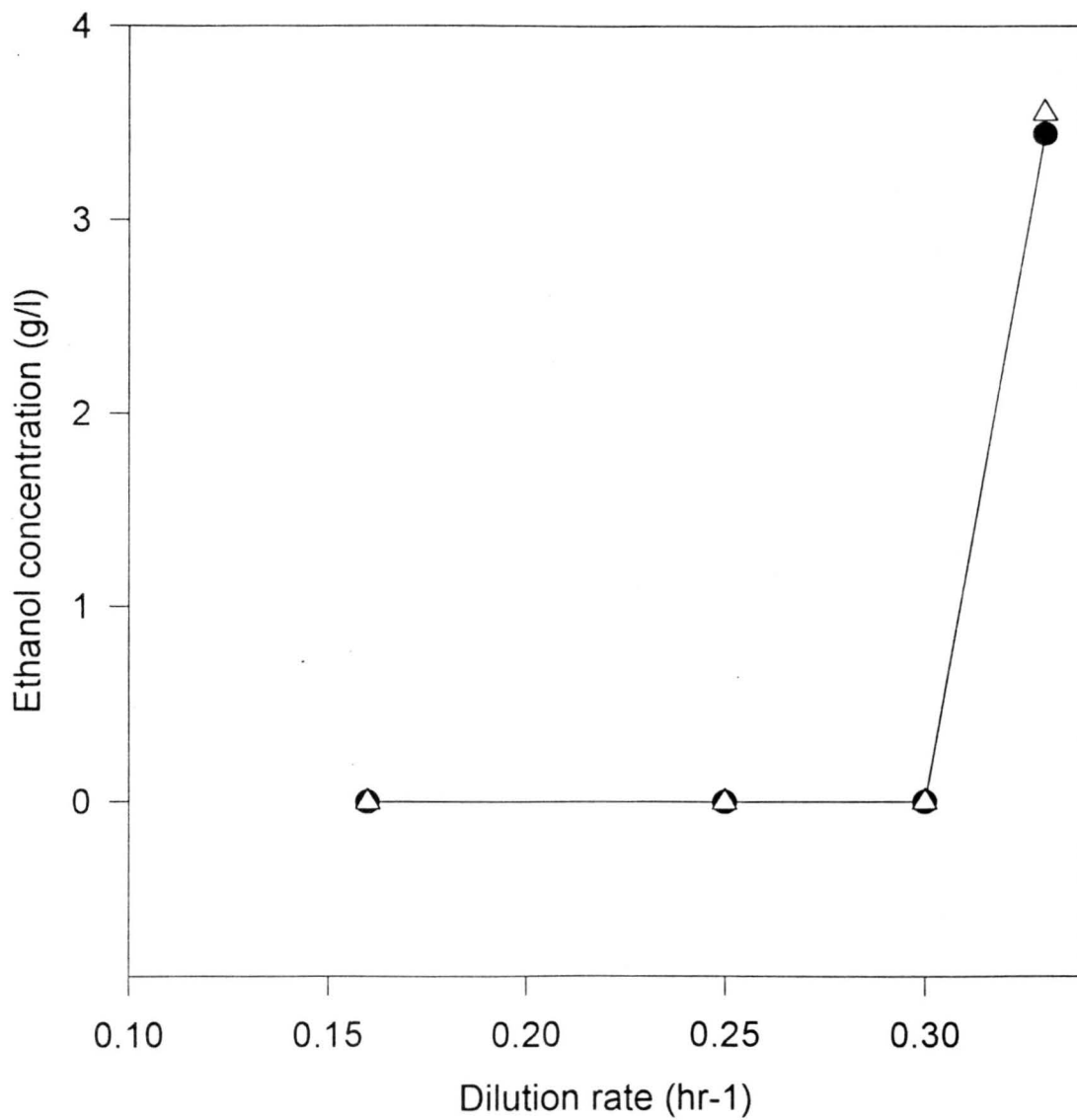


**Figure 3.2** Ethanol vs. Dilution rate -- FF1

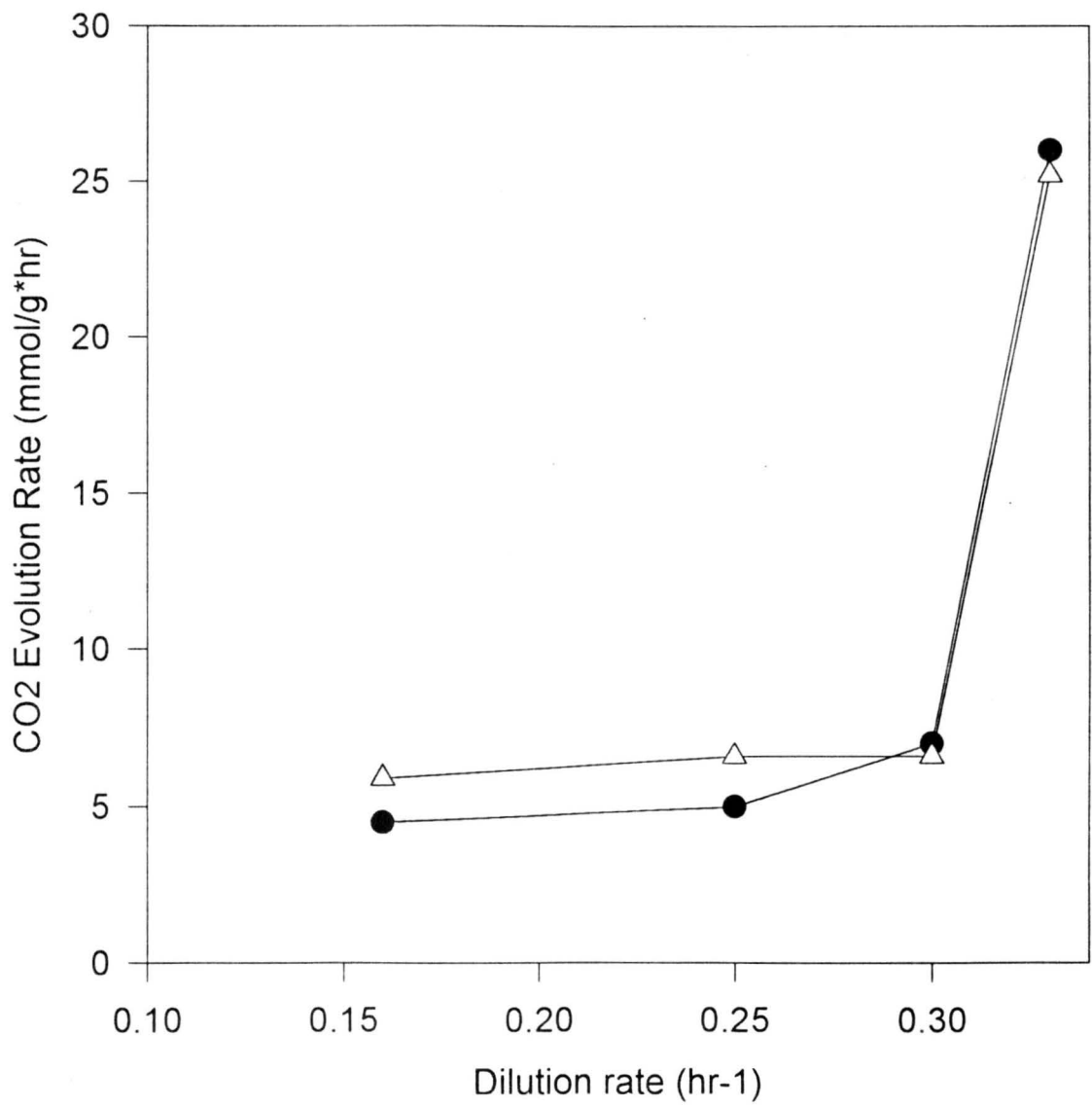


**Figure 3.3** Off Gas Data -- FF1

The difference in critical dilution rate of  $0.28 \text{ hr}^{-1}$  in FF1 and  $0.25 \text{ hr}^{-1}$  in the von Meyenberg reference data is reportedly due to the difference in substrate feed concentrations, 11.3 g/l vs. 30.0 g/l. This phenomena is discussed in von Meyenberg's thesis (1969).

### 3.2 Flip-Flop Experiment #2 (FF2)

#### *Preamble*

Again a continuous culture of *S. cerevisiae* was set up with the anticipation of seeing differences in biomass yield when feeding and mixing are flip-flopped. As insufficient monitoring of dissolved oxygen levels was pin pointed as a possible cause for the failure to see a response in the previous experiment, two alterations were made from conditions described in FF1. First, in order to properly monitor the dissolved oxygen throughout the system, an autoclavable stainless steel flow cell was constructed to house two 0.75 inch diameter probes (Figure 2.5). One site holds another Ingold Model 80 dissolved oxygen probe and the other, which was designed to hold a NADH fluorescence probe in future experiments, was plugged with a stainless steel rod. This flow cell was placed just after the end of the feed loop and just before re-entry to the stirred tank; this position allows the dissolved oxygen to be measured at the most oxygen deprived location within the system, at the end of the plug flow loop.

Secondly, the Applikon Biocontroller Model AD-1030 was programmed to sparge pure oxygen gas into the tank whenever the dissolved oxygen concentration at the end of the loop dropped to a repressive level. Several authors have reported

anaerobic behavior of *S. cerevisiae* cultures when the dissolved oxygen concentration falls below 1 milligram per liter (about 15% saturation at 30°C and 5000 feet elevation); this value was used as the control setpoint.

### *Results*

Figures 3.4, 3.5, and 3.6 show the results of experiment FF2. Again we see that differences in mixing intensity within the feed zone did not significantly effect the steady state outputs of the system. Oxidative behavior was displayed up to a dilution rate of  $0.32 \text{ hr}^{-1}$  and the culture became glucose repressed upon increasing the dilution rate to the  $0.35 - 0.36 \text{ hr}^{-1}$  domain. This critical dilution rate of  $0.32 \text{ hr}^{-1}$  is significantly higher than the value of  $0.25 \text{ hr}^{-1}$  reported by von Meyenberg (1969).

Figure 3.7 contains a graph tracing the dissolved oxygen concentration in the stirred tank and at the loop's end against time. When the mixing intensity was flip-flopped at  $t=140$  hours, the concentration of oxygen dissolved at the loop's end decreases while the dissolved oxygen level in the stirred tank remained constant.

### *Discussion*

The suspicion that inadequate oxygen transfer may have been responsible for the lack of response in FF1 did not prove to be insightful; as the results of this fermentation clearly display, flip-flopping the mixing intensity does not effect how carbon is converted at any of the dilution rates studied. It is worth noting the range of dilution rates studies here is wider than the range used by Dunlop and Ye (1990) and does include the value of  $0.16 \text{ hr}^{-1}$  where their reports indicate the most drastic sensitivity to mixing intensity. These results along with other unsuccessful attempts

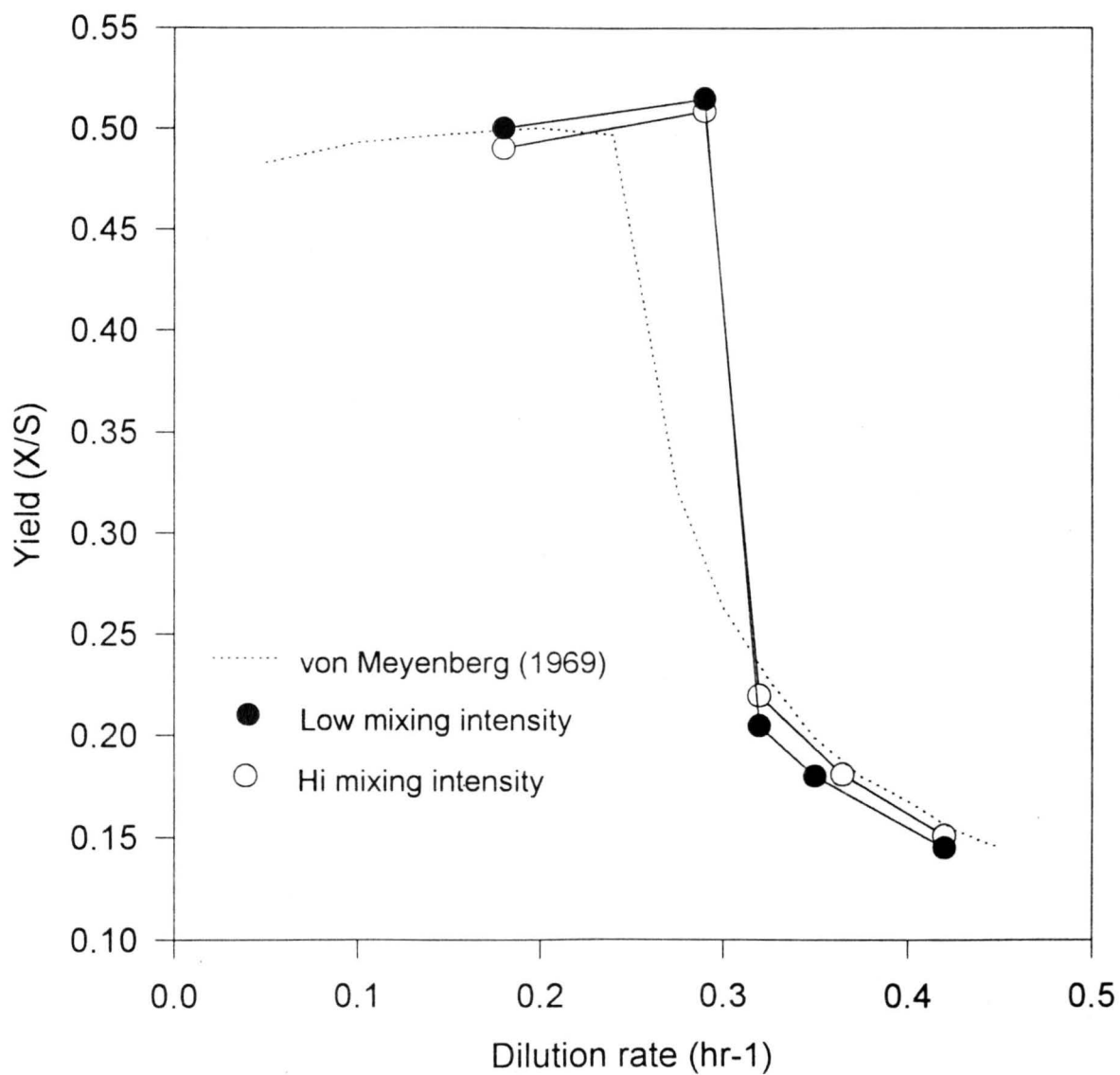


**Figure 3.4** Yield vs Dilution rate -- FF2

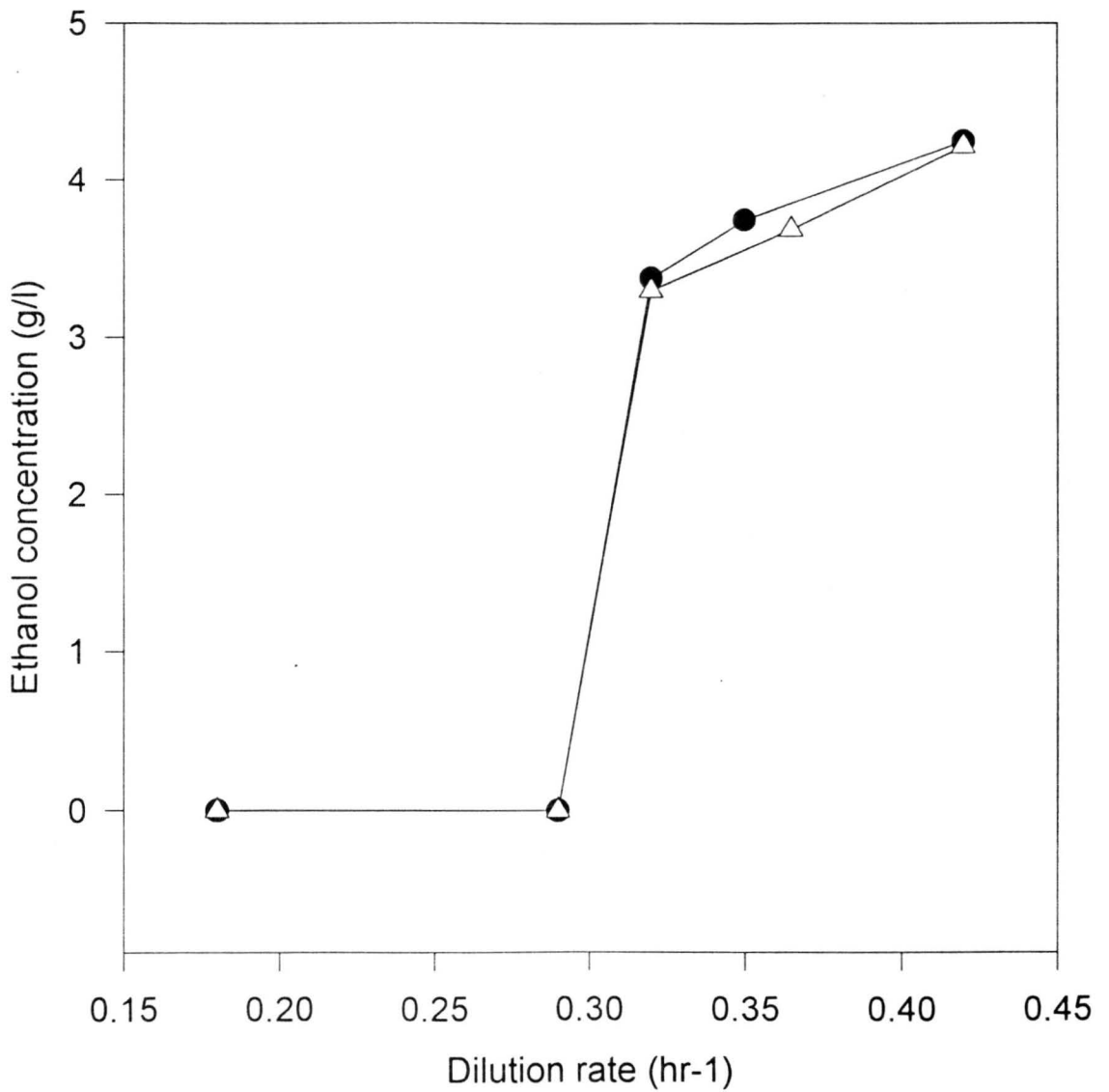


**Figure 3.5** Ethanol vs Dilution rate -- FF2

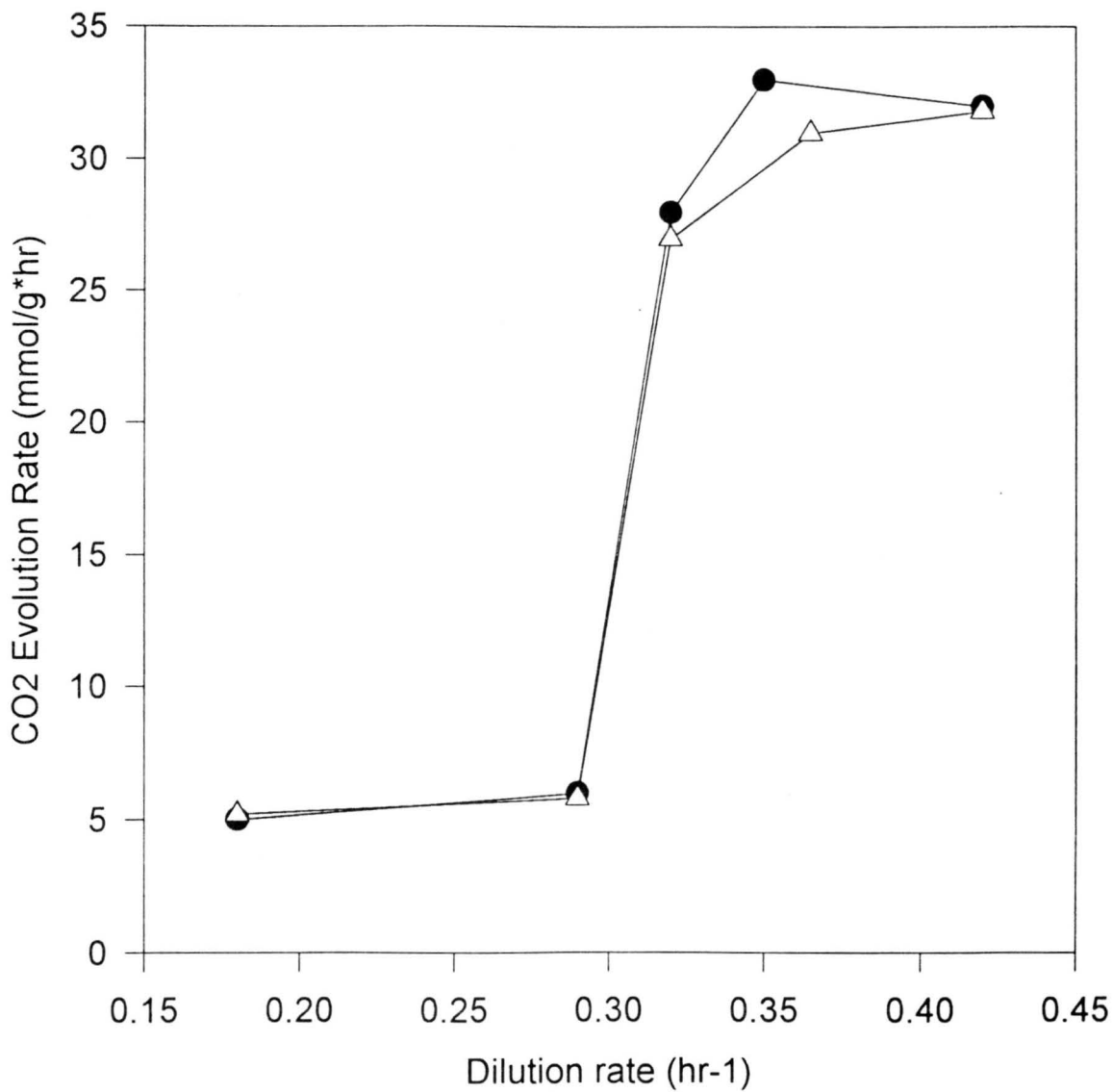


**Figure 3.6** Off Gas Data -- FF2

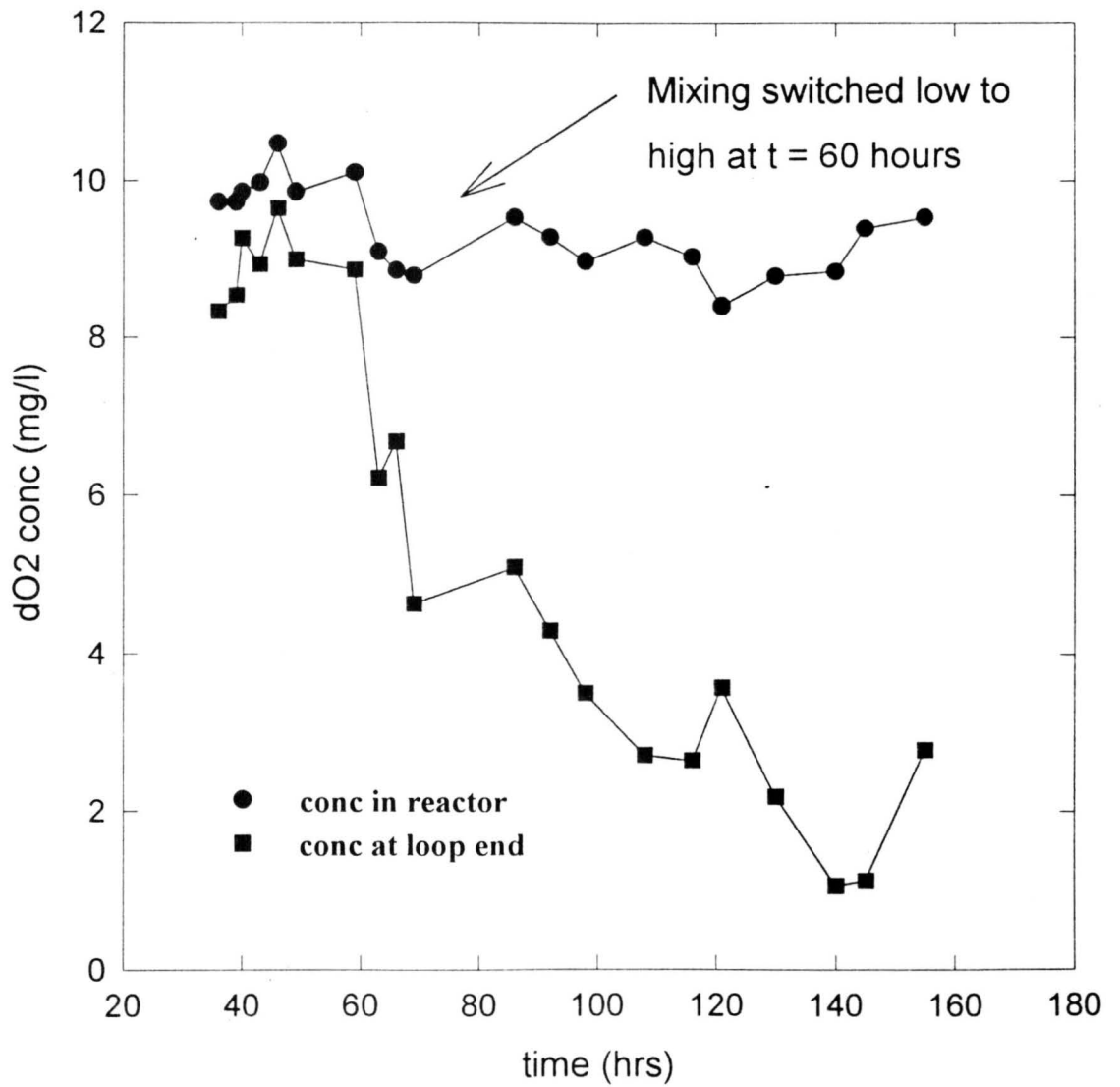


**Figure 3.7** Dissolved oxygen concentration vs Time

to reproduce this phenomena by Wenger (1994) suggest that micromixing's role in fermentation needed re-examining.

The results in Figure 3.7 are somewhat encouraging. After having achieved a new steady state condition at a dilution rate of  $0.25 \text{ hr}^{-1}$ , the mixing level was increased by sliding the mixer to the position 1 cm upstream of the feed needle. What occurred is the first evidence of a system response indebted to the degree of nutrient dispersion in the feed region. The level of dissolved oxygen at the end of the loop began to drop from 80% saturation and finally reached a new steady state value of 30% saturation about 6 hours or 1.5 residence times later.

A hypothesis for what happened in this figure follows: by increasing the feed zone mixing and therefore the availability of glucose to the cells, the amount of substrate consumed oxidatively, coupled with the mitochondria's need for more oxygen to metabolize the glucose, causes the amount of dissolved oxygen to slowly decrease in the plug flow feed region where consumed oxygen cannot be replaced. Also noteworthy is that the dissolved oxygen concentration in the fermenter remained constant at 90% saturation throughout this time range. It is reasonable that because the new steady state value of dissolved oxygen in the loop never dropped to a repressive level, the overall oxygen requirement for the system was not effected enough to alter the steady state biomass yield or fermentor dissolved oxygen concentration.

More evidence of a relation between the oxygen consumption and the biomass yield for the system as a whole exists if one compares the critical dilution rates in

experiments FF1 and FF2. The oxygen supplemented FF2 achieved derepressed growth up to  $D = 0.32 \text{ hr}^{-1}$  whereas the un-supplemented FF1 became glucose repressed after increasing the feed rate from  $D = 0.28 \text{ hr}^{-1}$ . The maintaining of oxygen levels above non-repressive regions allowed the culture to grow oxidatively up to higher dilution rate and therefore increased the biomass productivity of the system.

Given that: (1) Increased nutrient dispersion in this system may lead to lower values of dissolved oxygen in the loop and, (2) Maintenance of dissolved oxygen levels above non-repressive levels can help increase the critical dilution rate of the system, any micromixing effect seen would be in the nature of that reported by Fowler and Dunlop (1989). Specifically, lower steady state biomass yields as a result of repressive dissolved oxygen concentrations at higher mixing intensities. Therefore, we decided to focus our efforts on reproducing and improving upon their results.

As it is known that the extent of glucose repression is also effected by the dissolved oxygen concentration, levels of respiratory enzymes cytochrome oxidase and cytochrome reductase will also be measured in the next experiment. This may provide insight as to the mechanism by which the glucose effect represses the culture.

### 3.3 Culture History Effect Experiment #1 (CHE1)

#### *Preamble*

The major difference between a flip-flop type experiment and a culture history effect (CHE) type experiment lies in the feeding/mixing schedule used during the fermentation. In a CHE experiment, an entire yield versus dilution rate curve is collected at a single mixing extreme. After the last steady state is established at one extreme, the dilution rate is returned to its original position and the static mixer is slid to its other extreme. Another yield versus dilution rate curve is then obtained at the opposite extreme.

The last experiment indicated that this type of feeding/mixing schedule may be a better approach for obtaining the desired results. As we are trying to reproduce Fowler and Dunlop's results (1989), the culture conditions we used matched theirs with only a few exceptions. The system they used did not monitor dissolved oxygen levels in the loop. This may have been part of the reason they incorrectly assumed that oxygen would not reach repressive levels in their loop; nevertheless, it was decided that air only would be sparged into the tank as they has studied. The gas flowrate of 8 vvm used in their method was decreased to a more appropriate 2 vvm, as this flowrate is sufficient to keep stirred tank dissolved oxygen levels above the repressive threshold. All other system hardware remained identical to that described in experiment FF2.

## *Results*

Figures 3.8 through 3.12 contain the important results from experiment CHE1. Figure 3.8 shows the yield versus dilution rate curves for CHE1 and shows how the higher degree of nutrient dispersion created slightly lower steady state biomass yields than did the lesser dispersed feed curve. Figure 3.9 shows how this disparity in yields translates to the overall biomass productivity of the bioreactor; Figure 3.10 shows that the carbon which was not converted to biomass was instead fermented to ethanol. Off-gas concentrations, which are not reported here, were statistically similar in both mixing cases. In addition to differences in steady state biomass and ethanol yields, figure 3.11 shows that disparities exist in steady state dissolved oxygen levels as well. Figure 3.12 shows a normalized level of the electron transport chain enzymes, cytochrome oxidase and cytochrome reductase, at the different mixing states.

## *Discussion*

The disparity in yields in this experiment, albeit small, is still encouraging. The yields when the feed is more dispersed are 4-8% lower than when the feed is less dispersed. It translates to increased biomass productivity at all dilution rates, as can be seen in figure 3.9. In fact, three dilution rates in the poor mixed curve, 0.249, 0.283, and 0.323  $\text{hr}^{-1}$ , all have higher productivities than the optimum production feed rate, 0.328  $\text{hr}^{-1}$ , for the well mixed curve. The optimum production feed rate for the poor mixed curve is 0.283  $\text{hr}^{-1}$  and corresponds to a productivity of 1.31 grams of dry biomass per liter per hour; this is a 4 percent improvement over the

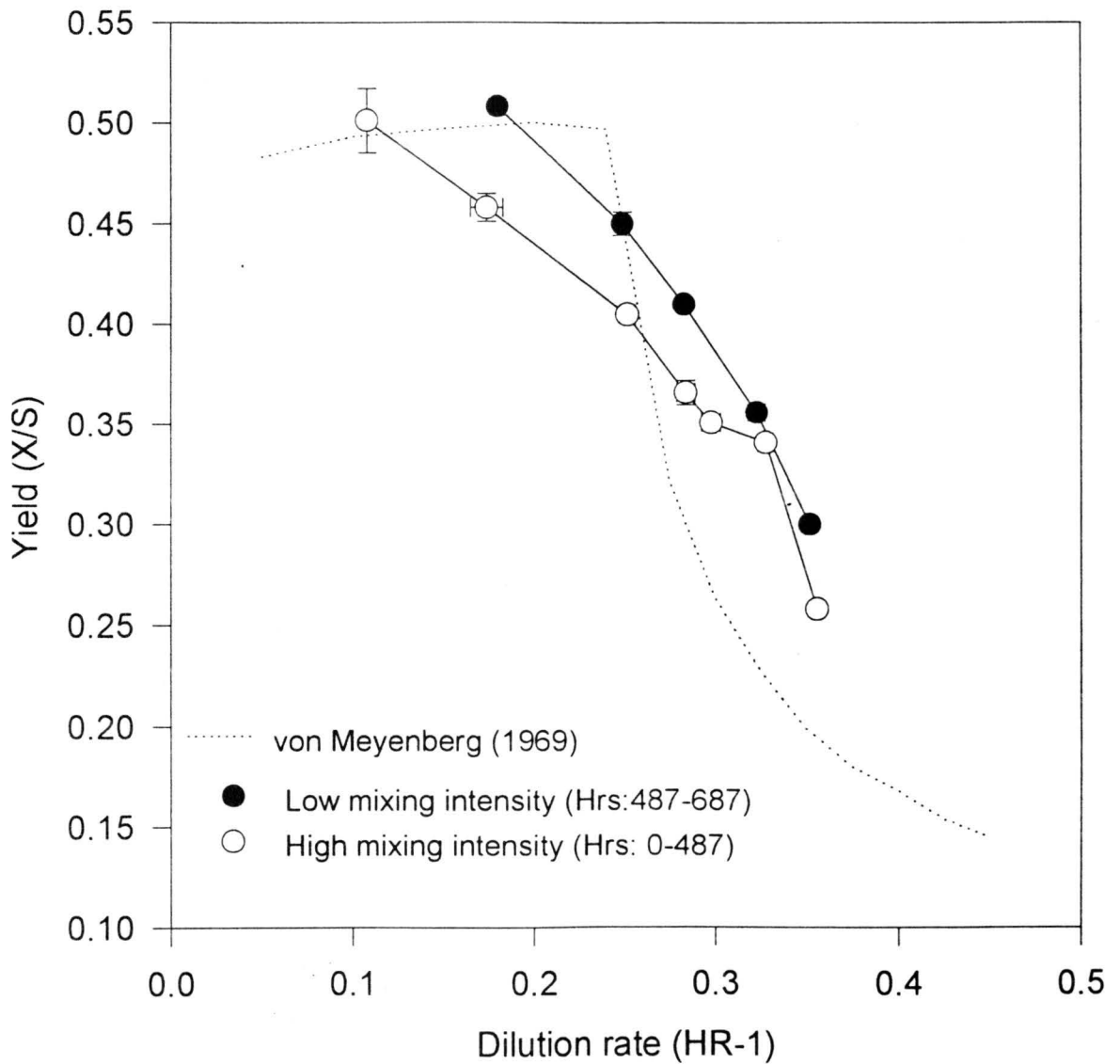


**Figure 3.8** Yield vs Dilution rate -- CHE1

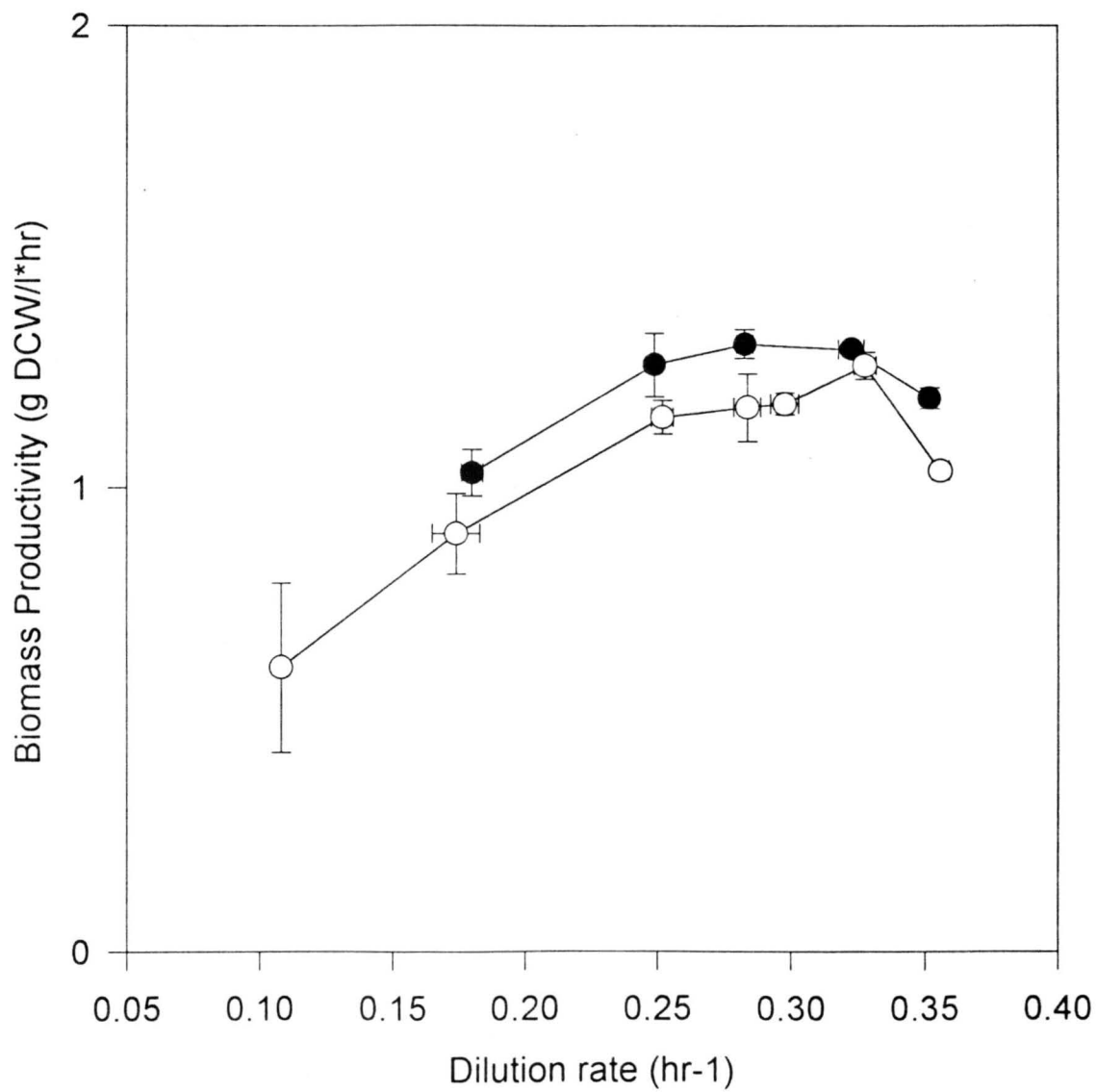


**Figure 3.9** Productivity vs Dilution rate -- CHE1

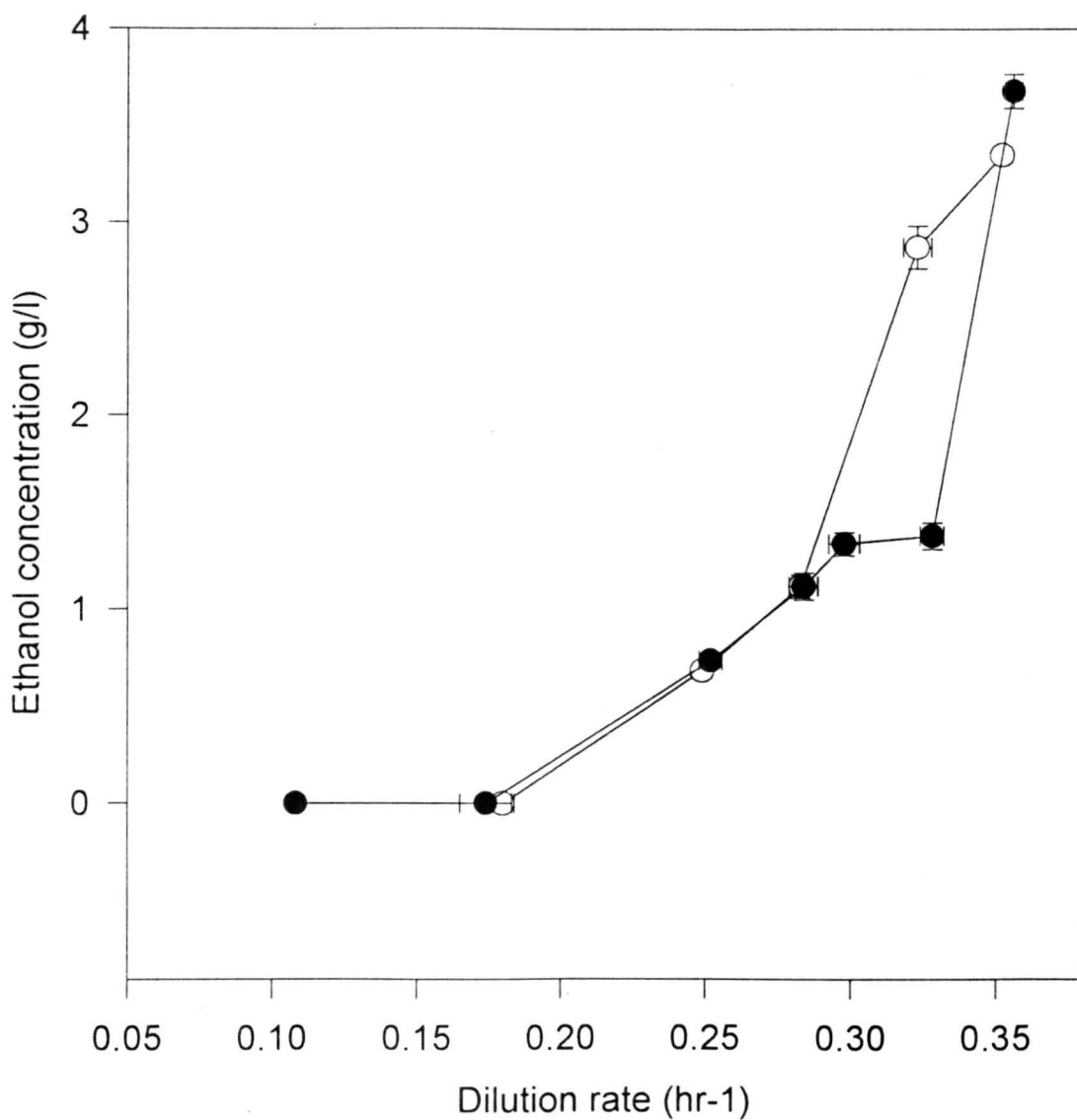


**Figure 3.10**

Ethanol concentration vs Dilution rate -- CHE1

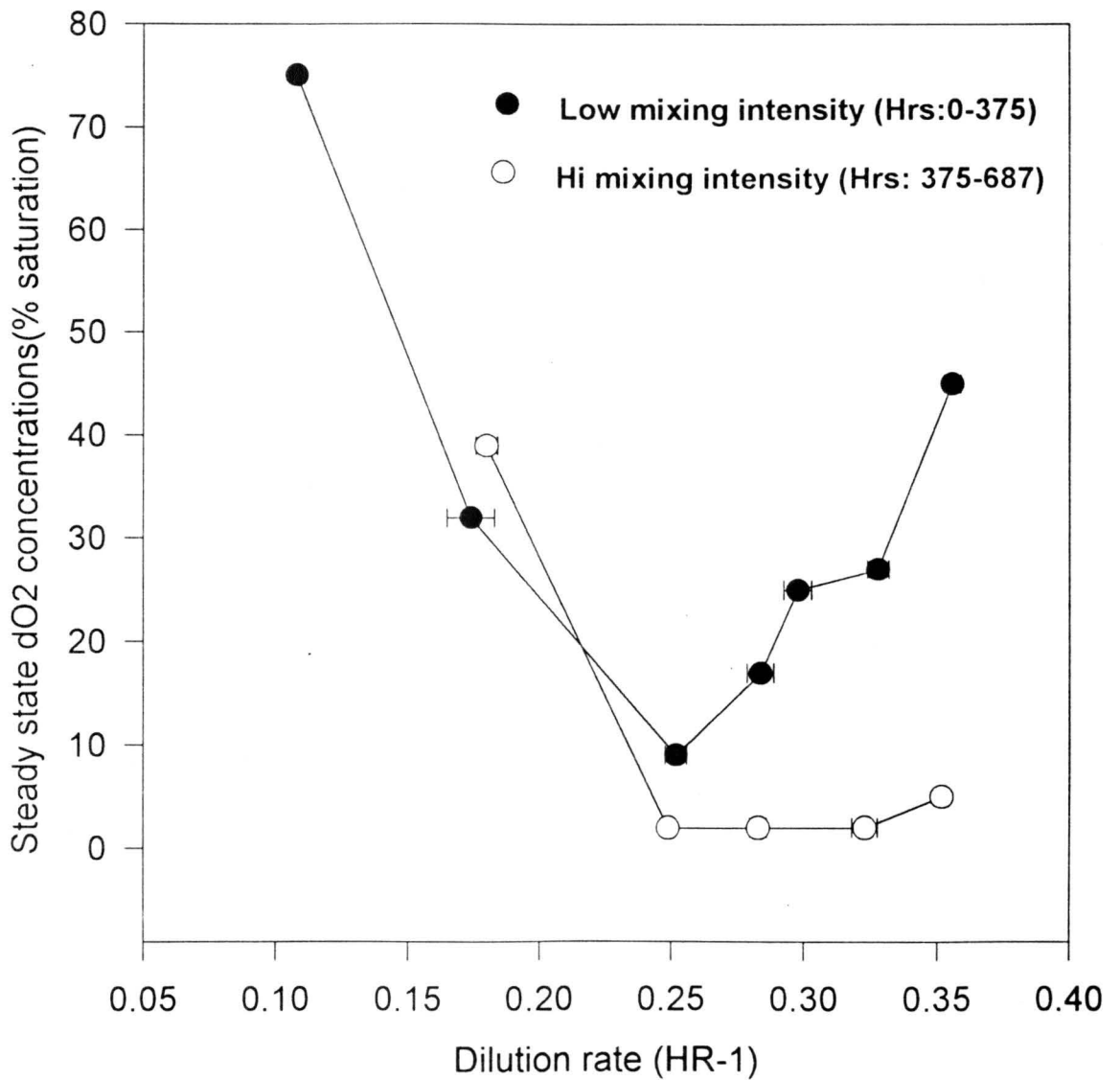


**Figure 3.11**

Dissolved oxygen levels vs Dilution rate -- CHE1

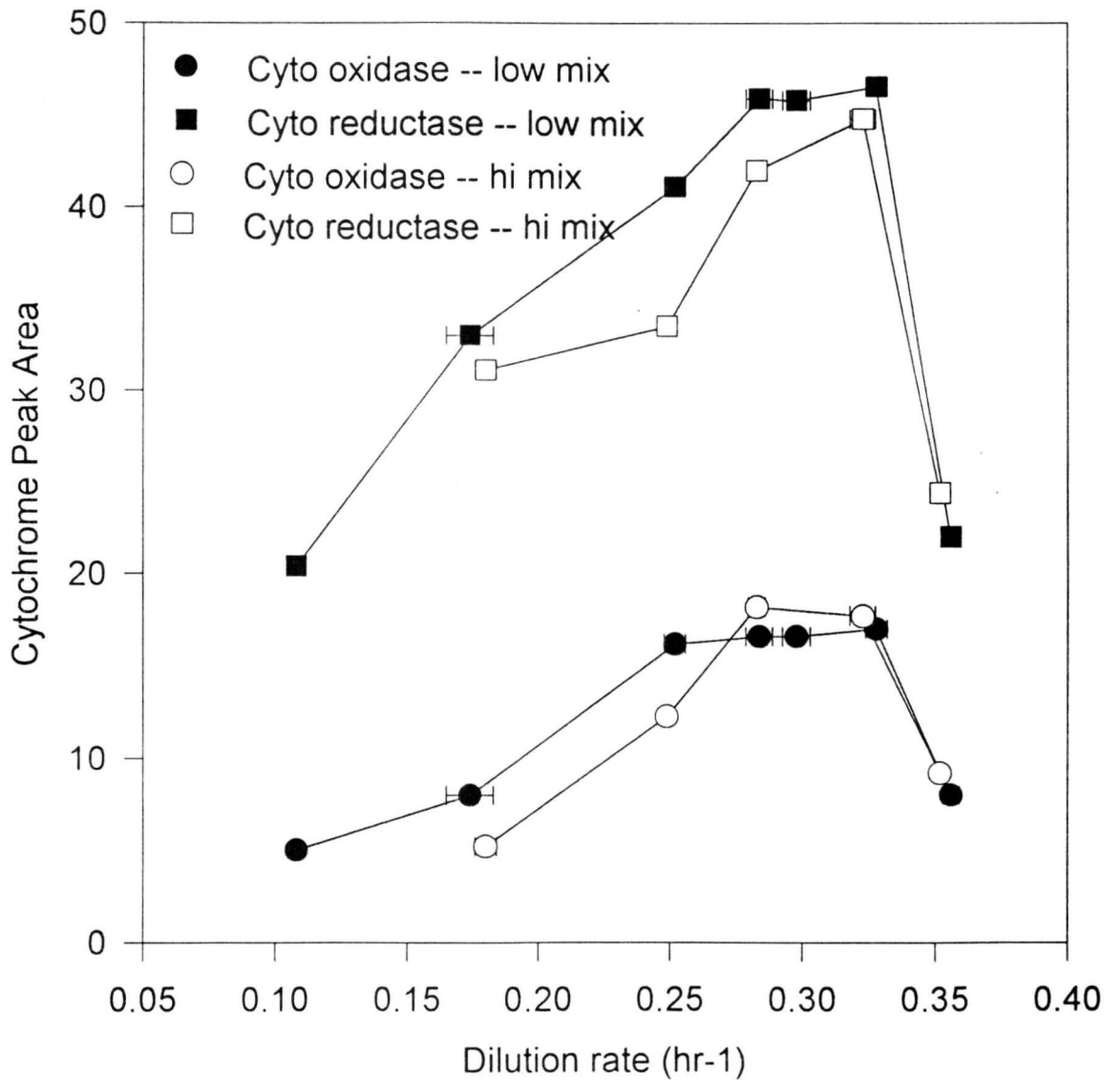


**Figure 3.12** Cytochrome levels vs Dilution rate -- CHE1

**maximum productivity of 1.26 g dry biomass per liter per hour in the well mixed curve.**

**Also noteworthy is the lower optimum production feed rate in the poor mixed curve. This will convert to less money spent on feed medium per unit time. Exactly which dilution rate optimizes the economics of biomass production cannot be determined without considering the cost of the feed medium. This significant portion of the working capital required to run a continuous bioreactor will certainly be different in an industrial setting than it is in our research setting. The cost of our defined medium is about \$3 per liter, not including preparation costs. It is possible that a 10 percent improvement on productivity per dollar spent could be achieved.**

**The inequality in steady state dissolved oxygen concentrations shown in figure 3.11 supports this entire theory well. On the poorly mixed curve, the steady state dissolved oxygen level at the loop's end dropped to a minimum of 9 percent saturation at 0.252 hr<sup>-1</sup> then returned to non-repressive concentrations at higher dilution rates. However, on the highly mixed curve, this same concentration dropped to a repressive level at 0.249 hr<sup>-1</sup> and stayed below 5 percent saturation for the remainder of the curve. This indicates that the more dispersed feed did indeed cause an anaerobic region within the system and this apparently caused an increase in ethanol production, which is shown in Figure 3.10.**

**To investigate the role glucose repression may have played in creating this system response, cytochrome levels within the culture were indirectly measured and results are displayed in Figure 3.11. If excessive glucose concentrations created saturated**

pathways and a bottleneck effect, the culture's cytochrome content should be very low because less oxygen is being consumed and most substrate is being fermented. If lack of oxygen is responsible for the decrease in yield, one would expect the cytochrome levels would be higher than a glucose repressed state because some substrate is still being consumed oxidatively. It is speculated that exposure to increased glucose levels may not only decrease the organism's respiratory capacity immediately, but also cause the organism to adapt over this long period of time causing permanent changes to the culture's electron transport chain enzymes. Furakawa et al. (1983) have reported such changes occurring in time spans around 300 hours. This certainly may be applicable to our system.

In light of this possibility, we felt it was important to note the chronological order in which the different mixing curves were obtained. In experiment CHE1, the poorly mixed curve was obtained first and the well mixed curve second. If permanent adaptation to the culture's respiratory enzymes occurs during the well mixed regime, then obtaining that curve first would prohibit obtaining higher biomass yields in the poor mixed regime at a later time.

This hypothesis is the basis for experiment CHE2, where all conditions will be left the same except for the order in which the mixing curves are obtained. This may provide prudent information as to the significance of the culture's history on its respiratory performance.

### 3.4 Culture History Experiment #2 (CHE2)

#### *Preamble*

The objective of this experiment is identical to that of CHE1, namely to establish if the steady state biomass yields will vary with the intensity of feed dispersion in the side loop. All conditions are similar to those described in the preamble for CHE1, except the chronological order in which the curves are obtained will be reversed to investigate if the culture's respiratory capacity irreversibly adapts when exposed to excessive glucose levels for several cell generations.

#### *Results*

Results of biomass yield, biomass productivity, ethanol concentration, and cytochrome levels for experiment CHE2 are reported in Figures 3.13 through 3.16, respectively. Quick examination of these figures indicates that no biological response occurred with varying feed mixing intensity at any dilution rate of this experiment. Figure 3.17 compares the low mixing curves obtained in experiments CHE1 and CHE2.

#### *Discussion*

There are a few interesting observations to be made with this data, even though it appears that the results are not profound. Figure 3.13 clearly shows the biomass yields were virtually identical for both mixing extremes. This data does support our theory that cytochrome performance is permanently modified by culture history exposure to glucose levels exceeding the threshold repression concentration.

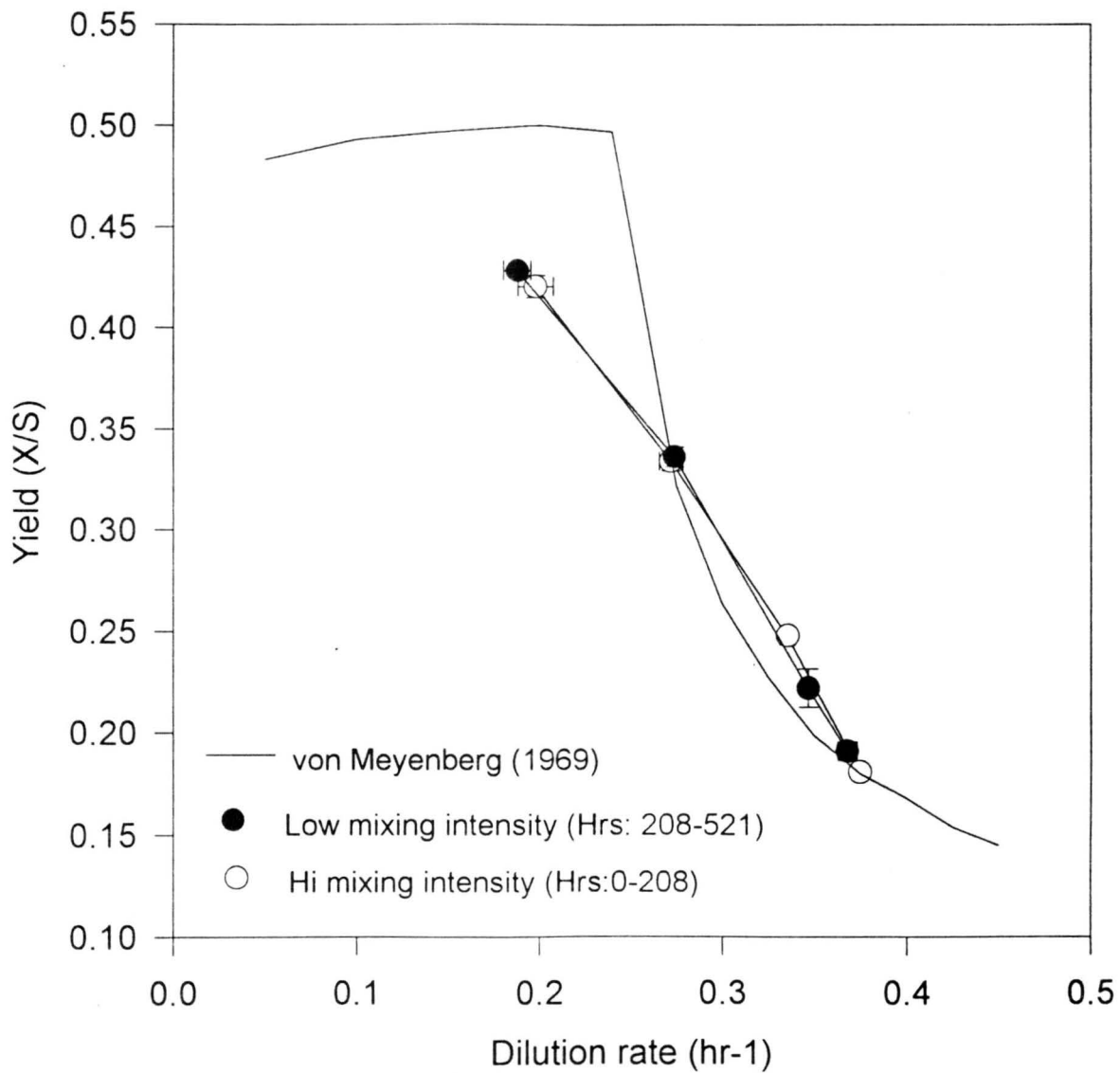


**Figure 3.13** Yield vs Dilution rate -- CHE2

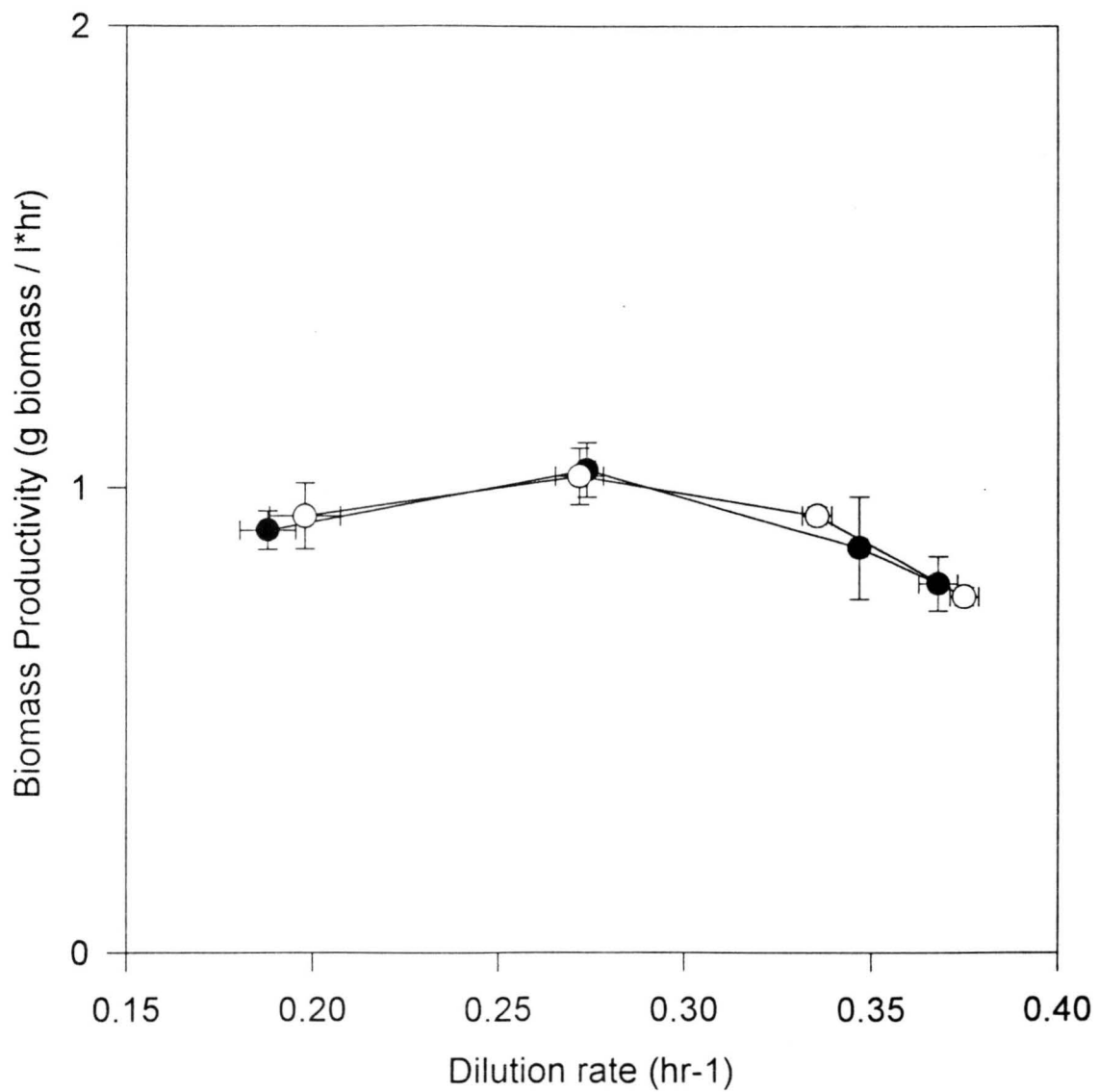


**Figure 3.14** Productivity vs Dilution rate -- CHE2

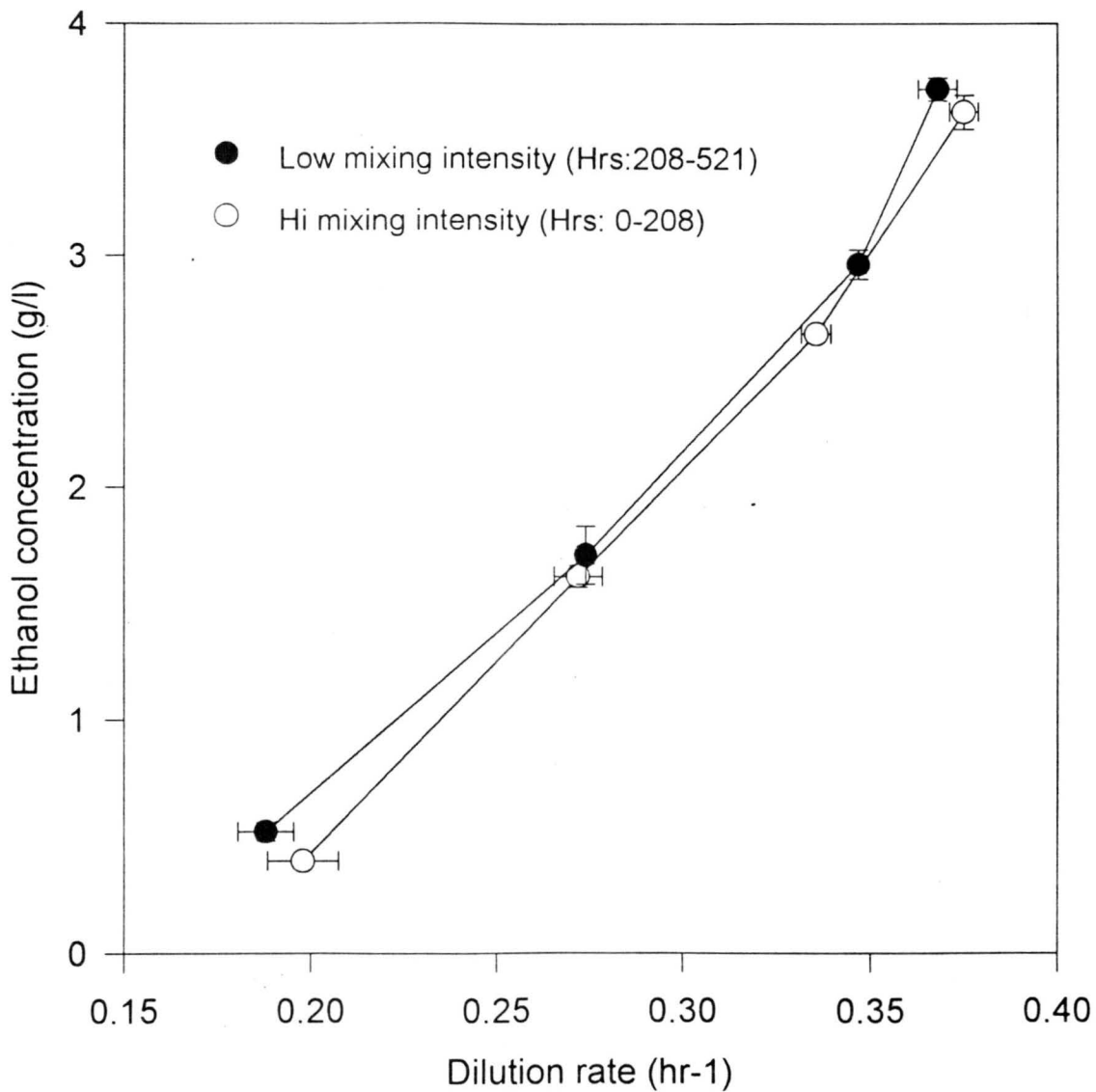


**Figure 3.15** Ethanol vs Dilution rate -- CHE2

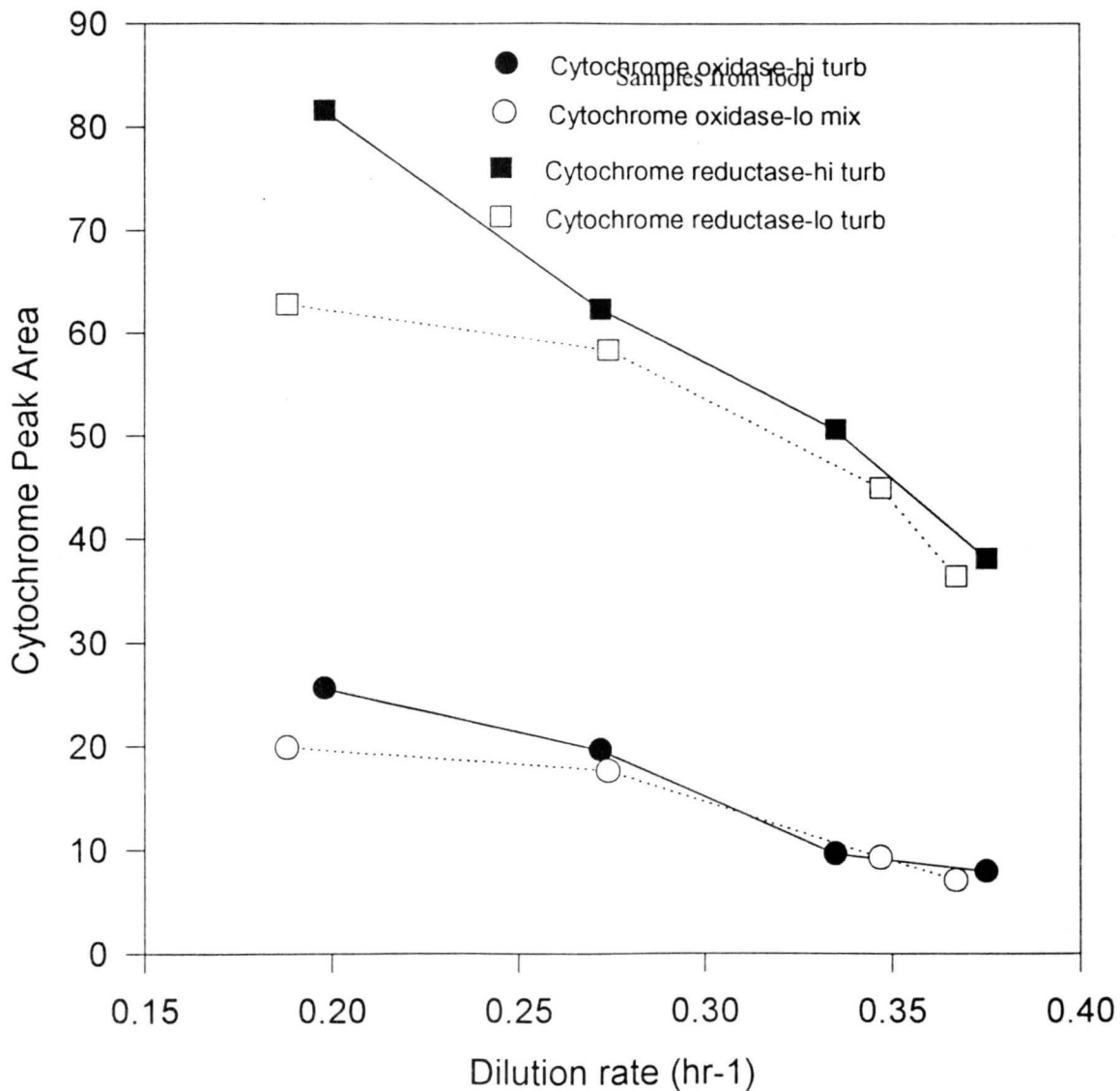


**Figure 3.16**

Cytochrome content at different mixing intensities

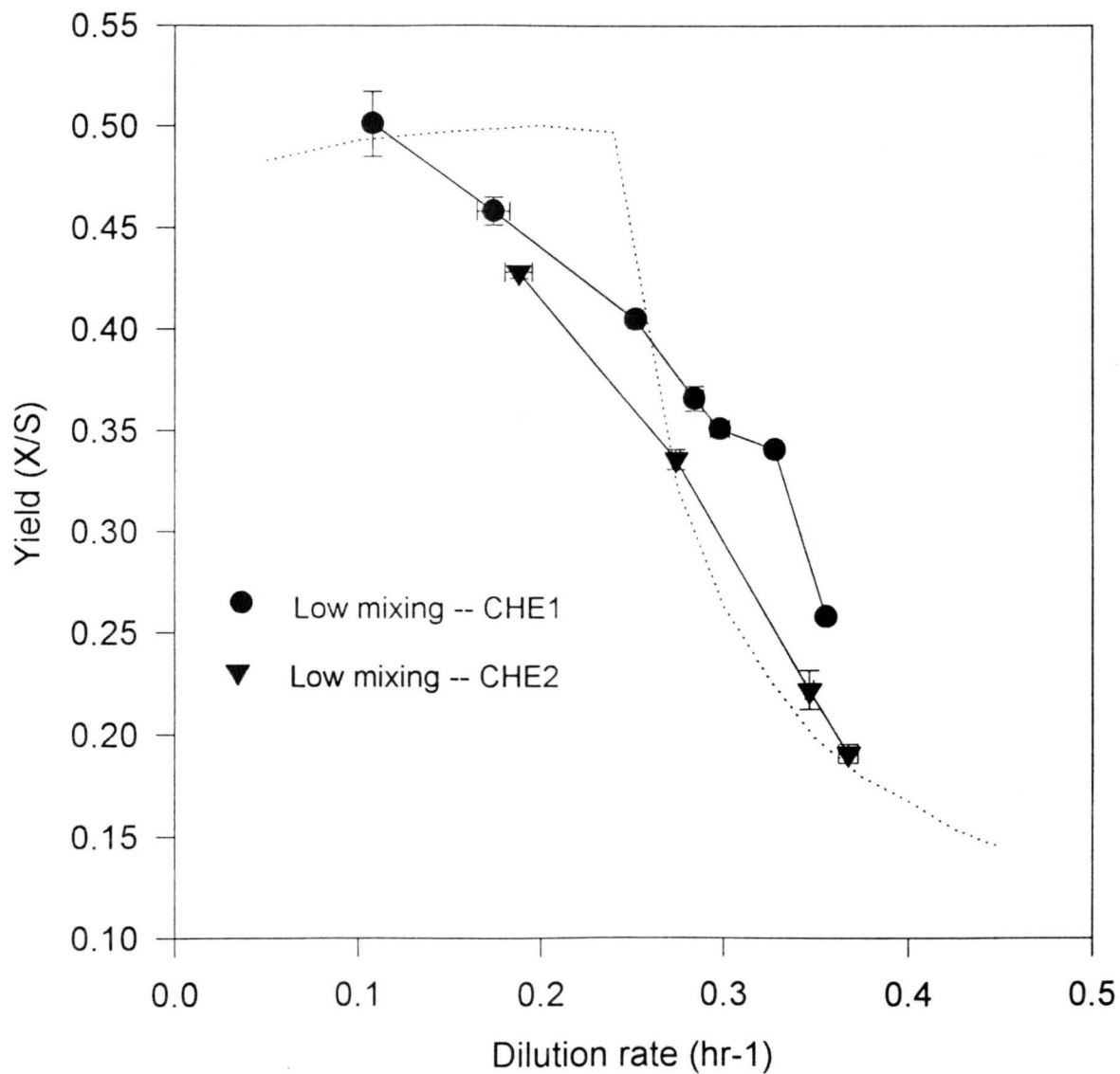


**Figure 3.17** Low Mixing Conditions -- CHE1 vs CHE2

During the first 208 hours of this fermentation, the fresh sterile medium was highly dispersed into the cell broth. If perfect mixing is assumed, the glucose concentration just downstream of the feed needle when the feed rate is 198 ml/hr equals 0.037 grams per liter; this is well below the reported threshold limit of 0.10 grams of glucose per liter and therefore one would not expect any repression to be occurring at this feed rate. However, as the feed rate increases, the steady state bulk glucose concentration rises above zero. This coupled with the fact that the feed rate is greater could bring perfectly mixed feed concentrations as high as 0.15 grams per liter. The results of this experiment support that exposure to an excessive glucose concentration for hundreds of hours may have caused the culture to sacrifice some of its respiratory abilities.

Another interesting observation is the large discrepancy between steady state biomass yields for the curves in CHE1 as compared to CHE2. As Figure 3.17 evidences, CHE2 has biomass yields about 0.04 to 0.08 grams biomass per gram glucose at all dilution rates. We attribute this significant difference to culture history as well. Because CHE2 was started at a dilution rate of  $0.188 \text{ hr}^{-1}$ , the culture never had an opportunity to reach its normal 0.5 yield at lower dilution rates. This fact appears to have prevented the culture from developing the enzymatic machinery necessary for maintaining higher yields at greater dilution rates. This same phenomenon was noticed in other fermentations which were not run to completion due to equipment failure or contamination.

**The author was not comfortable with the validity of this experiment's results for the following reason: the vented pulse dampener upstream of the feed loop was not sufficiently separating the gas phase from the liquid phase before entry to the loop. When these large and somewhat frequent bubbles dislodged from the pulse dampener they undoubtedly disturbed the parabolic laminar flow profile in the poorly mixed feed zone. We suspect that this disruption probably created enough mixing at the feed site to decrease the microscale dimension significantly.**

**To test the extent to which this inefficient separation effects the feed dispersion two studies were conducted. First, micromixing sensitive dye reactions were performed with and without gas-liquid separation at both mixing intensities to see if substantial differences occurred in microscale prediction (Section 4.2.2). Secondly, pure monazo dye R was fed through the needle into a clear distilled water bulk. From visualizing the dye dispersing at these different mixing conditions (Section 4.3) and from the dye results, it was determined that a full-proof method of consistently and dependably removing gas bubbles before the feed loop is essential for creating the desired mixing extremes. It was decided the next experiment would essentially repeat the same conditions as CHE2 with the addition of a cyclone separator in the recirculation loop to insure bubbles are not disturbing the desired mixing conditions.**

## CHAPTER IV: Results and Discussion

### 4.1 Fermentation Results

#### *Introduction*

This chapter contains results and discussion of the two fermentation experiments which had the cyclone separator in-line as well as the various methods used to quantify the microscale in the feed zone. The Bourne dye reaction predicts Kolmogorov diameters of 34 and 160 microns for the well-mixed and poorly-mixed cases in these experiments, respectively.

#### 4.1.1 Culture History Experiment #3 (CHE3)

##### *Preamble*

Again, we are trying to determine if the chronological order in which the mixing curves are obtained is important for eliciting a biological response. As dependable gas-liquid separation is essential to produce the desired microscales at the feed site, the cyclone separator shown in Figure 2.2 was placed just down stream of the peristaltic recirculation pump to help insure reliable separation. The gas-liquid mixture sucked from beneath the sparger in the stirred tank enters near the top and through the side of the cyclone. The cyclone is positioned so that a swirling action occurs as the mixture enters the vessel. This swirling creates a "dead zone" for a few moments which allows gravity to separate the phases. The liquid is forced

through the bottom of the cyclone and heads for the feed loop while the gas escapes through the roof. The gas outlet is fitted with a sterile air filter to prevent contamination entering this port.

The escaping gas has to be collected in a closed vessel so that the cell broth is not pumped through the cyclone's peak. A 10 liter plastic carboy was used for this purpose. Because this carboy would eventually fill with gas and create enough pressure to negate gravity's effect, the pressure in the gas collecting needed to be relieved periodically. To solve this problem, a repeat cycle timer (Omron H3BF) was wired to a solenoid valve which was set to open for a few seconds every 4 minutes. The opening of the valve for this small period of time not only obviates excessive pressure building in the gas collection vessel but also prevents the broth mixture from being pumped out the roof of the separator.

The well mixed curve was again collected first and the poorly mixed second. The tank was sparged with 2 vvm air. Cytochrome measurements were taken at every steady state sample in order to gather more reliable steady state averages.

### *Results*

Figure 4.1 shows that the low mixing curve again produced slightly higher biomass yields than the high mixing curve. Bioreactor performance was again increased by the less dispersed feed, as evidenced by the productivity versus dilution rate plot in Figure 4.2. The carbon not converted to biomass was instead fermented to ethanol, as the increased levels of ethanol detected in the well mixed curve (Figure 4.3). Increased feed zone mixing also appeared to slightly decrease the culture

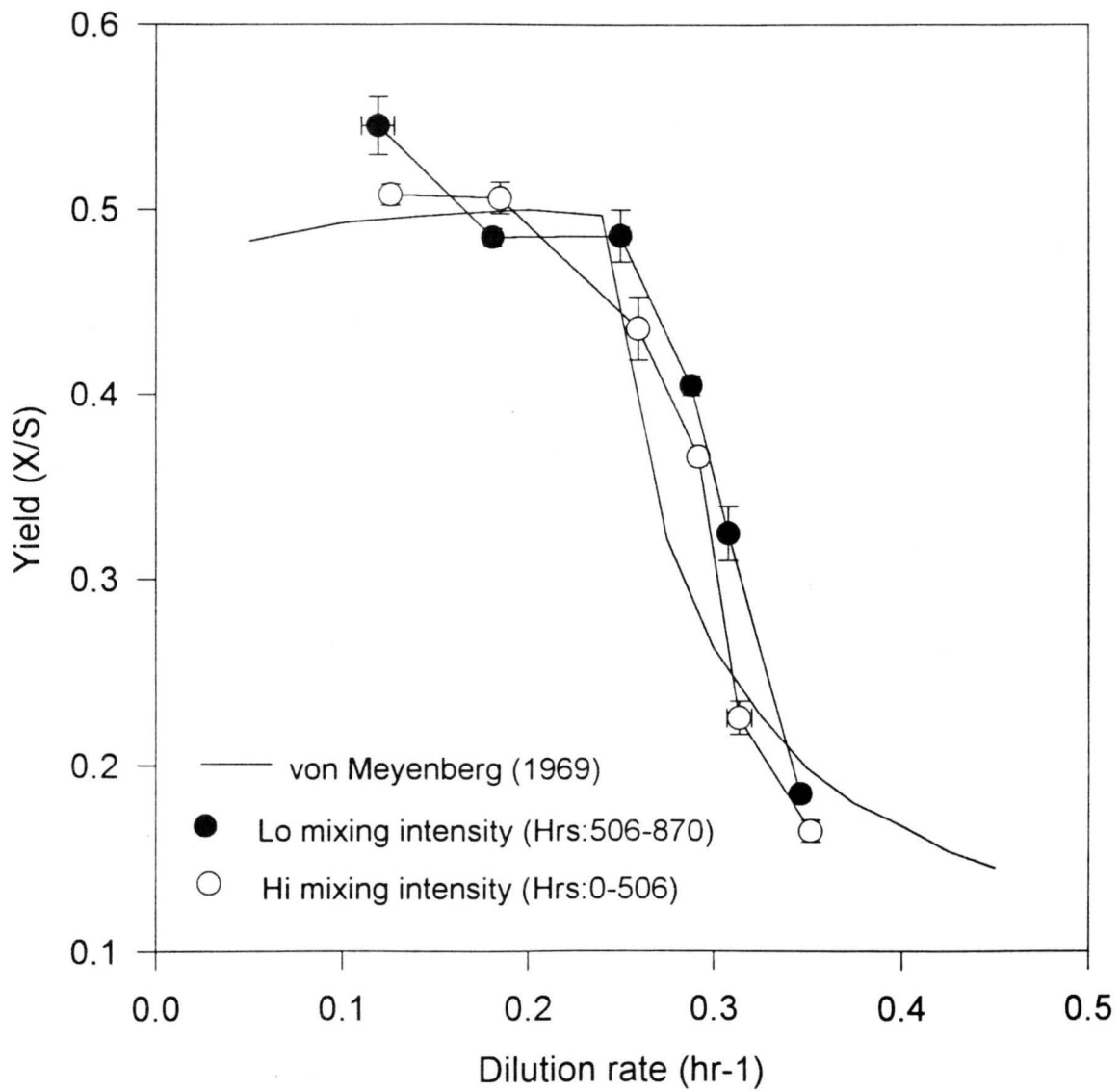


**Figure 4.1** Yield vs Dilution rate -- CHE3

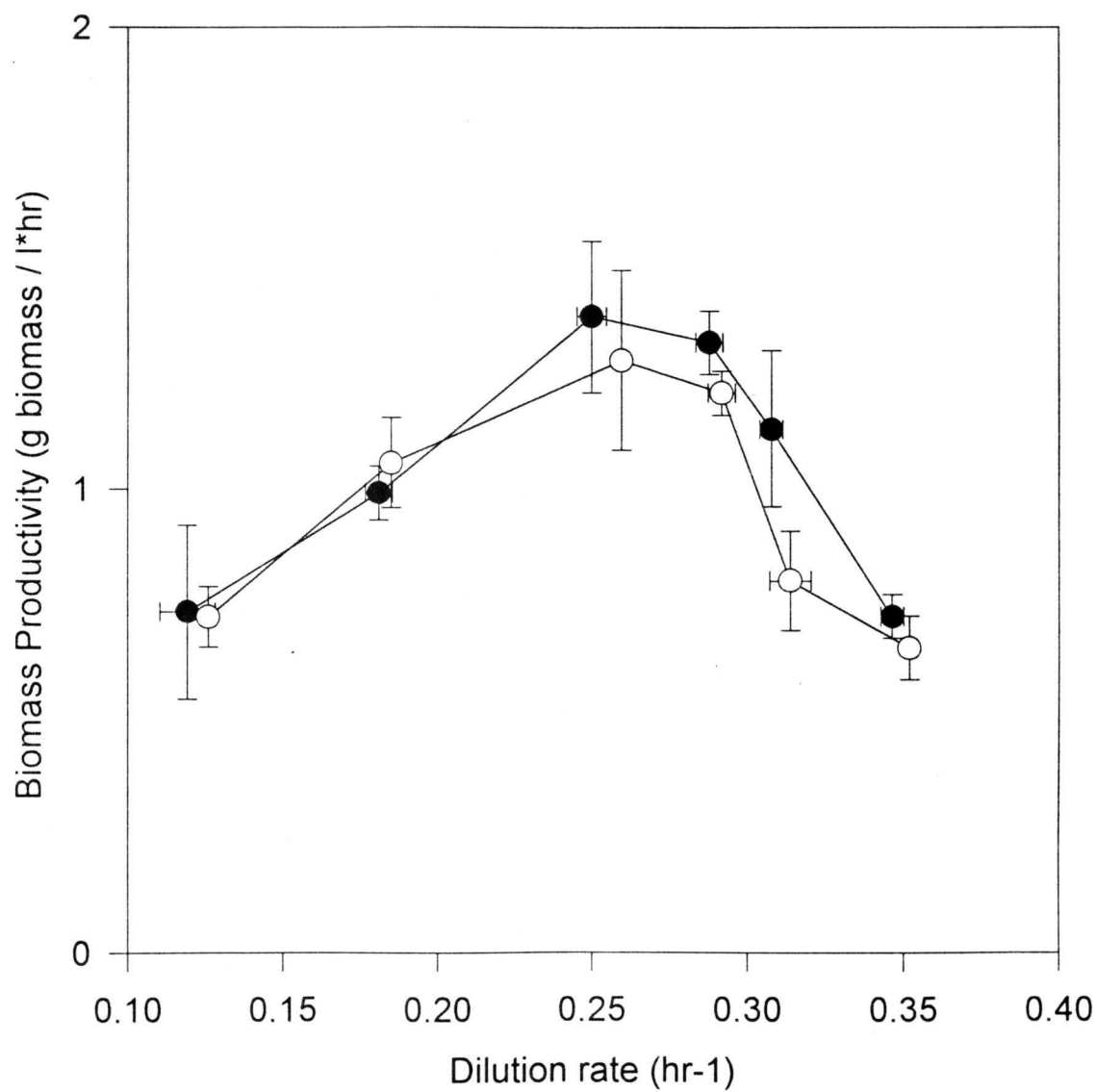


**Figure 4.2** Productivity vs Dilution rate -- CHE3

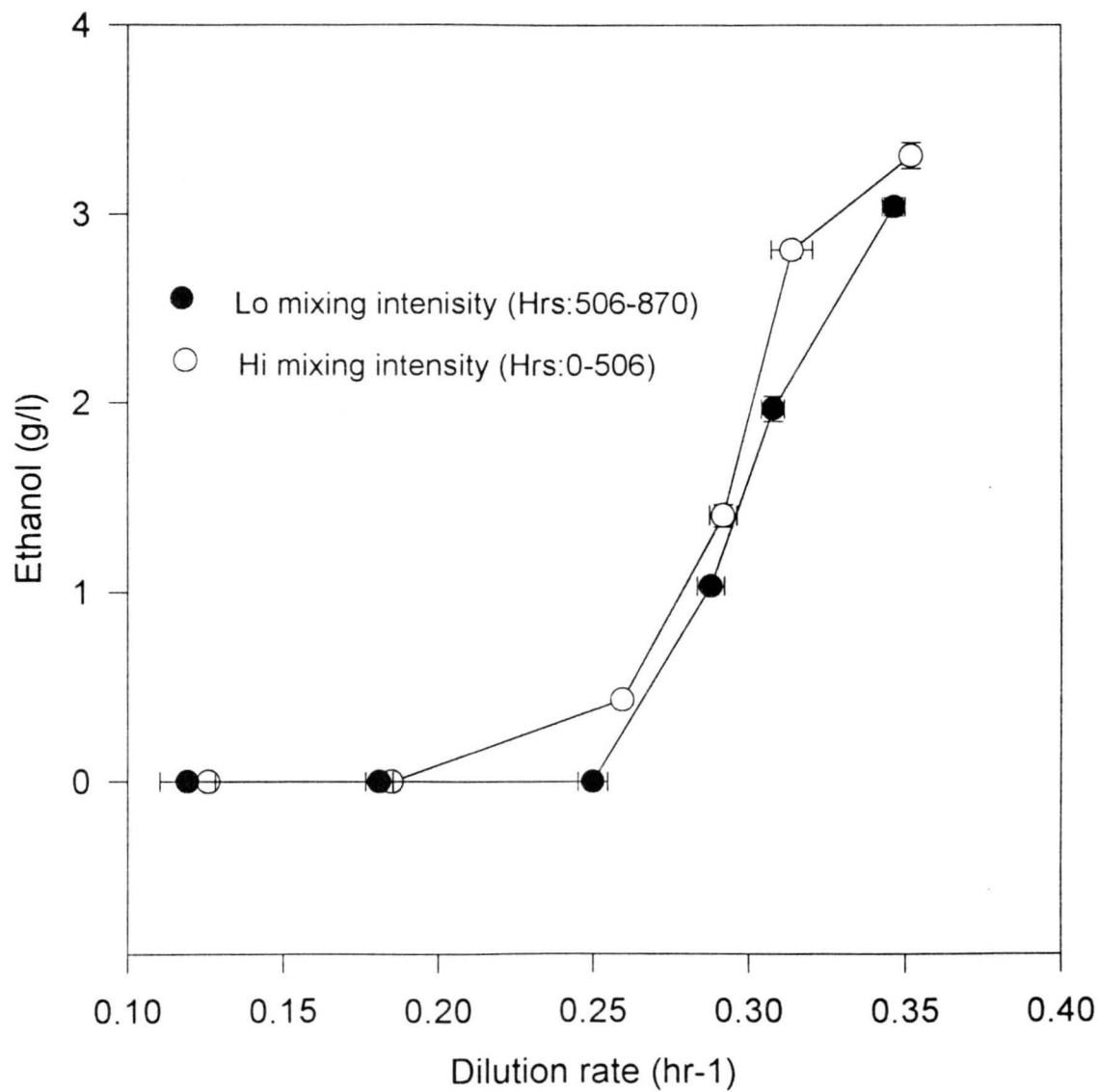


**Figure 4.3** Ethanol vs Dilution rate -- CHE3

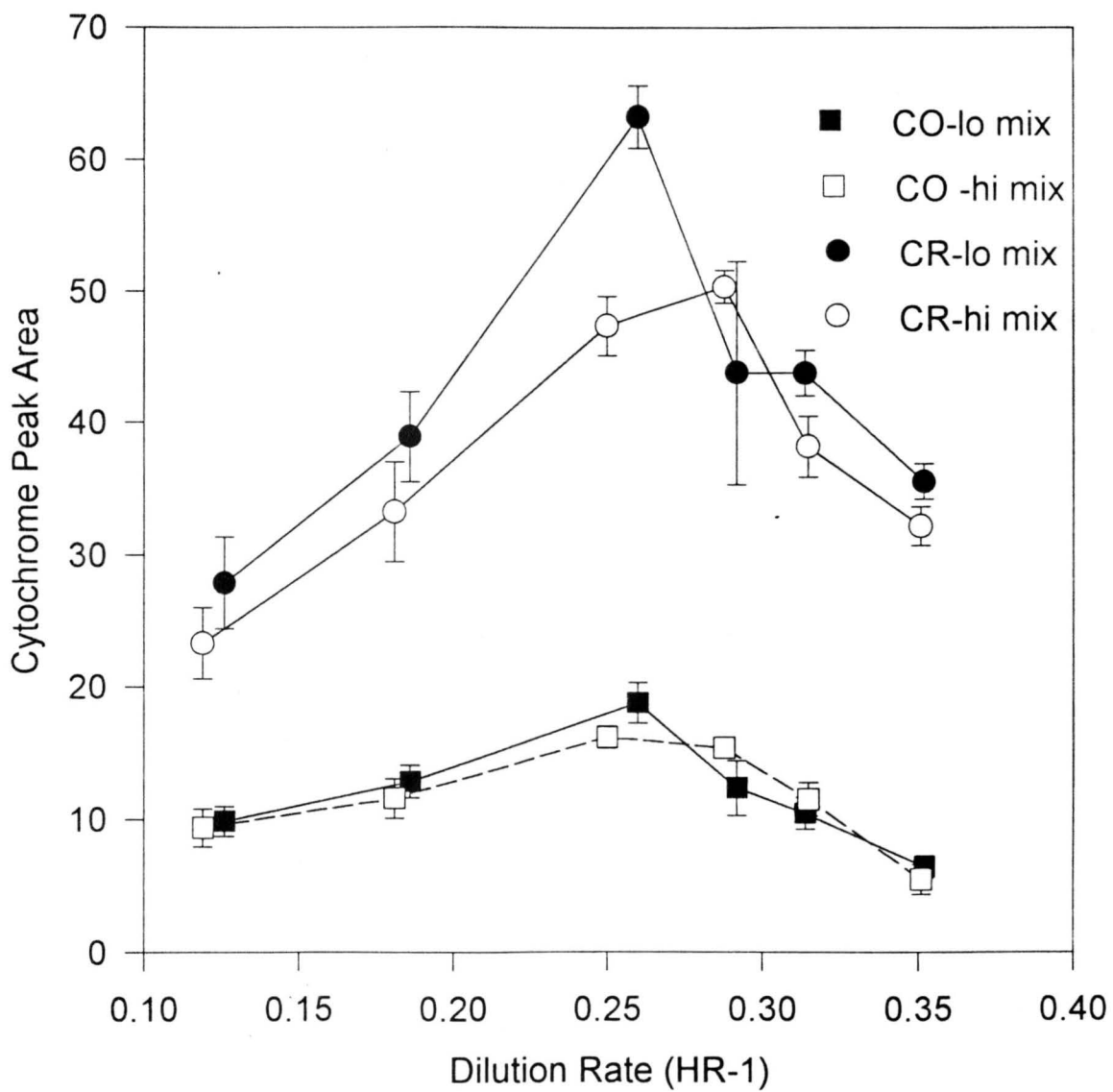


**Figure 4.4** Cytochrome content vs Dilution rate -- CHE3

respiratory capabilities, as steady state cytochrome reductase levels in Figure 4.4 show.

### *Discussion*

The discrepancies in steady state biomass yields are greater in this experiment than for CHE1 and CHE2, as differences become as great as 0.10 g biomass per g substrate at dilution rate of  $0.31 \text{ hr}^{-1}$ . This supports our suspicion that the lack of response in CHE2 may have been due to insufficient separation of gas bubbles before the feed zone. It does not support the theory that cytochrome performance is irreversibly affected by culture history exposure to excessive glucose concentrations, as the first 500 hours of exposure to the well mixed condition did not prevent the culture from recovering to yield higher biomass coefficients and cytochrome reductase levels during the last 300 hours.

Again, the improved yield translated to improved productivities at all dilution rates. However, the reactor's maximum performance was not statistically effected as the optimum production feed rate of  $0.25 \text{ hr}^{-1}$  outputted approximately 1.2 grams of biomass per liter per hour at both mixing conditions. It is important to note that the optimum production feed rate of  $0.25 \text{ hr}^{-1}$  in CHE3 is lower than the  $0.328$  and  $0.283 \text{ hr}^{-1}$  reported in CHE1. Again, by getting maximum productivity at lower feed rates, the economics of the process may be improved.

As the cyclone separator was not used in experiment CHE1, it was decided to repeat this chronological order again with the separator in place insuring that

microscale levels in the feed zone are as distant as possible. It may be possible to improve on the results obtained in CHE1 for this reason.

#### 4.1.2 Culture History Experiment #4 (CHE4)

##### *Preamble*

Experiment CHE4 was an attempt to reproduce the response seen in experiment CHE1 with the addition of the cyclone separator to help achieve the desired microscales in the feed zone. Because the method of degassing used in CHE1 was sporadic and unreliable, it is suspected that microscale separation at varying mixing extremes was not 34-160 microns but closer to 65-127 microns. This was due to the intermittent disruption of feed zone by bubbles that were not removed through the vented pulse dampener used in CHE1.

The poorly mixed curve was collected first and the well mixed curve second. Air flowrate was kept at 2 vvm. Cytochrome samples were collected only once per steady state condition.

##### *Results and Discussion*

Figure 4.5 contains the yield versus dilution rate data for experiment CHE4. The behavior of this culture was much different from CHE1. Small variations in biomass yield occurred in CHE4 until a dilution rate of  $0.30 \text{ hr}^{-1}$ , when the well mixed curve's yield dove to repressive yields. The poorly mixed curve maintained higher yield up to and including a dilution rate of  $0.325 \text{ hr}^{-1}$ . Again, it does not appear that the chronological order in which the curves are obtained is important.

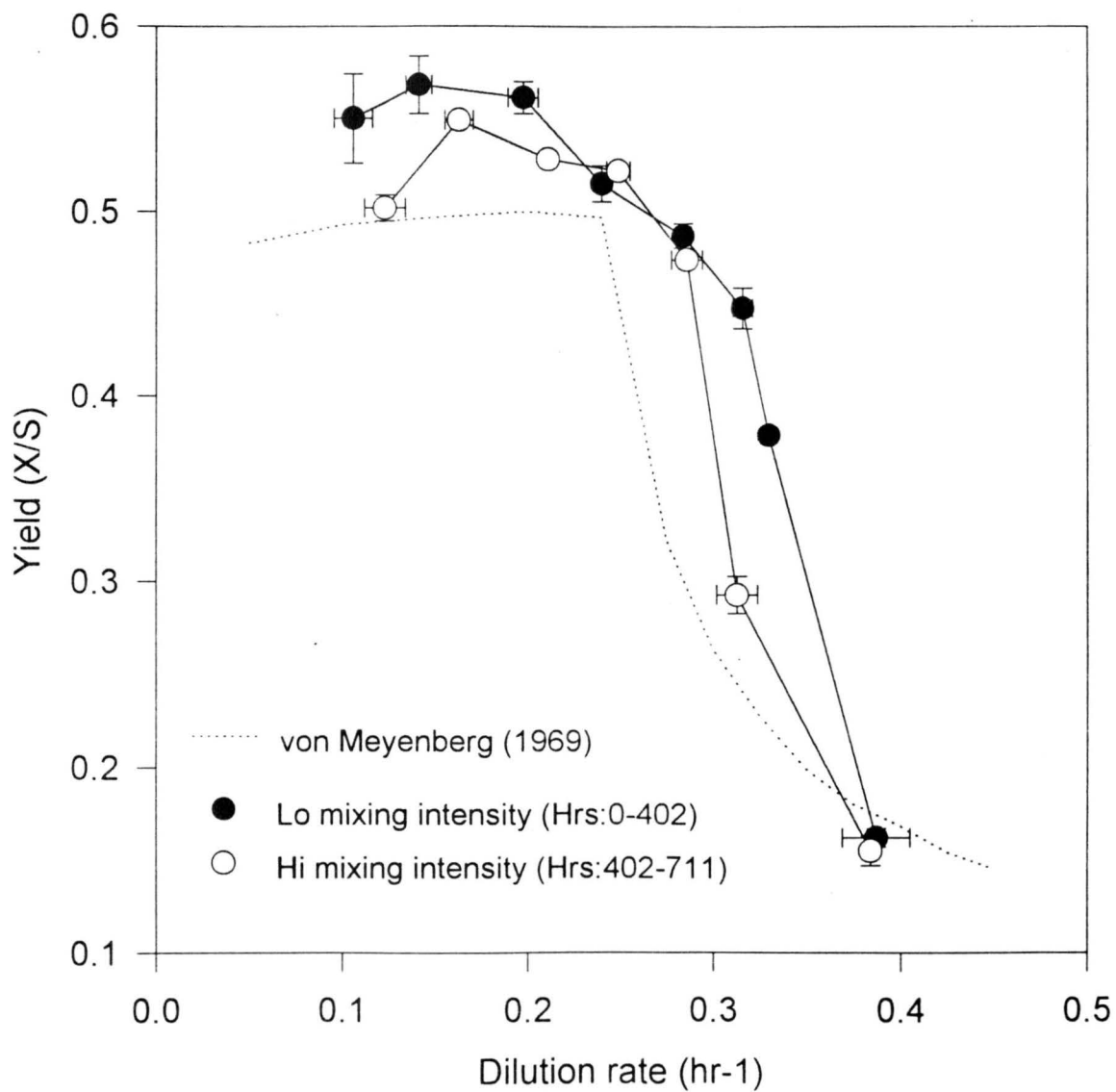


**Figure 4.5** Yield vs Dilution rate -- CHE4

This phenomenon is the opposite of that reported by Wenger (1994) where increased mixing intensity in a stirred tank increased critical dilution rates.

There is, however, a very significant difference between this system and the ones Wenger used: the recirculation loop. The existence of the side loop in this system serves to clutter the overall picture because the culture is spending 20 percent of its time in a region where oxygen transfer cannot occur; of course, the loop is necessary for isolating micromixing's effects from macromixing's.

This air only system frequently reported intermediate steady state biomass yields below the fully respirative yields of 0.5 and above fully repressed yields of 0.15. In system's, such as von Meyenberg's (1969) and Wenger's (1994), where dissolved oxygen is kept above repressive levels at all times, intermediate steady state values were rarely observed. This is evidence of the critical role dissolved oxygen plays in the onset of glucose repression.

The next logical experiment to perform with this system is to repeat CHE4 with pure oxygen gas being supplemented when the dissolved oxygen concentration at the end of the loop drops below 0.1 mg/liter, as was done in experiment FF2. When dissolved oxygen is kept at non-repressive levels, fully respiratory yields of about 0.5 are maintained to a higher dilution rate. Controlling the micromixing may enable a higher critical dilution rate to be achieved, thus improving the bioreactor performance.

Figure 4.6 shows the bioreactor's productivity for experiment CHE4. At a dilution rate of  $0.316 \text{ hr}^{-1}$ , the productivity reached as high as 1.6 grams biomass

per liter per hour in the poorly mixed curve. The productivity dropped to about 1.0 g biomass/l\*hr at this same dilution rate in the well mixed curve. The steady state ethanol concentrations were again higher in the well mixed curve than the poorly mixed one, as Figure 4.7 shows.

Figure 4.8 shows peak areas for cytochrome  $aa_3$  at the two different mixing states. One assay was done at each steady state with the sample being the last collected at that steady state. The cytochrome  $aa_3$  level is indeed lower at the critical values in the well mixed curve. This suggests that cytochrome performance is related to the decrease in yield, a phenomenon also reported by Wenger (1994). Evidently, the loss of cytochrome enzymes occurs in a time scale on the order to several cell generations. This may be the reason for the failure to see the desired system response in the flip-flop experiments. Better success may be found in a flip-flop experiment if a value just below the critical dilution rate is held, the mixing intensity is flip-flopped, and the culture is watched for several residence times longer than reported in Ye and Dunlop (1990) or in FF1 or FF2.

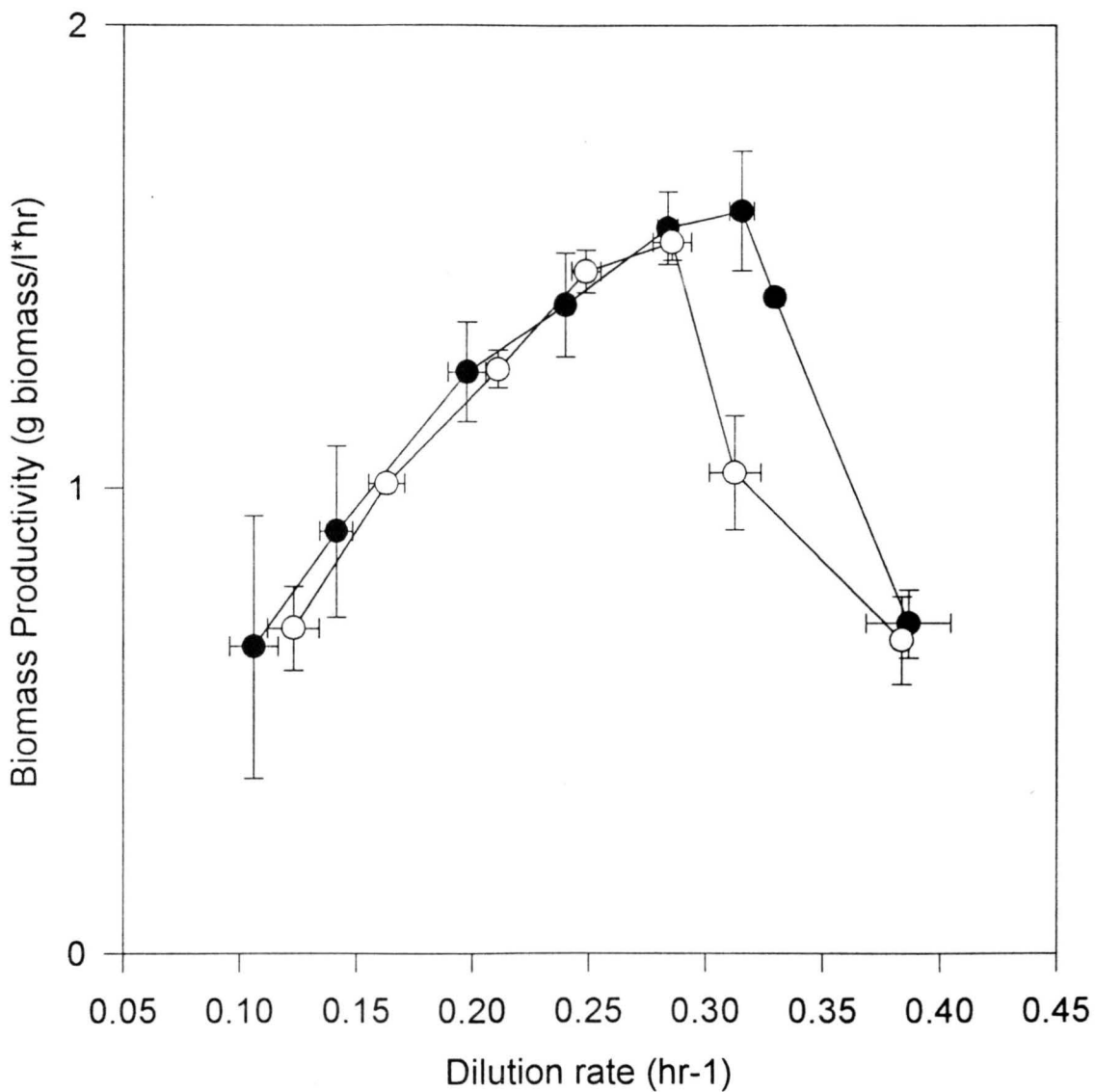


**Figure 4.6** Productivity vs Dilution rate -- CHE4

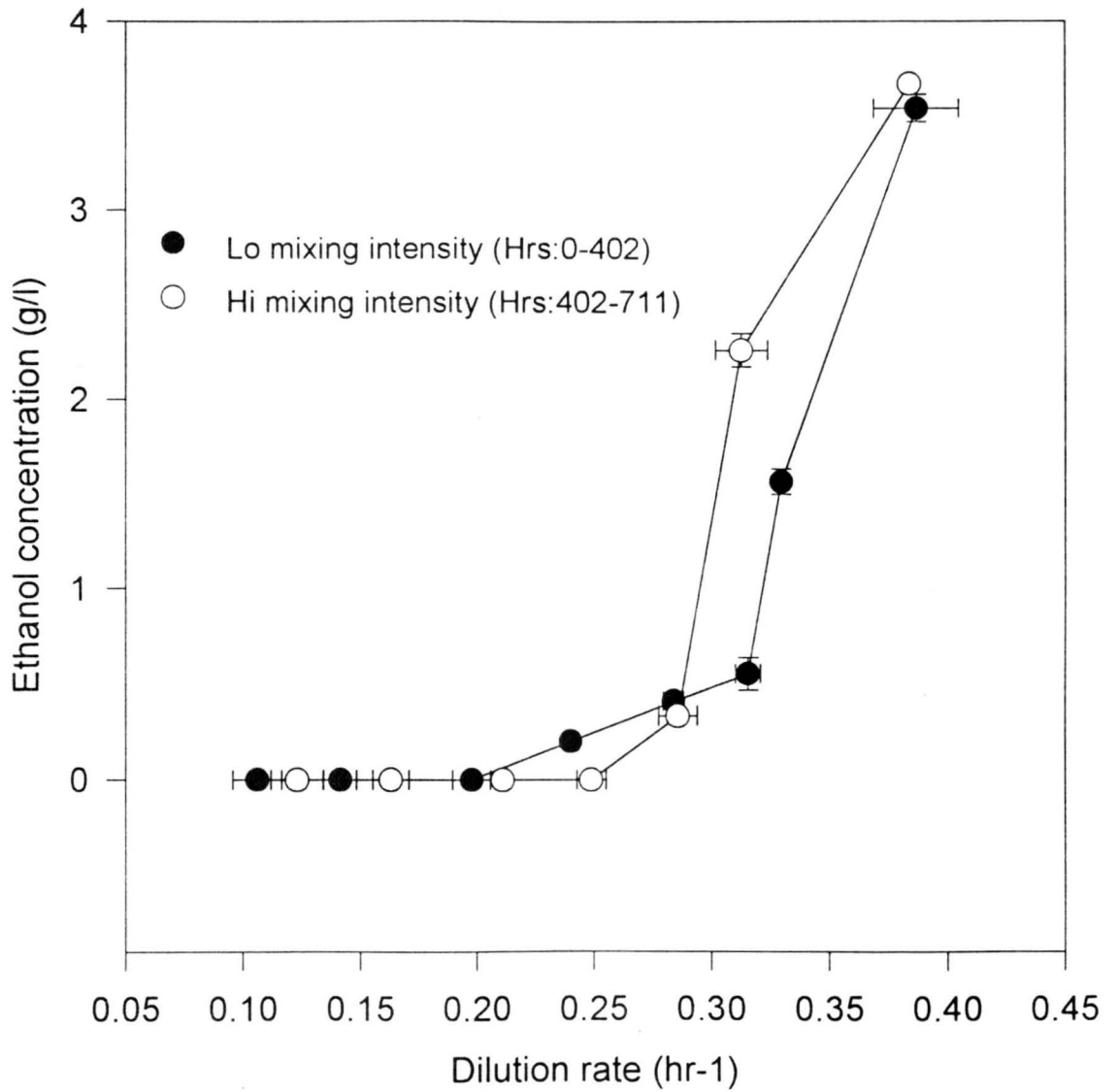


**Figure 4.7** Ethanol vs Dilution rate -- CHE4

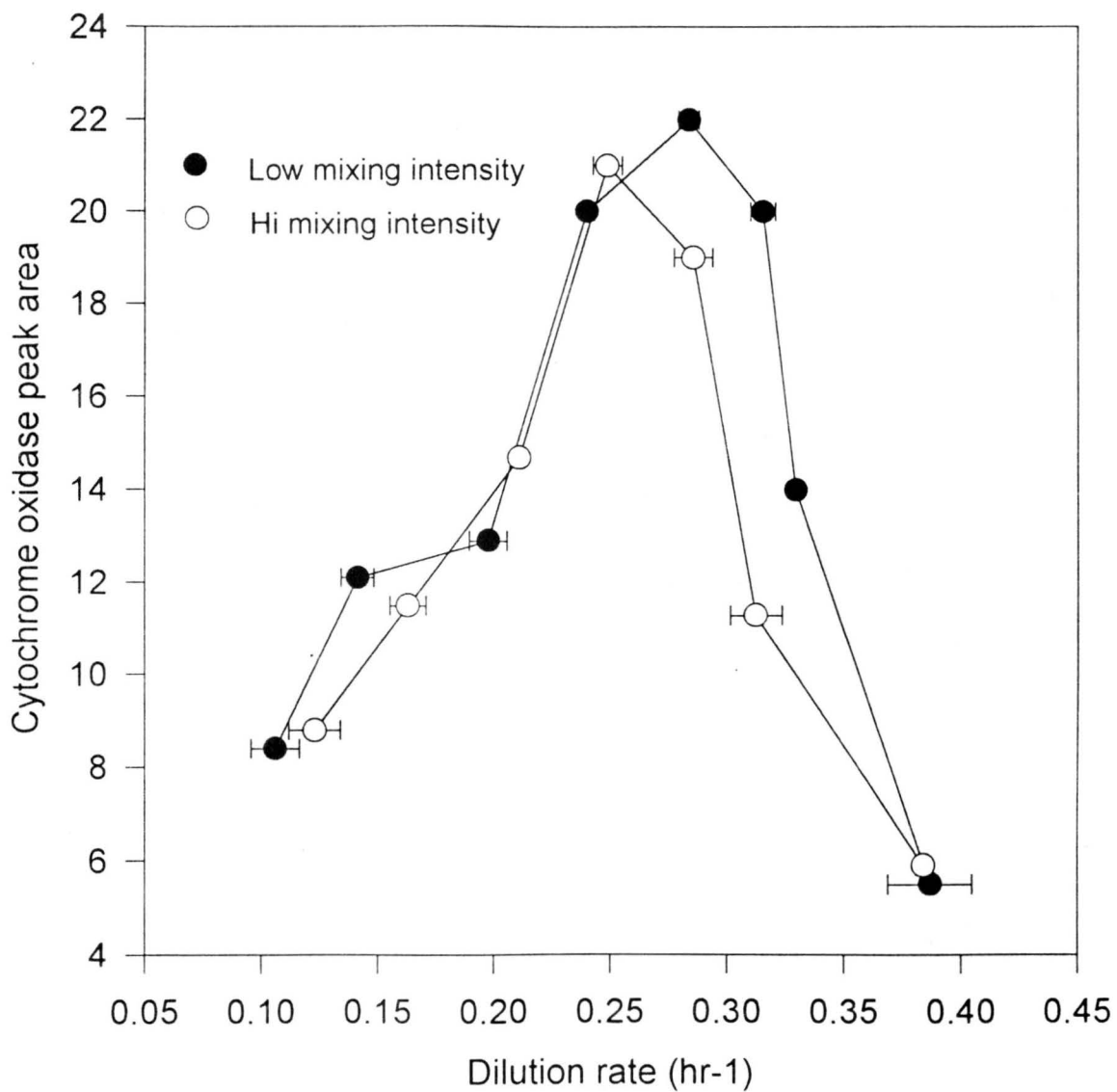


**Figure 4.8** Cytochrome content vs Dilution rate - CHE4

## 4.2 Turbulence Quantification

### 4.2.1 Scale Determination from LDV Time Series

The autocorrelation function of a time series taken one centimeter downstream of the static mixer at the pipe's center is shown in Figure 4.9. Integration of the autocorrelation function provides reasonable values for the integral scale of 0.240 cm for the poorly mixed series and 0.070 cm for the well mixed time series. Figure 4.10 contains the turbulence spectrum for the well mixed time series. The peak at 16 Hz may be related to the eddy shedding frequency, although, the value calculated with the Strouhal number for the eddy shedding frequency is 7.6 Hz. Calculating the Taylor microscales and the energy dissipation rate per unit mass,  $\varepsilon$ , requires integrating the dissipation spectrum. This integral diverges in the measured frequency range; obtaining a valid integral requires the dissipation spectrum converging to zero, the value where the inertial forces of the eddy finally balance the viscous forces of the fluid and energy is no longer dissipated. This is not possible given the size of microscale relative to the measuring volume of the probe.

The problem here arises because the instantaneous velocity distribution is not uniform within the measuring elements region. Because a valid velocity measurement requires a consistent set of Doppler frequencies across 10 fringes 4.88 microns apart, any particle traveling in an eddy smaller than this 48 micron distance will create data which is unacceptable to the signal analyzer. Hinze (1975) discusses this in his list of seven requirements that the measuring element must satisfy for calculations to be reliable.

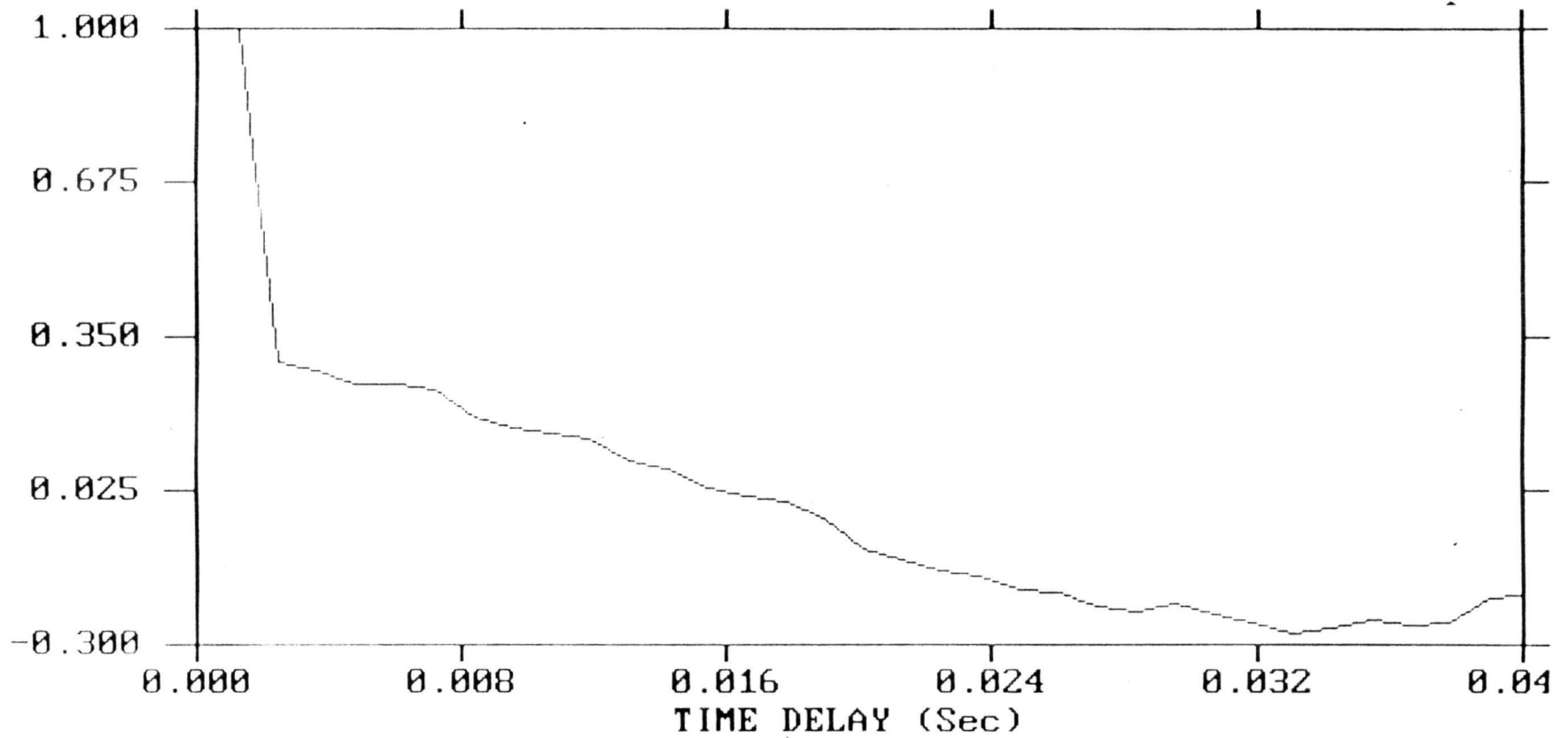
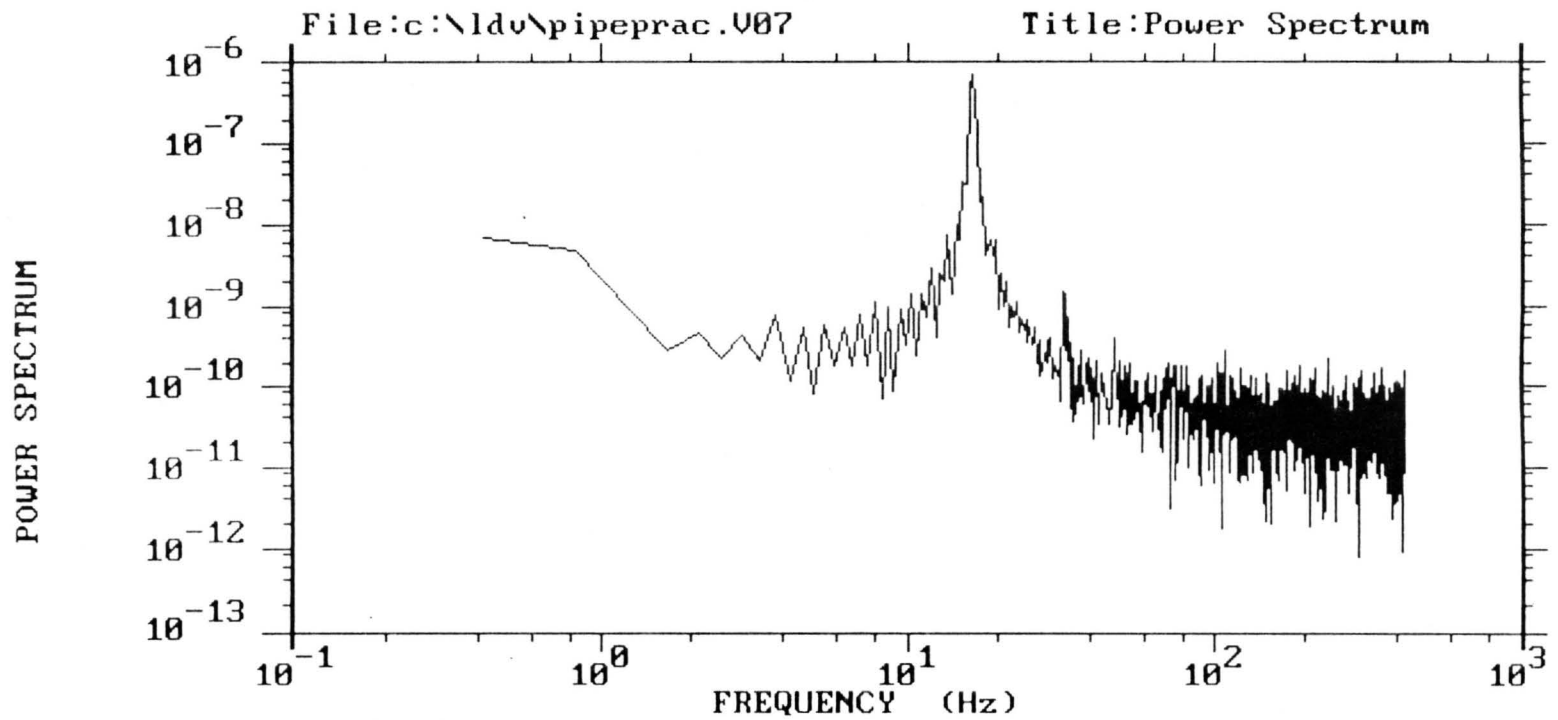


Figure 4.9 -- The autocorrelation function of a velocity time series collected one centimeter downstream of the static mixer.



Graph Component: V  
% of Bins Containing Data = 100  
Scaling Factors (X,Y) = 1.0 , 1.0

Figure 4.10 -- The power spectrum of a velocity time series collected one centimeter downstream of the static mixer.

Srikantaiah (1985) first suggested indirectly measuring the energy dissipation rate by the following means. The distribution of radially averaged turbulent energies was measured at increasing axial distances from the mixer. A decrease in turbulent energy from one position downstream to the next is multiplied by the average bulk convection velocity and divided by the axial distance interval. The resulting value gives a reasonable estimate of the rate at which energy is dissipating; a value which is needed for calculating the microscales describing the eddy diameter and turnover rate. Figure 4.11 shows the radially averaged values of total turbulent energy at positions 0.9, 1.0, and 1.1 centimeters downstream of the mixer, for approximating the well mixed domain. The average energy dissipation rate from this data is calculated to be  $1.59 \text{ m}^2/\text{s}^3$ , corresponding to a smallest eddy diameter equal to 25 microns. Figure 4.12 shows the same turbulent energy values at distances 19.0, 19.5, 20.0, 20.5, and 21.0 cm downstream of the mixer. The large scatter here is due to the fact the energy dissipation has reached a small and steady level where energy differences approach zero. Prediction of microscales by this method for the poorly mixed extreme are unreliable as sample errors approach 100 percent.

Calculation of energy dissipation rate in a smooth laminar pipe can be done using Poiseuille's law,  $f=16/\text{Re}$ , where  $f$  is the Fanning friction factor. This method gives a value of  $5.90 (10)^{-4} \text{ m}^2/\text{s}^3$ , estimating the smallest eddy diameter at these operating conditions to be 180 microns.

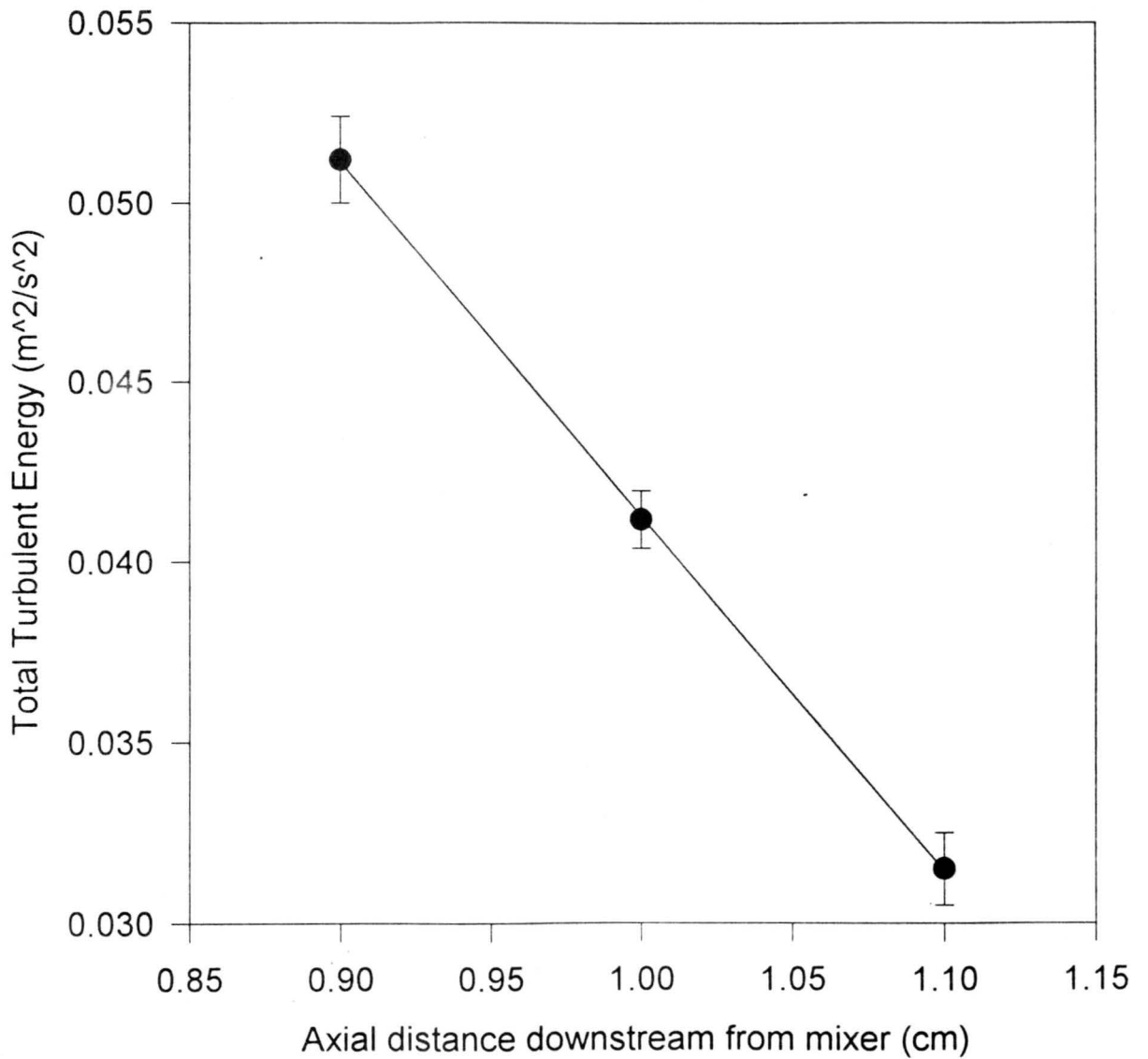


**Figure 4.11**

Radially averaged values of total turbulent energy  
High mixing condition

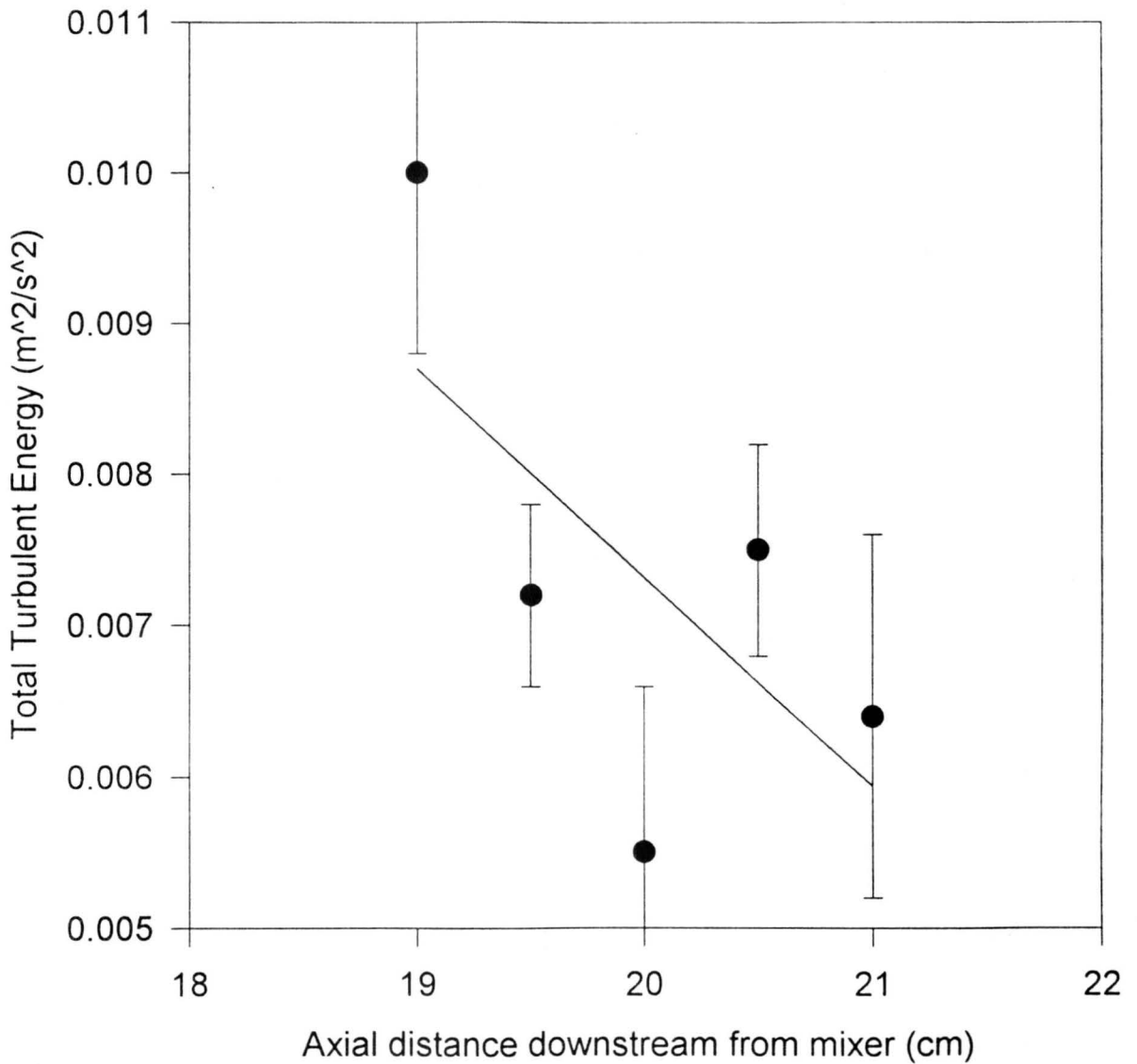


**Figure 4.12**

Radially averaged values of total turbulent energy  
Low mixing condition

If the instantaneous velocity,  $U$ , is replaced by  $\underline{U} + u$ , the mean and fluctuating component of velocity, in the Navier-Stokes equations, and it is expanded along with the continuity equation, terms appear which are responsible for creating tangential stresses. These stresses, which were identified by Osbourne Reynolds in 1888, are often called Reynolds' stresses and are solely responsible for creating the instabilities which create turbulence. Our two-dimensional LDV is capable of quantifying this particular stress component when placed in coincidence mode. The FIND software calculated a value of  $0.549 \times 10^{-2} \text{ m}^2/\text{s}^2$  for the Reynolds' stress in the well mixed condition. Like attempts to calculate total turbulent energy in the poorly mixed condition, the LDV proved ineffective. The instrument was not capable of acquiring data in the coincidence mode due to the small variance in velocities in the poorly mixed state.

#### 4.2.2 Scale Determination from Bourne Dye Reaction

This fast, competitive, consecutive reaction described in Section 2.2.2. was used to characterize the microscale at four different mixing levels. The four levels studied were each of the two mixing conditions with and without the benefit of the cyclone degasser. The reaction procedure was carried out five times at each mixing condition. When the absorbance spectrum is regressed against the extinction coefficients in Table 4.1, the resulting product yields defined by the equation:  $X_s = 2C_s / (2C_s + C_{o-R} + C_{p-R})$ , are plugged into the E model and the predicted microscale dimensions are shown in Figure 4.13.

**Table 4.1 -- Extinction Coefficients for Dye Products**

Wavelength (nm)	<i>ortho</i> -R	<i>para</i> -R	S
690	0.05	1	37.8
680	0.22	1.21	67.6
675	0.35	1.13	89.7
670	0.49	0.9	122
665	0.67	0.87	161
660	0.86	0.85	211
655	1.06	0.9	272
650	1.66	1.41	348
645	2.37	2.03	434
640	3.46	2.95	533
635	5.06	4.36	648
630	7.73	6.46	776
625	12	9.69	918
620	19	14.5	1,070
615	30.3	22.1	1,230
610	48.7	33.4	1,390
605	77.8	49.9	1,540
600	122	74.1	1,690
595	215	120	1,830
590	313	173	1,950
585	443	253	2,070
580	614	357	2,160
575	819	495	2,240
570	1,050	655	2,290
565	1,300	830	2,310
560	1,570	1,020	2,320
555	1,840	1,230	2,310
550	2,120	1,430	2,280
545	2,380	1,630	2,240

540	2,610	1,810	2,180
535	2,820	1,980	2,120
530	2,980	2,120	2,050
525	3,090	2,230	1,990
520	3,160	2,320	1,940
515	3,190	2,370	1,900
510	3,170	2,380	1,880
505	3,100	2,360	1,890
500	3,000	2,310	1,920
495	2,860	2,230	1,950
490	2,710	2,130	1,990
485	2,540	2,010	2,030
480	2,360	1,880	2,050
475	2,190	1,740	2,070
470	2,010	1,610	2,060
465	1,860	1,470	2,040
460	1,710	1,350	2,010
455	1,570	1,230	1,940
450	1,440	1,120	1,860
445	1,340	1,010	1,770
440	1,230	914	1,660
435	1,120	824	1,540
430	1,020	740	1,420
425	916	664	1,290
420	807	595	1,170
415	703	533	1,040
410	608	480	933
400	441	407	749

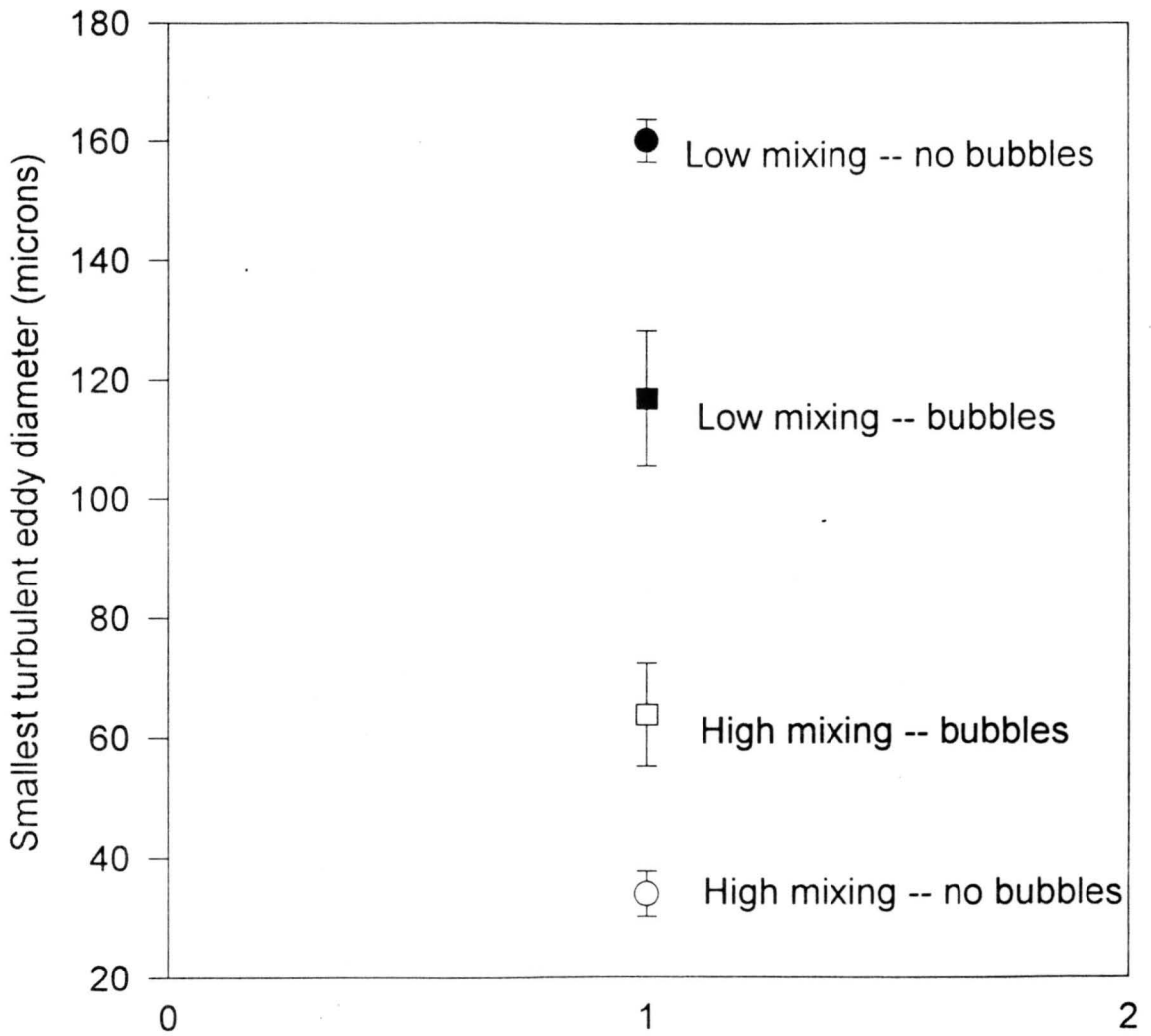


**Figure 4.13**

Dye reaction & E model microscale quantification  
at four different mixing conditions

**It was suspected from the results of fermentation experiment CHE2 that the presence of excessive bubbles in the side loop would significantly hinder the formation of parabolic profiles and decrease microscale dimensions. The values predicted for the Kolmogorov length scales with and without the cyclone are 160 and 127 microns, respectively. The separator helps to increase the poorly mixed microscale by about 40 microns or one third again its gassed value.**

**A surprise was found in the results for the well mixed extreme. Predictions of smallest turbulent eddy diameter are 65 microns for the gassed experiments and 34 microns for the degassed, about half the diameter. While it was not expected that the presence of bubbles would have a dramatic effect on the well mixed condition, these results indicate otherwise. This discrepancy can be explained as follows: given the constant kinematic viscosity of our medium, the only parameter affecting the Kolmogorov scales is the energy dissipation rate per unit mass. In order for the scales to be small, energy dissipation must be large, and in order for energy dissipation to be large, the fluid must be dense (i.e., a liquid). The air bubbles prevent the separation of streamlines which disrupts the formation of vortices just downstream of the mixer. Vortex formation and stretching between fluids creates laminated structures in which diffusion length is decreased and reaction rate is increased. It is in this manner that air bubbles so significantly lengthen the average microscale during the well mixed condition.**

**In conclusion, the presence of air bubbles in the recirculation loop both decreased the microscale in the poorly mixed state and increased it in the well mixed**

state. To achieve the maximum degree of separation in microscales at the feed site, some reliable and continuous method must be implemented that insures no gas phase material can disrupt the energy dissipation.

#### 4.2.3 Comparison of Different Mixing Results

Table 4.2 shows all the microscale predictions made at the various mixing conditons studied in this thesis. Laser Doppler velocimetry provides the most quantitative information of the methods studied here, but proved capable of estimating the smallest turbulent eddy at the well mixed degassed condition only. The Bourne dye reaction is most applicable for microscale prediction, but has the disadvantages of not predicting other

**Table 4.2 -- Comparison of Microscale Diameters at Different Mixing Conditions by Different Methods.**

<i>Mixing Conditon</i>	<i>Method</i>	<i>Estimate of Komogorov eddy diameter (microns)</i>
Low/no bubbles	Bourne Dye	160
Low/no bubbles	Blasius Eqn	180
Low/bubbles	Bourne Dye	127
High/no bubbles	Bourne Dye	34
High/no bubbles	LDV	28
High/bubbles	Bourne Dye	65

scales and also being quite time consuming. Using the Blasius equation is only applicable for completely laminar flows, but appears to give reasonable estimations. The other popular experimental method of turbulence scale quantification is

piezoelectric transduction. Its disadvantages include its large probe size and its intrusiveness of the flow field. Exactly which of these methods is most appropriate will be dependent on the particular system being studied and the type of information needed.

Table 4.3 compares the mixers used in this system with mixers of Beyerinck (1991) and Fowler (1985). The difference in microscale in this system is greater than either of the previous two as are the Reynolds numbers of the pipe and the mixer.

Table 4.3 -- Comparison of Feed Zone Mixing Conditions in Similar Systems

	Fowler (1985)	Beyerinck (1992)	Current
Re--pipe	940	1340	2000
Re--mixer	5-17	500	750
Agitation rate (RPM)	500	700	700
Aeration rate (VVM)	8.7	2.0	2.0
Pipe diameter	33 mm	10.7 mm	10.7 mm
Loop residence time	6.4 seconds	19.5 seconds	13.8 seconds
% time in loop	26%	20%	20%

#### 4.3 Photographs of Dye Dispersion at the Different Mixing Conditions

The figures 4.14a and 4.14b contain slides of the monazo dye product R dispersing into the bulk flow at the different mixing conditions studies in this thesis.

**Figure 4.14a shows the well mixed state, where vortex formation and stretching causes the dye to explode outward, as the axial and radial components of the turbulent velocities approach the same magnitude. Total mixedness appears to occur within 10 mixer diameters downstream. Conversely, the dye in the poorly mixed condition shown in figure 4.14b appears to remain completely segregated. All turbulent fluctuations have approached zero and the dye remains separated from the bulk for over 20 mixer diameters downstream.**

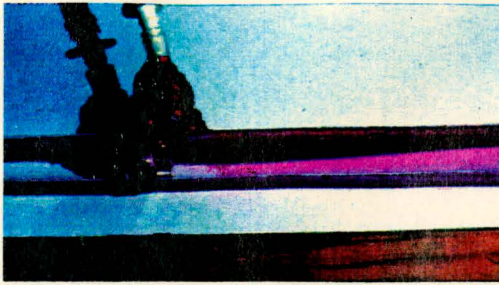


Figure 4.14a

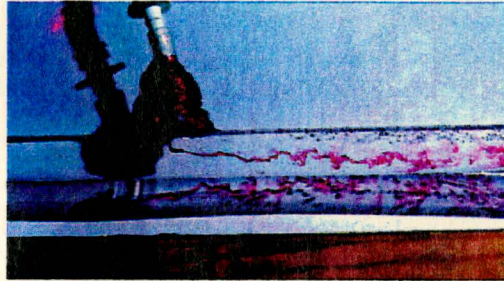


Figure 4.14b

**Figure 4.14a:**

The static mixer is placed directly upstream of the feed needle. Streamlines become separated, creating vortices just downstream of the mixer. The laminated structures formed in the decay of turbulence reduce the effective mixing length.

**Figure 4.14b:**

The static mixer is placed far upstream of the feed needle. The dye enters isokinetically into a streamline. Mass and momentum transfer across streamlines is negligible, as the dye remains segregated from the bulk.

## CHAPTER V: Conclusions

The glucose effect metabolism of *Saccharomyces cerevisiae* makes continuous cultures of this organism a good method for studying the role of substrate micromixing in bioreactors. In industrial fermentations, the use of a heavily agitated side loop for feed dispersion may allow lower power inputs to the stirred tank, resulting in lower operating costs. The use of more costly non-repressive substrates may be justified if either the side loop mixer or cost to sufficiently agitate the vessel are not practical. This has implications towards other organisms with similar types of substrate repressive metabolisms.

The use of a recirculating side loop and static mixer to control micromixing at the feed site in this study has provided the following insights:

- 1) When a flip-flop feeding/mixing strategy is used, no significant change in the cell yield or ethanol produced was observed. When dissolved oxygen levels were maintained above non-repressive levels, the critical dilution rate was greater and the bioreactor productivity was improved. It appears that the mixing condition must be imposed over longer periods of time than those measured in these flip-flop experiments.

2) When a culture history feeding/mixing strategy is used, and dissolved oxygen is not controlled, poor substrate dispersion increased steady state biomass yields in the range of dilution rates where the organism is beginning transition from oxidative to fermentative metabolism. Cytochrome performance appears to play a key role in determining which metabolism is dominant.

3) Culture history plays perhaps the most critical role in determining any particular steady state condition. This has ramifications right from the moment of culture is started, even the number of colonies removed from the slant could be significant.

4) The respiratory capacity of the culture does not seem to deteriorate over long periods of time. This was evidenced by higher cytochrome levels in the poor mixed culture, regardless of the chronological order in which the feeding curves are obtained.

The following conclusions can be made about microscale quantification at the mixing conditions used in this study:

1) The LDV cannot directly measure microscales but can give potentially useful turbulence parameters based on statistical methods. These include: the autocorrelation function, the energy spectrum, the dissipation spectrum, Reynolds' stresses, and total turbulent energies. The energy dissipation rate per unit mass can be indirectly calculated and the smallest turbulent eddy diameter from it.

2) Of the four mixing conditions in this study, LDV can reasonably predict only one of them. An estimation of 25 microns for the well mixed degassed situation is of the same order as predictions by mixing models and other experimental methods. The plenitude of data provided by the LDV is offset by the restricted set of conditions the instrument is operable under.

3) The Bourne dye reaction provides reasonable estimations of microscale parameters at every mixing condition in question. The length microscales for the degassed side loop were 34 and 160 microns, as compared to 65 and 117 microns without gas separation. This suggests that to maximize the difference in scales in this sort of nutrient delivery system, a full-proof method of degassing the fluid before the feed site is essential.

4) The flexibility of this method is its major advantage. The major disadvantage is that the models developed to this date can only provide quantitative information regarding the length microscale and the Damkohler number for each investigated state.

In the author's opinion, the critical experiment to decide the honest utility of this approach has yet to be conducted. This same side loop should be used to deliver fresh feed to a 100 liter stirred tank bioreactor. If the necessary power requirements for sufficiently agitating larger vessels can be reduced by this feeding scheme, while maintaining similar productivity, then its implementation can be justified. Other experiments in laboratory scale fermenters may too be useful. In particular, a culture history type experiment where dissolved oxygen is kept at non-repressive

**levels may provide additional insight about the glucose effect's intracellular mechanism.**

## CHAPTER VI: List of Symbols

<b>A</b>	<b>1-naphthol or its reagent solution</b>
<b>B</b>	<b>Diazotized sulfanilic acid or its reagent solution</b>
<b>C</b>	<b>Concentration (mol/l)</b>
<b>D</b>	<b>Dilution rate (<math>\text{hr}^{-1}</math>)</b>
<b>D<sub>crit</sub></b>	<b>Critical dilution rate (<math>\text{hr}^{-1}</math>)</b>
<b>Da</b>	<b>Damkohler number</b>
<b>E</b>	<b>Engulfment rate (<math>\text{sec}^{-1}</math>)</b>
<b>F</b>	<b>Dimensionless concentration ratio of B/A</b>
<b>f</b>	<b>Fanning friction factor</b>
<b>k<sub>r</sub></b>	<b>Reaction rate constant</b>
<b>k<sub>a</sub></b>	<b>Volumetric liquid mass transfer coefficient</b>
<b>kW</b>	<b>Kilowatt</b>
<b>nm</b>	<b>Nanometer</b>
<b>R</b>	<b>Either <i>ortho</i>- or <i>para</i>- isomer of monazo dye product</b>
<b>RPM</b>	<b>Revolutions per minute</b>
<b>S</b>	<b>diazo dye product</b>
<b>Sc</b>	<b>Schmidt number</b>
<b>U<sub>i</sub></b>	<b>Instantaneous velocity component</b>
<b><u>U</u></b>	<b>Average velocity component</b>
<b>u</b>	<b>Fluctuating velocity component</b>
<b>u<sup>2</sup></b>	<b>Mean square velocity</b>
<b>vvm</b>	<b>volumes of air per volume of liquid per minute</b>

### Greek letters

<b>ε</b>	<b>Energy dissipation rate (<math>\text{m}^2/\text{sec}^3</math>)</b>
<b>η</b>	<b>Kolmogorov eddy diameter</b>
<b>ν</b>	<b>Kinematic viscosity (<math>\text{m}^2/\text{sec}</math>)</b>
<b>τ</b>	<b>Kolmogorov eddy turnover rate (<math>\text{sec}^{-1}</math>)</b>

## CHAPTER VII: Acknowledgements

I would especially like to thank my advisor, Dr. Eric Dunlop, for his untiring support and guidance in the preparation of this thesis and for the many opportunities he has provided me to explore the world, both physically and geographically. The Colorado Bioprocessing Center also needs to be thanked for the use of its facility and supplies.

Without the laboratory assistance of Kevin Wenger (Homebrew God), Hugh Graham (Computer God) and Pradyumna Kumar Namdev (Confucius), this thesis would not be what it is today. The nifty color shots of dye dispersion were taken with photographic expertise of Hugh, and the layout designed by pighed.

Unspeakable appreciation goes to Kevin, Hugh, Phil Benstein, Jenny Conde, Lisa Jones, and SPECTRE for helping me to drink and laugh away the agony of continuous fermentation. For putting up with my constant deafening rock n' roll muzak, SPECTRE deserves acknowledgment and some earmuffs. Greg Holloway deserves credit for teaching me to play Disc Golf; the student will undoubtedly someday surpass his teacher.

Richard Taylor, pighed and his mother, Sally, are thanked for instilling in me a passion and curiosity for the world and its beauty. I am, however, most indebted to my parents, Gene and Lucie Mondani, to whom I owe pretty much everything.

## CHAPTER VIII: Literature Cited

- Alberts B., D. Bray, J. Lewis, M. Raff, K. Roberts and J.D. Watson, *Molecular Biology of the Cell*, Garland, New York, (1983).
- Armenante, P.M. and D.J. Kirwan, "Mass Transfer to Microparticles in Agitated Systems," *Chem. Eng. Sci.*, 44:2781-2796 (1989).
- Bajpai, R.K. and M. Reuss, "Coupling of Mixing and Microbial Kinetics for Evaluating the Performance of Bioreactors," *Canadian J. Chem. Eng.*, 60: 384-392 (1982).
- Baldyga, J. and J.R. Bourne, ""Simplification of Micromixing Calculations. I. Derivation and Application of a New Model," *Chem. Eng. Journal*, 42: 83-92 (1989).
- Barthole, J.P., R. David and J. Villermaux, "A New Chemical Method for the Study of Local Micromixing Conditions in Industrial Stirred Tanks," *Chem. Reaction Eng.*, 42: 545-554 (1982).
- Bennett, C.O. and J.E. Myers, *Momentum, Heat, and Mass Transfer, 3rd ed.*, McGraw-Hill Chemical Engineering Series, New York, (1982).
- Beyerinck, R. "Feed Zone Turbulence as Measured by Laser Doppler Velocimetry and Baker's Yeast Growth in a Chemostat," Masters Thesis, Colorado State University, Fort Collins, CO, (1991).
- Borrvalho, L.M., D.R. Malamud, A.D. Panek, M.N. Tenan, D.E. Olivera, and J.R. Mattoon, "Parallel Changes in Catabolite Repression of Haem Biosynthesis and Cytochromes in Repression-resistant Mutants of *Saccharomyces cerevisiae*," *J. Gen. Microbiology*, 135: 1217-1227 (1989).
- Bourne J.R., P. Rys and K. Suter, "Mixing Effects in the Bromination of Resorcin," *Chem. Eng. Sci.*, 32: 711-716 (1977).
- Bourne, J.R., F. Kozicki, and P. Rys, "Mixing and Fast Chemical Reaction," *Chem. Eng. Sci.*, 36 10:1643 (1981).

- Bourne J.R., C. Hilber, and G. Tovstiga, "Kinetics of the Azo Coupling Reactions Between 1-Naphthol and Diazotized Sulfanilic Acid," *Chem. Eng. Communications*, 37: 293 (1985).
- Brooks, J.D. and J.L. Meers, "The Effect of Discontinuous Methanol Addition on the Growth of a Carbon Limited Culture of *Pseudomonas*," *J. Gen. Microbiology*, 77: 513-519 (1983).
- Cherry, R.S. and E.T. Papoutsakis, *Biotech. Bioeng.* 32: 1001 (1988).
- Corrsin, S., "Simple Theory of an Idealized Turbulent Mixer," *AIChE J.*, 3: 329-330 (1957).
- Crabtree, H.G., "Observations on the Carbohydrate Metabolism in Tumours," *Biochem. J.*, 23: 536-545 (1929).
- Curl R.L., "Dispersed Phase Mixing I: Theory and Effects in Simple Reactors," *AIChE J.*, 9: 175 (1963).
- Danckwerts P.V., "Continuous Flow Systems, Distribution of Residence Times," *Chem. Eng. Sci.*, 1 1 (1953).
- Dunlop, E.H. and S.J. Ye, "Micromixing in Fermenters: Metabolic Changes in *Saccharomyces cerevisiae* and their Relationship to Fluid Turbulence," *Biotech. Bioeng.*, 36: 854-864 (1990).
- Els, H., "LDV Measurements in pipe flow: problems and experiences," International Symposium on Laser Anemometry, ASME, Miami, Florida (1985).
- Fiechter, A., and H.K. von Meyenberg, *Proc. 2nd Int. Symp. Yeast*, A. Kockova-Kratochilova, ed., p. 387, Slovenskej Akademie Vied (1966).
- Fiechter A., "Continuous Cultivation of Yeasts," Chapter 6 in *Methods in Cell Biology*, 11: D.M. Prescott, ed., (1978).
- Fields, P.R. and N.H. Slater, "The Influence of Fluid Mixing Upon Respiratory Patterns for Extended Growth of a Methyloph in an Air-Lift Fermenter," *Biotech. Bioeng.*, 26: 719-726 (1984).
- Fowler, J.D. and E.H. Dunlop, "Effects of Reactant Heterogeneity and Mixing on Catabolite Repression in Cultures of *Saccharomyces cerevisiae*," *Biotech. Bioeng.*, 33: 1039-1046 (1989).

- Fowler, J.D. "Mixing and Nutrient Dispersal in Cultures of *S. cerevisiae*,"  
Masters Thesis, Washington University, Saint Louis, Missouri (1985).
- Frey, J.H. and C.D. Denson, "Imidization Reaction Parameters in Inert  
Molten Polymers For Micromixing Tracer Studies," *Chem. Eng. Sci.*,  
43 8: 1967-1973 (1988).
- Funahashi, H. and M. Maehara, "Effects of Agitation by Flat-Bladed  
Turbine Impeller on Microbial Production of Xanthan Gum," *J.*  
*Chem. Eng. Japan*, 20 1 16-22 (1987).
- Furakawa, K. E. Heinzle, and I.J. Dunn, "Influence of Oxygen on the  
Growth of *Saccharomyces cerevisiae* in Continuous Culture," *Biotech.*  
*Bioeng.*, 15: 2293-2317 (1983).
- Hansford, G.S. and A.E. Humphrey, "The Effect of Equipment Scale and  
Degree of Mixing on Continuous Fermentation Yield at Low Dilution  
Rates," *Biotech. Bioeng.*, 8: 85-96 (1966).
- Helgesen, J.K. and M.J. Matteson, "Particle Mixing and Diffusion in the  
Turbulent Wake of Cylinder Arrays," *Experiments in Fluids* 10:  
333-340 (1991).
- Hinze, J.O. *Turbulence*, McGraw-Hill, New York, 1975.
- Jeffries T.W. and M.A. Alexander, "Respiratory Efficiency and Metabolite  
Partitioning as Regulatory Phenomena in Yeasts," *Enzyme Microb.*  
*Tech.*, 12: 2-19 (1990).
- Kindler, P., M.A. Elliot, B.K. Stephenson and M.J. Matteson, "Particle  
Deposition after Crossing a Sudden Expansion," *J. of Aerosol Science*  
22 3: 259-266 (1991).
- Lievense, J.C. and H.C. Lim, "The Growth and Dynamics of *Saccharomyces*  
*cerevisiae*," *Annual Reports on Fermentation Processes*, G.T. Tsao, ed.,  
22: 123-183 (1981).
- Moes J., M. Griot, J. Keller, and E.A. Heinzle, "A Microbial Culture with  
Oxygen-Sensitive Product Distribution as a Potential Tool for  
Characterizing Bioreactor Oxygen Transport," *Biotech. Bioeng.* 27:  
482-489 (1985).
- Nauman E.B. "Residence Time Distribution and Micromixing", *Chem. Eng.*  
*Communications*, 8: 53 (1981).

- Ottino, J.M., "Lamellar Mixing Models for Structured Chemical Reactions and Their Relationship to Statistical Models; Macro- and Micromixing and the Problem of Averages.," *Chem. Eng. Sci.* **35**: 1377-1391 (1980).
- Pastuer, L. *Compt. Rend. Acad. Sci.*, **75**: 784-790 (1872).
- Paul, E.L. and R.E. Treybal, "Mixing and Product Distribution for a Liquid Phase, Second Order, Competitive Consecutive Reaction," *AIChE J.* **17** 3: 718-724 (1971).
- Plasari, E., R. David, and J. Villermaux, "Micromixing Phenomena in Continuous Stirred Reactors Using a Michaelis-Menten Reaction in the Liquid Phase," *ACS Symp. Series*, **65**: 125-139 (1978).
- Potsma E., W.A. Scheffers, and J.P. van Duken, "Kinetics of Growth and Glucose Transport in Glucose-Limited Chemostat Cultures of *Saccharomyces cerevisiae* CBS 8066," *Yeast*, **5**: 159-165 (1989).
- Ranade, V.V., and J.B. Joshi, "Flow Generated by a Disc Turbine: Part I Experimental," *Chem. Eng. Research and Design* **68**: 19-33 (1990).
- Ratledge, C., "Yeast Physiology -- A Micro-Synopsis," *Bioprocess Engineering*, **6**: 195-203 (1991).
- Roshko, A., "On the Development of Turbulent Wakes from Vortex Streets," Report 1191, *National Advisory Committee for Aeronautics*, Washington D.C., (1954).
- Ruklisha, M.P., J.J. Vanags, M.A. Rikmanis, M.K. Toma, and U.E. Viesturs, "Biochemical Reactions of *Brevibacterium flavum* Depending on Medium Stirring Intensity and Flow Structure," *Acta Biotechnology*, **9** 6: 565-575 (1989).
- Senior, P.J., and J. Windass, "The ICI Single Cell Protein Process," *Biotech. Letters* **2**: 205-210 (1980).
- Sonnleitner, B. and O. Kappeli, "Growth of *Saccharomyces cerevisiae* is Controlled by Its Limited Respiratory Capacity: Formulation and Verification of a Hypothesis," *Biotech. Bioeng.*, **28**: 927-937 (1986).
- Sonnleitner B., "Dynamics of Yeast Metabolism and Regulation," *Bioprocess Eng.*, **6**: 187-193 (1991).

- Srikantaiah, D.V. and H.W. Coleman, "Turbulence Spectra from Individual Realization Laser Velocimetry Data," *Experiments in Fluids* 3: 35-44 (1985).
- Sweere, A. "Response of Bakers' Yeast to Transient Environmental Conditions Relevant to Large-Scale Fermentation Processes," Chapter 6, Ph.D. Thesis, Delft University of Technology, (1988).
- Tennekes, H. and J.L. Lumley, *A First Course in Turbulence*, MIT Press, Cambridge, Mass., (1972).
- Thoma, S., V.V. Ranade, and J.R. Bourne, "Interaction Between Micro- and Macromixing during Reactions in Agitated Tanks," *Canadian J. of Chem Eng.* 69: 1135-1141 (1991).
- Townsend, A.A., "The Measurement of Double and Triple Correlation Derivatives in Isotropic Turbulence," *Proc. of the Cambridge Phil. Soc.* 43: 560-570 (1947).
- Townsend, A.A., "Momentum and Energy Diffusion in the Turbulent Wake of a Cylinder," *Proceedings of the Royal Society of London*, 197(A): 124-140 (1949).
- Tsai, B.I., L.E. Erickson, and L.T. Fan, "The Effect of Micromixing on Growth Processes," *Biotech. Bioeng.*, 11: 181-205 (1969).
- Villermaux, J., "Micromixing Phenomena in Stirred Reactors," *Encycl. Fluid Mech.*, 2 27: 707-769 (1986).
- von Meyenberg, K. "Catabolite Repression and the Germination Cycle of *Saccharomyces cerevisiae* (German)," Ph.D. Dissertation #4279, ETH, Zurich (1969).
- Wenger, K.S., I.D. MacGilp, and E.H. Dunlop, "Investigation of the Chemistry of a Diazo Micromixing Test Reaction," *AIChE Journal*, 38 7: 11105-11114 (1992).
- Wenger, K.S., "Substrate Mixing and the Glucose Effect Metabolism of *Saccharomyces cerevisiae*," Ph.D. Dissertation, Colorado State University, Fort Collins, CO, (1994).
- Yeh, T.T., B. Robertson, and M.W. Matter, "LDV Measurements near a Vortex Shedding Strut Mounted in a Pipe," *J. of Fluids Eng.* 105: 185-196 (1983).

## **Appendix A-- Diazotization of Sulfanilic Acid**

**Recipe is for 1 liter with concentrations 5.5 mol/m<sup>3</sup>.**

- 1) Dissolved 0.2915 g (0.00275 mol) Na<sub>2</sub>CO<sub>3</sub> in 5.5 ml distilled H<sub>2</sub>O.**
- 2) Slowly add 0.9526 g (0.00550 mol) sulfanilic acid. Stir mixture and warm gently until all of sulfanilic acid is dissolved.**
- 3) Meanwhile, dissolve 0.3947 g (0.00572 mol) NaNO<sub>2</sub> in approx. 1 ml distilled H<sub>2</sub>O.**
- 4) Prepare a slurry of 1.25 ml conc. HCl with 6.6 g of ice.**
- 5) Cool the sulfanilic acid to 15°C. With good stirring, add the NaNO<sub>2</sub> solution to the sulfanilic acid solution. Quickly add the ice/HCl slurry. Allow the mixture to stir for approx. 1 minute before rinsing any residulas into the mixture. Within approx. 1 minute, a white precipitate of diazotized sulfanilic acid should be seen.**
- 6) Allow the mixture to stir in an ice bath for 30 minutes.**
- 7) Add 0.016 g (2.67 (10<sup>-4</sup>) mol) urea followed quickly by 2.5 ml conc. HCl.**
- 8) Dilute to 1 liter volume with distilled H<sub>2</sub>O.**

**Note: The white precipitate of diazotized sulfanilic acid should be kept in suspension, as it is explosive when dried. The solution should also be kept refridgerated and it good for only 24-36 hours.**

**Recipe for 5 liters of 1-naphthol with concentration 0.0055 mol/m<sup>3</sup>.**

- 1) With vigorous stirring, dissolve 58.29 g Na<sub>2</sub>CO<sub>3</sub> in approx 2 liters distilled water.**
- 2) Add 46.20 g NaHCO<sub>3</sub> to solution, allow to dissolve completely.**
- 3) Slowly add 0.4165 g 1-naphthol. It takes about 1 hour of vigorous stirring to dissolve completely. If possible, the solution should be sparged with nitrogen gas during the dissolution process.**